NAVAL POSTGRADUATE SCHOOL
Monterey, California

THESIS

OPTIMAL STOCHASTIC SLIDING MODE CONTROL OF UNDERWAY REPLENISHMENT IN A RANDOM SEA

by

Fu, Hsu-Sheng

December, 1991

Thesis Advisor: Fotis A. Papoulias

Approved for public release; distribution is unlimited.

REPORT DOCUMENTATION PAGE

1a REPORT SECURITY CLASSIFICATION UNCLASSIFIED	1b RESTRICTIVE MARKINGS
2a SECURITY CLASSIFICATION AUTHORITY	3 DISTRIBUTION/AVAILABILITY OF REPORT Approved for public release; distribution is unlimited.
2b DECLASSIFICATION/DOWNGRADING SCHEDULE	
4 PERFORMING ORGANIZATION REPORT NUMBER(S)	5 MONITORING ORGANIZATION REPORT NUMBER(S)
6a NAME OF PERFORMING ORGANIZATION Naval Postgraduate School 6b OFFICE SYMBOL *(If applicable)*	7a NAME OF MONITORING ORGANIZATION Naval Postgraduate School
6c ADDRESS (*City, State, and ZIP Code*) Monterey, CA 93943-5000	7b ADDRESS (*City, State, and ZIP Code*) Monterey, CA 93943-5000
8a NAME OF FUNDING/SPONSORING ORGANIZATION 8b OFFICE SYMBOL *(If applicable)*	9 PROCUREMENT INSTRUMENT IDENTIFICATION NUMBER
8c ADDRESS (*City, State, and ZIP Code*)	10 SOURCE OF FUNDING NUMBERS Program Element No. / Project No. / Task No. / Work Unit Accession Number

11 TITLE (*Include Security Classification*)
OPTIMAL STOCHASTIC SLIDING MODE CONTROL OF UNDERWAY REPLENISHMENT IN A RANDOM SEA (U)

12 PERSONAL AUTHOR(S) Fu, Hsu Sheng

13a TYPE OF REPORT	13b TIME COVERED	14 DATE OF REPORT (*year, month, day*)	15 PAGE COUNT
Master's Thesis	From To	December 1991	127

16 SUPPLEMENTARY NOTATION
The views expressed in this thesis are those of the author and do not reflect the official policy or position of the Department of Defense or the U.S. Government

17 COSATI CODES			18 SUBJECT TERMS (*continue on reverse if necessary and identify by block number*)
FIELD	GROUP	SUBGROUP	

19 ABSTRACT (*continue on reverse if necessary and identify by block number*)

Motion control of underway replenishment operations is achieved through the use of sliding mode control with a Linear Quadratic Gaussian compensator design. External disturbances include first-order wave force and moment as well as slowly varying interaction forces and moments between the two ships. Feedback control is used to provide adequate stability of motions while feedforward control with disturbance estimation and compensation achieves the desired steady state accuracy. The results demonstrate that satisfactory path keeping during operations can be maintained for various ship proximity distances and enviromental conditions.

20 DISTRIBUTION/AVAILABILITY OF ABSTRACT	21 ABSTRACT SECURITY CLASSIFICATION
☒ UNCLASSIFIED/UNLIMITED ☐ SAME AS RPT ☐ DTIC USERS	UNCLASSIFIED
22a NAME OF RESPONSIBLE INDIVIDUAL Fotis A. Papoulias	22b TELEPHONE (*Include Area code*) (408)646-3381 22c OFFICE SYMBOL ME/Pa

DD FORM 1473, 84 MAR 83 APR edition may be used until exhausted
All other editions are obsolete

SECURITY CLASSIFICATION OF THIS PAGE
Unclassified

Approved for public release; distribution is unlimited.

Optimal Stochastic Sliding Mode Control of
Underway Replenishment in
A Random Sea

by

Fu, Hsu-Sheng
Lieutenant, Taiwan, Republic of China Navy
B.S., Chinese Naval Academy 1987

Submitted in partial fulfillment
of the requirements for the degree of

MASTER OF SCIENCE IN MECHANICAL ENGINEERING

from the

NAVAL POSTGRADUATE SCHOOL
December 1991

Author: _____
Fu, Hsu-Sheng

Approved by: _____
Fotis A. Papoulias, Thesis Advisor

_____
Anthony J. Healey, Chairman
Department of Mechanical Engineering

ABSTRACT

Motion control of underway replenishment operations is achieved through the use of sliding mode control with a Linear Quadratic Gaussian compensator design. External disturbances include first-order wave force and moment as well as slowly varying interaction forces and moments between the two ships. Feedback control is used to provide adequate stability of motions while feedforward control with disturbance estimation and compensation achieves the desired steady state accuracy. The results demonstrate that satisfactory path keeping during operations can be maintained for various ship proximity distances and environmental conditions.

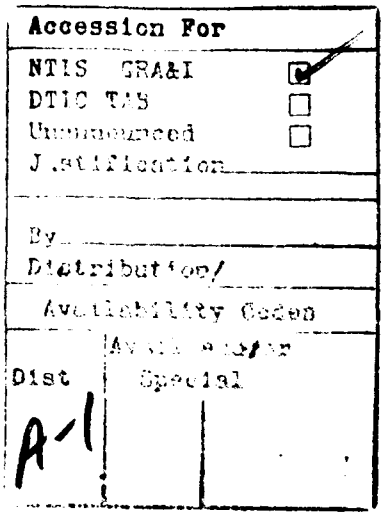

TABLE OF CONTENTS

LIST OF TABLES

LIST OF FIGURES

ACKNOWLEDGMENTS

I would like to express my sincere gratitude to my thesis adviser, Professor Fotis A. Papoulias. His expert assistance and continued guidance allowed me to overcome many intractable difficulties.

To Professor George J. Thaler my heartfelt thanks for his knowledgeable advice and patience throughout the course of this research. I really appreciate the time and effort they spent with me.

I. INTRODUCTION

A. AIM OF THIS STUDY

Accurate course keeping is one of the most important problems for ship maneuvering and especially in an underway replenishment in an open sea. There is an apparent danger in such an operation due to the complex effects of the seaway, and the conventionally slow control loop indicated in Figure 1.1.

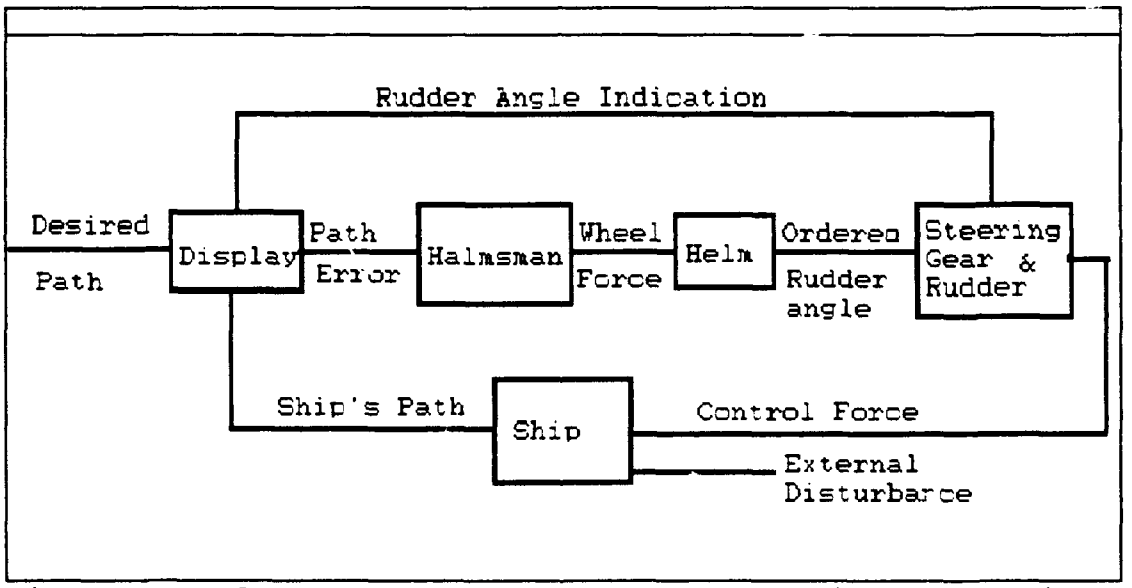

Figure 1.1 Close Loop Control System for Ship Maneuvering

In particular, during underway replenishment the ship is subject to a variety of forces and environmental disturbances. The most important of these are the interaction forces and

moments that are generated as a result of the two ships in proximity with one another[Ref.7][Ref.8]. These forces depend on the relative positions of the two ships and both their magnitude and sign is not easily predictable by analytical techniques In a random seaway there exist also first-order irregular wave forces and second-order wave drift forces. The latter appear in the form of long term slowly varying excitations and do not have a significant effect on lateral separation control[Ref.8]. In this thesis we focus our attention on the effects of the interaction forces and first-order wave forces on the system response. We employ a sliding mode feedback control law due to its robustness characteristics with regard to unmodeled dynamics and disturbances. The sliding surface is based on the Linear Quadratic Regulator. Partial state measurement is assumed and a Kalman filter is designed to provide an accurate estimate of the unmeasurable states and to minimize the effects of measurement noises. Disturbance estimation and compensation is used in order to ensure the desired steady state accuracy. A schematic block diagram of the control design is shown in Figure 1.2.

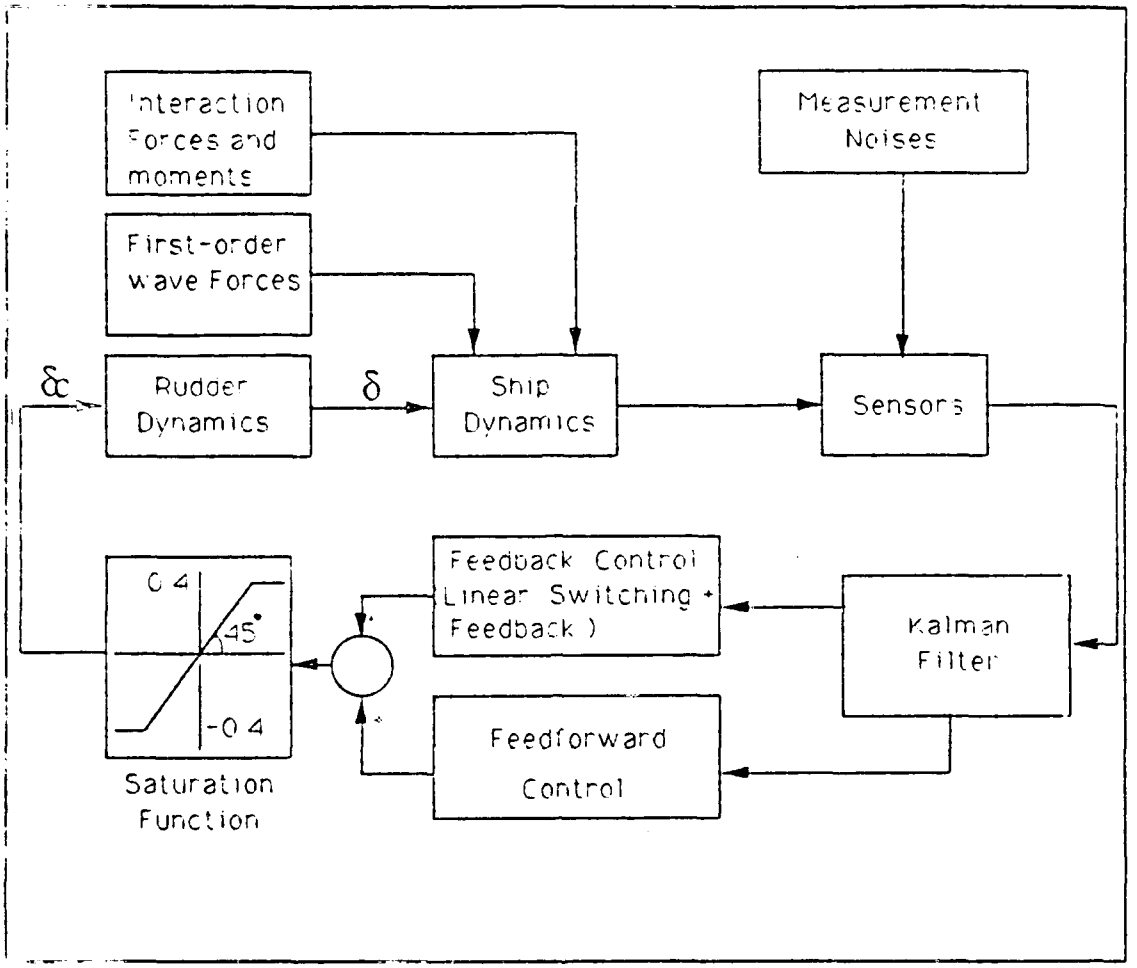

Figure 1.2 Automatic Control of Ship Replenishment at Sea

B. THESIS OUTLINE

In Chapter II, the LQR method of sliding mode controller design is developed and simulated at calm sea. Chapter III is conserned with the Kalman filter design. Simulations of the UNREP with open sea effects are presented in Chapter III.

II. MATHEMATICAL MODEL IN THE HORIZONTAL PLANE

A. NONLINEAR STEERING EQUATIONS IN THE OPEN SEA

The UNREP operation at sea is schematically depicted in Figure 2.1 where Y and N are the interaction forces and moments. The leading ship keeps its course unchanged and the tracking ship keeps the separation distance constant, normally less then 100 feet (depending on the type of ship).

Figure 2.6 and Figure 2.7 show the interaction forces and moments on the tracking ship due to the interaction effect of the leading ship. The interaction force Y(A,B) acts through the ship's center of gravity and the moment N(A,B) about the center of gravity in the horizontal plane. The two curves used in this study are for a typical Mariner ship at a nominal speed of 15 knots and for different relative positions. In applying these curves to the leading ship, the interaction force and moment need to be changed to -Y(-A,B) and -N(-A,B), respectively. For each figure, the curves for B=50 ft and B=100 ft were determined from experimental model testing results[Ref.6][Ref.8], and the curves in between were determined by interpolation. The data were also extrapolated up to B=150 ft. A and B are continually read by the simulation program as input data to a two dimensional interpolation

routine which calculates the base line interaction forces and moments acting on the ship.

The coordinate system used in this study follows the standard system from Principles of Naval Architecture[Ref.11]. In practice, the leading ship keeps constant heading, while the tracking ship maintains a constant lateral separation distance. Different configurations and the directions of variations of the interaction force and moment as the tracking ship moves from -524 ft to 524 ft are shown in Figure 2.2.

The primary consern for UNREP simulation is related to the space coordinates (longitudinal and lateral separation distance, yaw angle, and yaw rate). So the equations of motion are first expressed in ship velocity coordinates (u, v) and then transformed to space coordinates(x, y) (Figure 2.3). The transformation equations are

$$\dot{x}=u\cos\psi-v\sin\psi \tag{2.1}$$

$$\dot{y}=u\sin\psi+v\cos\psi \tag{2.2}$$

The ship's coordinates are assumed to be at the ship's center of gravity ($x_G=0$, $y_G=0$).

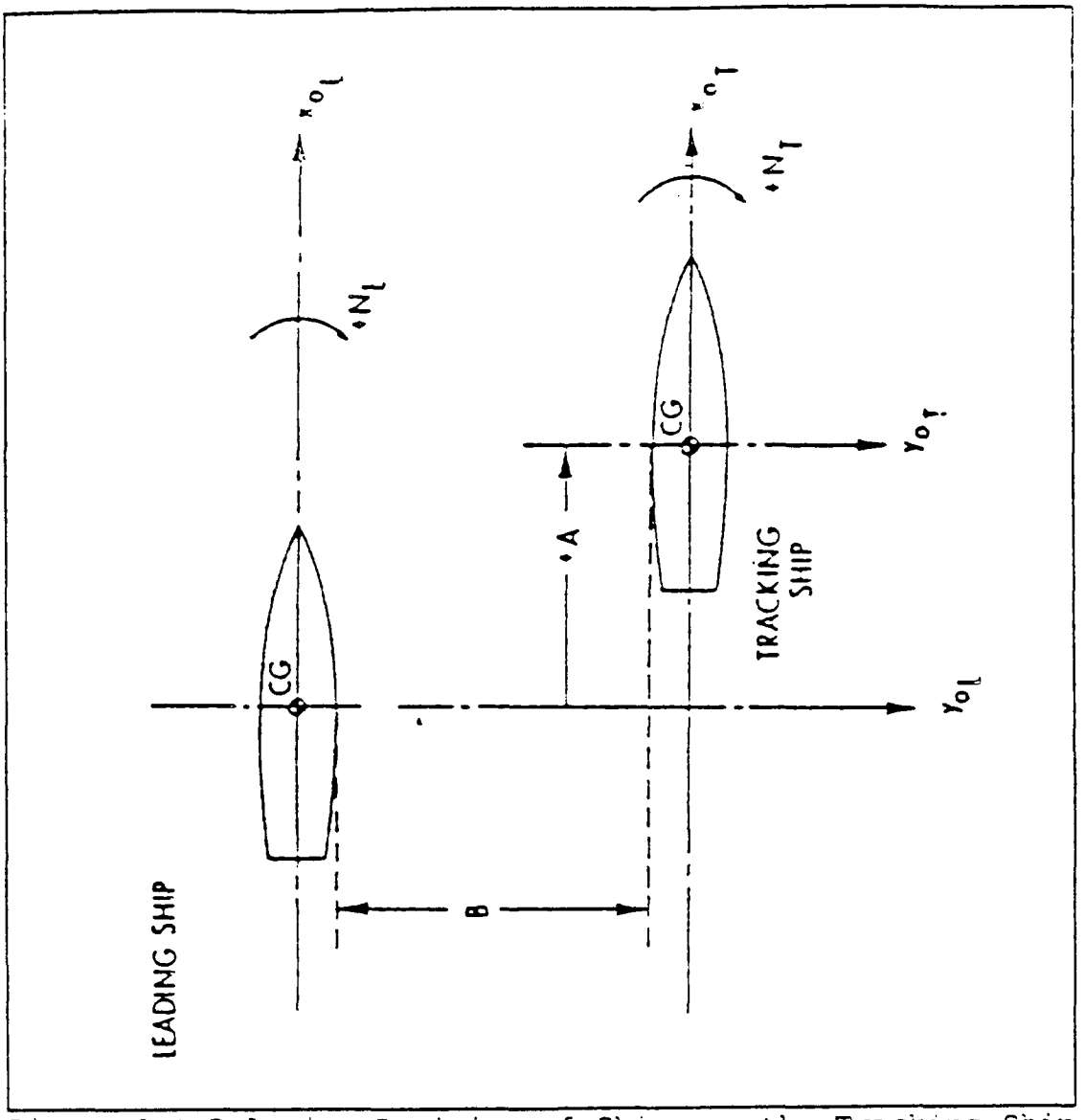

Figure 2.1 Relative Position of Ships as the Tracking Ship Passes the Leading Ship

* Note :

A: longitudinal separation distance.

B: lateral separation distance.

Arrows indicate positive directions according to established sign convention[Ref.13].

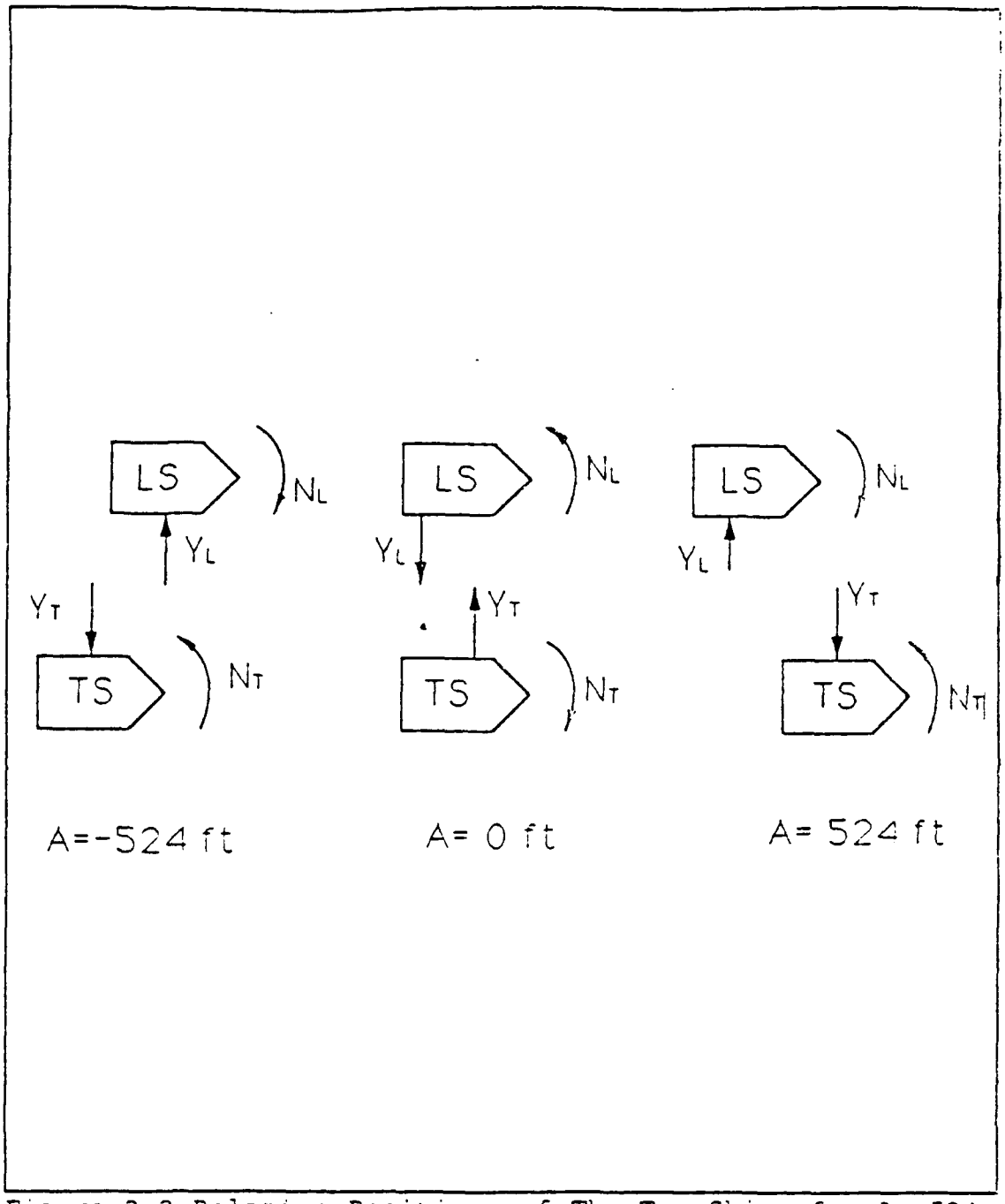

Figure 2.2 Relative Positions of The Two Ships for A=-524 ft, 0, and +524 ft and Corresponding Interaction Forces and Moments.

* Note: LS: Leading Ship.

TS: Tracking Ship.

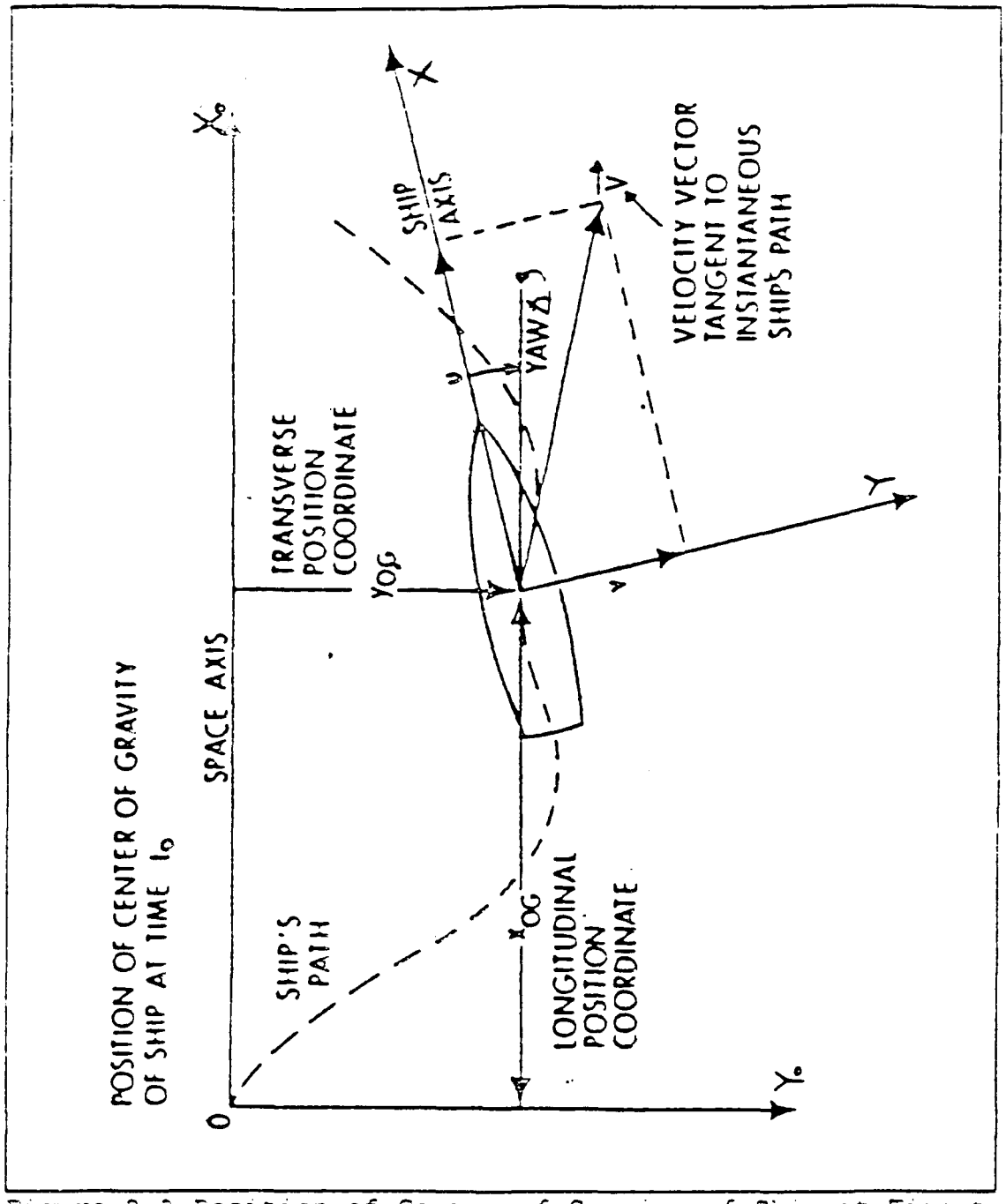

Figure 2.3 Position of Center of Gravity of Ship at Time t_0 in Space Axes

* Note:

V: Velocity vector tangent to instantaneous ship path.

B. MANEUVERING MATHEMATICAL MODEL

The nonlinear maneuvering equations of motion and the hydrodynamic interaction forces and moments that act on the ship's hull are modeled for 15 knots nondimensional forward speed. In an UNREP control simulation, the ability to manually or automatically control the rudder and propeller speed must be present. Only rudder input is considered here, and the ship forward speed is assumed constant by the propulsion control. The basic mariner study ship characteristics are presented at Table 2.1.

Table 2.1 Characteristics of Mariner-type Study Ship

Length between perpendicular	527.8 ft(160.87 m)
Beam	76.0 ft(23.26 m)
Draft	29.75 ft(9.06 m)
Displacement	16800.0 tons (15120 t)
Block coefficient(C_b)	0.6

* The ship's coordinate system is assumed to be at the ship's center of gravity(x_G, y_G= 0).

The goal of this study is to present an alternative way of steering control based on sliding modes. For this reason the simulation does not concentrate on the derivation of ship dynamic and hydrodynamic effects, but on the results of control and observer feedback. Only the tracking ship is the major consideration, and we assume a reliable lateral distance measurement. The ship hydrodynamic maneuvering model for the study ship consists of the nonlinear equations of motion in the horizontal plane (sway and yaw). The hydrodynamic coefficients are presented in Table 2.3, and the nondimensional equations of motion are:

SWAY EQUATION:

$$(m-Y_{\dot{v}})\,\dot{v}+(mx_G-Y_{\dot{r}})\,\dot{r}=F_2(u,v,r,\delta) \tag{2.3}$$

YAW EQUATION:

$$(mx_G-N_{\dot{v}})+(I_z-N_{\dot{r}})\,\dot{r}=F_3(u,v,r,\delta) \tag{2.4}$$

where

$$F_2(u,v,r,\delta)=Y_v v+(Y_r-mu_1)\,r+Y_\delta\delta+Y_n n+Y(A,B)+f_1+f_2 \tag{2.5}$$

and

$$F_3(u,v,r,\delta) = N_v v + (N_r - mx_G u_1) r + N_\delta \delta + N_n \Delta n + N(A,B) + n_1 + n_2 \quad (2.6)$$

Y(A,B) nondimensional hydrodynamic interaction force caused by leading ship.

N(A,B) nondimensional hydrodynamic interaction moment caused by leading ship.

f_1, n_1 first-order component of random sea.

f_2, n_2 second-order component of random sea.

Some assumptions were made for simplification without any significant physical effects. First, the ship's coordinates are assumed to be at the ship's center of gravity (x_G, $y_G \approx 0$); second, $Y_n n$ and $N_n n$ are small terms also neglected from the simulation; and third, the second-order force and sway moment f_2 and n_2 are not considered in this thesis. This is because the effect of these slowly varying forces and moments is similar to the interaction forces and moments which are analyzed in detail.

1. Rudder Dynamics Model

There are two limiters for modeling rudder dynamics, the first limiter models the rudder saturation limits at ±0.4 radians. The second limiter models the proportional band of a variable-displacement pump by limiting its maximum percent stroke, the limits for this nonlinear element have been found to be 0.297 radians for this study case. [Ref.1] [Ref.6]

The lag time and "dead band" in the rudder dynamics when a helm angle is commanded are important aspects of the manuvering control problem. The rate of change of the rudder angle was assumed to be inversely proportional to the error signal, subject to a maximum rudder rate of .0698 rad/sec, and a maximum error input of 0.297 radians.

The system gain can be defined as:

k_r = Maximum rudder rate/Maximum error input

= 0.0689/0.298 = 0.234 /sec

We nondimensionalize this system gain as:

$k_r' = k_r * L/u_l$ = 0.234*527.8 ft/(15*1.689) ft/sec =4.89

Where

L = ship length= 527.8 ft

u_l= ship forward speed= 15 knots= 15*1.689 ft/sec

This again was taken approximately equal to 5 in this study; and $\tau_r = 1/k_r'$ is defined as the nondimensional rudder system time constant.

The rudder "dead band" was set to ± 0.5 deg. An analog diagram of the rudder dynamics is shown in Figure 2.4 [Ref.8], which includes the response of the rudder system to step commands. The equivalent rudder dynamics are described by a first order lag, see Figure 2.5, where

$$\dot{\delta} = -\frac{1}{\tau_r}\delta + \frac{1}{\tau_r}\delta_c \qquad (2.7)$$

τ_r is the rudder dynamics time constant, and

δ_c is the commanded rudder angle.

2. State Space Representation

The mathematical model consists of the previous sway and yaw equations of motion

$$(m - Y_{\dot{v}})\dot{v} + (mx_G - Y_{\dot{r}})\dot{r} = Y_v v + (Y_r - mu)r + Y_\delta \delta + Y(A,B) + f_1 \qquad (2.8)$$

$$(mx_G - N_{\dot{v}})\dot{v} + (I_z - N_{\dot{r}})\dot{r} = N_v v + (N_r - mx_G u)r + N_\delta \delta + N(A,B) + n_1 \qquad (2.9)$$

and the rudder dynamics

$$\dot{\delta} = -\frac{1}{\tau_r}\delta + \frac{1}{\tau_r}\delta_c \qquad (2.10)$$

The lateral separation rate can be calculated from the components of lateral direction of ship forward speed (u) lateral speed (v), and heading angle (ψ)

$$\dot{y} = u\sin\psi + v\cos\psi \qquad (2.11)$$

With the small angle assumption we can linearize this equation as:

$$\dot{y}=\psi+v \tag{2.12}$$

where the dimensionless forward speed is one.

The last kinematic relation is between the ship heading ψ and heading rate $\dot{\psi}$=r. The first-order wave force f_1 and moment n_1 in (2.8) and (2.9) vary much rapidly compared to the dynamics of the ship and for control/observer design, they can be effectively modeled as white noise components. This is, however, not true for the interaction forces and moments Y(A,B) and N(A,B). These vary at approximately the same rate as the ship dynamics since they depend on the relative separation between the two ships. They are best modeled as colored noise components: the response of a first-order shaping filter driven by white noise

$$T_N\dot{N}=-N+W_N \tag{2.13}$$

$$T_Y\dot{Y}=-Y+W_Y \tag{2.14}$$

where the dimensionless time constants T_N and T_Y are equal to 1(i.e. the time that it takes to travel one ship length).

Collecting the above equations we get a seven order system in state space form. The control input is the commanded rudder angle δ_c and the augmented state vector contains the actual rudder angle δ, heading angle ψ, sway velocity v, yaw rate r, lateral separation distance y, and the two components of the interaction force Y and moment N. In a compact vector notation, the complete state space system is written as follows.

$$\dot{x}=Ax+B_1\delta_c+B_2w_1+B_3w_2 \tag{2.15}$$

where

$$x=\begin{bmatrix}\delta\\ \psi\\ v\\ r\\ y\\ N\\ Y\end{bmatrix} \tag{2.16}$$

$$w_1=\begin{bmatrix}W_N\\ W_Y\end{bmatrix} \tag{2.17}$$

$$W_2=\begin{bmatrix} n_1 \\ f_1 \end{bmatrix} \tag{2.18}$$

$$A=[a_{ij}],\quad i=1\sim 7;\ j=1\sim 7. \tag{2.19}$$

$$B_1=\begin{bmatrix} \frac{1}{\tau_r} \\ 0 \\ 0 \\ 0 \\ 0 \\ 0 \\ 0 \end{bmatrix} \tag{2.20}$$

$$B_2=\begin{bmatrix} 0 & 0 \\ 0 & 0 \\ 0 & 0 \\ 0 & 0 \\ 0 & 0 \\ 1 & 0 \\ 0 & 1 \end{bmatrix} \tag{2.21}$$

$$B_3=\begin{bmatrix} b_{11} & b_{12} \\ b_{21} & b_{22} \\ b_{31} & b_{32} \\ b_{41} & b_{42} \\ b_{51} & b_{52} \\ b_{61} & b_{62} \\ b_{71} & b_{72} \end{bmatrix} \tag{2.22}$$

$$a_{11} = -\frac{1}{\tau_r} \tag{2.23}$$

$$a_{24} = 1 \tag{2.24}$$

$$a_{31} = -\frac{Y_\delta (N_t - I_z) - N_\delta (Y_t - mX_G)}{(Y_{\dot{v}} - m)(N_t - I_z) - (Y_t - mX_G)(N_{\dot{v}} - mX_G)} \tag{2.25}$$

$$a_{33} = -\frac{Y_v (N_t - I_z) - N_v (Y_t - mX_G)}{(Y_{\dot{v}} - m)(N_t - I_z) - (Y_t - mX_G)(N_{\dot{v}} - mX_G)} \tag{2.26}$$

$$a_{34} = -\frac{(Y_r - mu)(N_t - I_z) - (Y_t - mX_G)(N_r - mX_G u)}{(Y_{\dot{v}} - m)(N_t - I_z) - (Y_{\dot{v}} - mX_G)(N_{\dot{v}} - mX_G)} \tag{2.27}$$

$$a_{36} = \frac{Y_t - mx_G}{(Y_{\dot{v}} - m)(N_t - I_z) - (Y_t - mX_G)(N_{\dot{v}} - mX_G)} \tag{2.28}$$

$$a_{37} = -\frac{N_t - I_z}{(Y_{\dot{v}} - m)(N_t - I_z) - (Y_t - mX_G)(N_{\dot{v}} - mX_G)} \tag{2.29}$$

$$a_{41} = -\frac{Y_\delta (N_{\dot{v}} - mX_G) - N_\delta (Y_{\dot{v}} - m)}{F4} \tag{2.30}$$

$$a_{43} = -\frac{Y_v (N_{\dot{v}} - mX_G) - N_v (Y_{\dot{v}} - m)}{F4} \tag{2.31}$$

$$a_{44} = \frac{(N_{\dot{v}} - mX_G)\ (Y_r - mu) - (N_r - mX_G u)\ (Y_{\dot{v}} - m)}{F4} \tag{2.32}$$

$$a_{46} = \frac{Y_{\dot{v}} - m}{F4} \tag{2.33}$$

$$a_{47} = -\frac{N_{\dot{r}} - I_z}{F4} \tag{2.34}$$

$$b_{31} = \frac{Y_{\dot{r}} - mX_G}{(Y_{\dot{v}} - m)\ (N_{\dot{r}} - I_z) - (Y_{\dot{r}} - mX_G)\ (N_{\dot{v}} - mX_G)} \tag{2.35}$$

$$b_{32} = -\frac{N_{\dot{r}} - I_z}{(Y_{\dot{v}} - m)\ (N_{\dot{r}} - I_z) - (Y_{\dot{r}} - mX_G)\ (N - \dot{v} - mX_G)} \tag{2.36}$$

$$b_{41} = \frac{Y_{\dot{v}} - m}{F4} \tag{2.37}$$

$$b_{42} = -\frac{N_{\dot{v}} - mX_G}{F4} \qquad (2.38)$$

$$F_4 = (N_{\dot{v}} - mX_G)\,(Y_t - mX_G) - (N_t - I_z)\,(Y_{\dot{v}} - m) \qquad (2.39)$$

a_{52}, a_{53} = 1,

a_{66}, a_{77} = -1,

τ_r = 0.2,

All other terms in the matrices are zero.

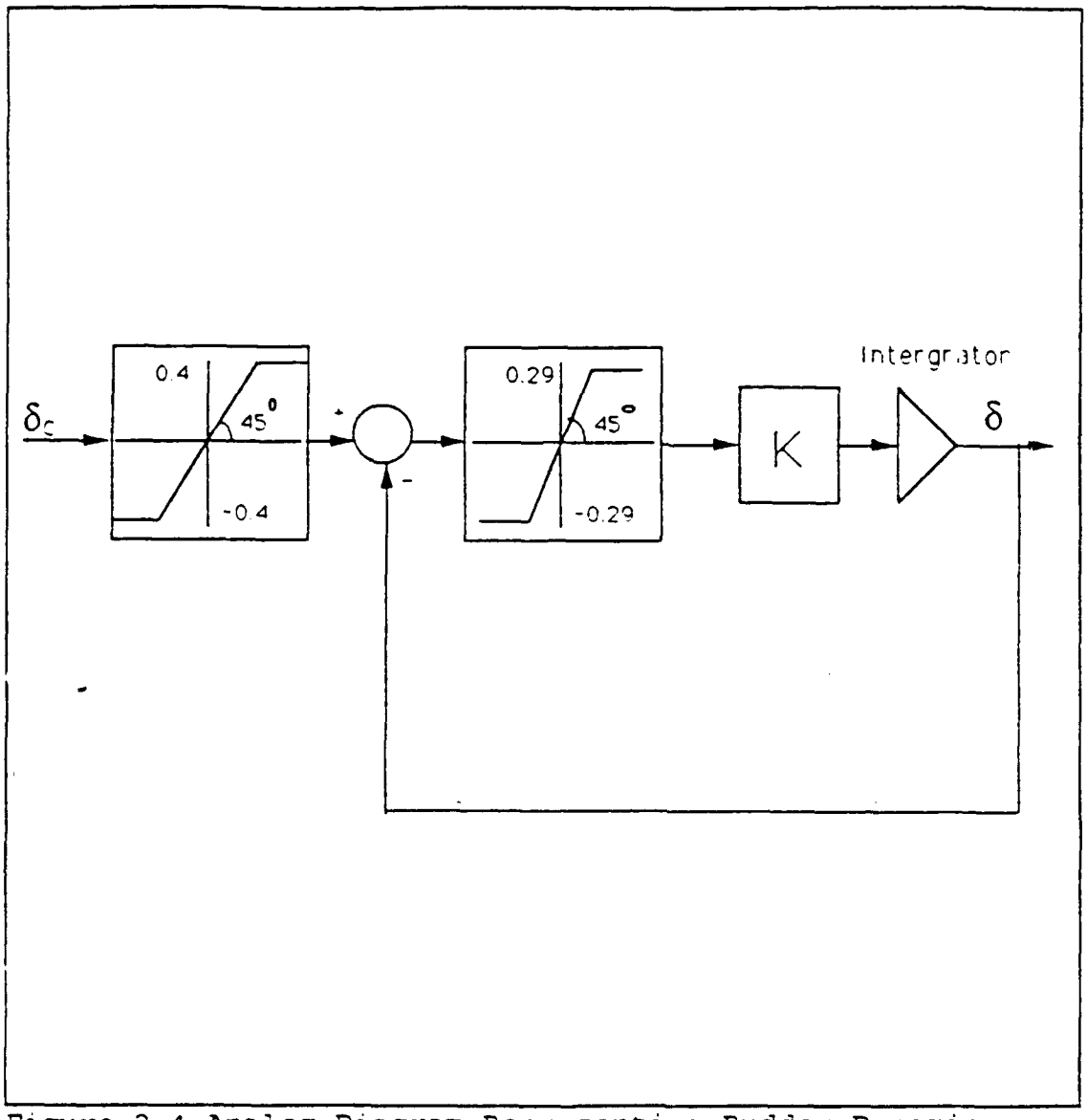

Figure 2.4 Analog Diagram Representing Rudder Dynamics

* Note:

Maximum rudder error signal ± 0.29 rad(17 degree).

K= 0.2/sec.

Maximum rudder rate 0.0698 rad/sec(3.5 deg/sec).

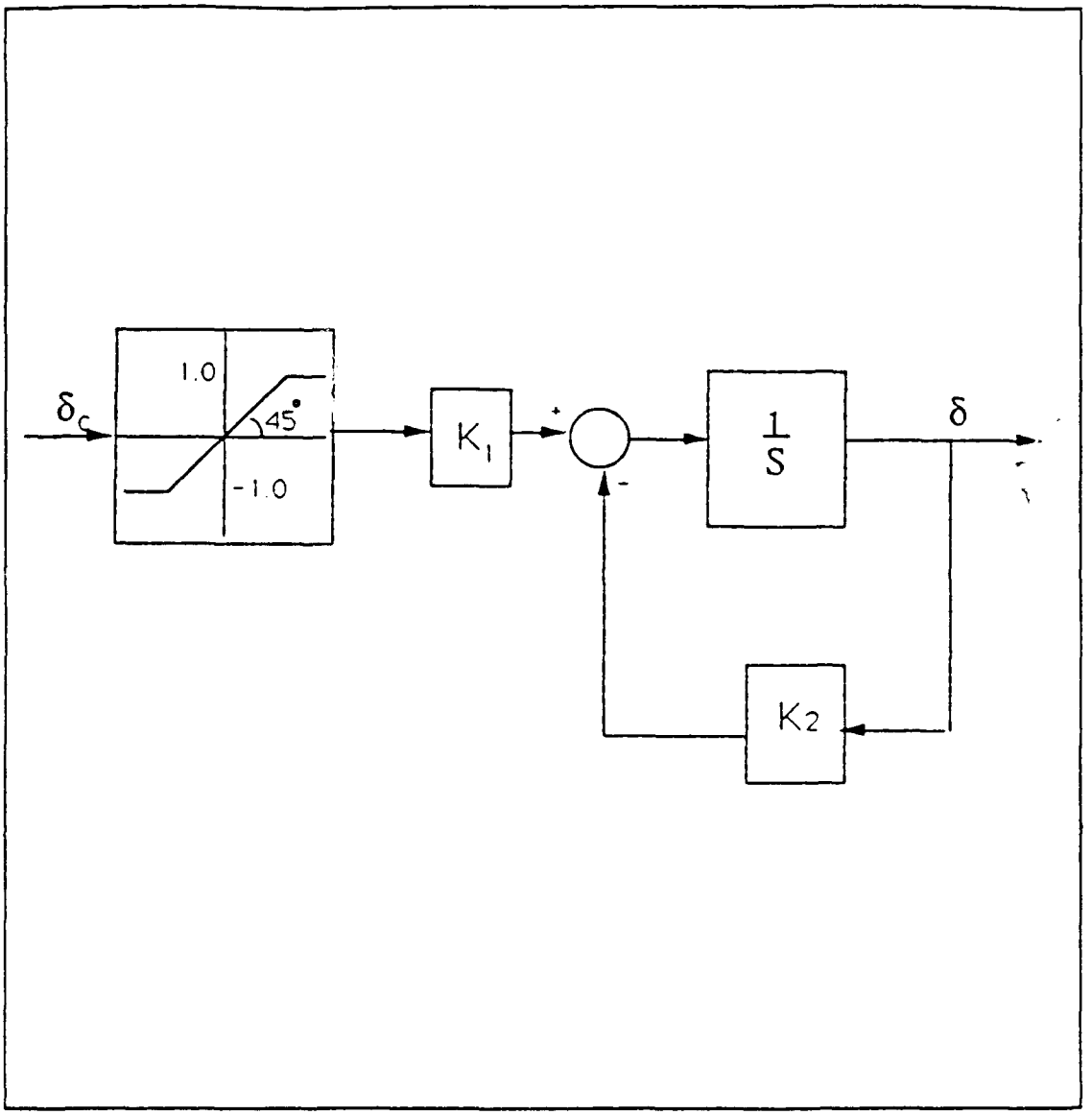

Figure 2.5 Equivalent First-order Lag Rudder Dynamics

* Note:

$K_1 = 1/\tau_r$.

$K_2 = 1/\tau_r$.

$\tau_r = 0.2$.

C. EXTERNAL FORCES AND MOMENTS

External disturbances that act on a ship during underway replenishment operations are due to several sources. First, the first order wave forces which are rapidly varying forces that depend on the seakeeping qualities of the ship and the particular seaway during operations. Slowly varying wave second order drift forces are important for long term moving and positioning operations while the same is true for current loads. On the other hand, of particular significance to the UNREP problem are the interaction forcesa and moments caused by the proximity of the two ships. For this reason we concentrate our efforts in the analysis on the control system performance of the two categories of forces: First order wave and interaction.

1. Interaction Force and Moment

These forces arise mainly due to changes in the flow field between two ships in proximity to one another and are modeled according to the data presented in [Ref.3] [Ref.8]. As shown in Figure 2.6 and Figure 2.7 these interaction forces are functions of both the longitudinal and lateral separation distances of the two ships. Furthermore, they are not of consistent signs which makes their effect on path keeping control especially troublesome. For simulation purposes the data of these two figures are used with bilinear interpolation

for the actual values of longitudinal and lateral ship to ship separation distances.

2. First-Order Irregular Wave Effects

The nondimensional first-order irregular sway force and yaw moment are functions of the regular wave encounter frequency. The Pierson-Moskowitz energy density spectrum is used here as a computer input to characterize the sea state. The nondimensional force and moment can be expressed as [Ref.8]

$$Y^1(t) = \int \cos(\omega_e t - \varepsilon_f(\omega_e)) \sqrt{2 S_x(\omega_e) |H_y(\omega_e)|^2} d\omega_e \qquad (2.40)$$

$$N^1(t) = \int \cos(\omega_e t - \varepsilon_m(\omega_e)) \sqrt{2 S_x(\omega_e) |H_n(\omega_e)|^2} d\omega_e \qquad (2.41)$$

where

$Y^1(t)$ is first-order irregular sway force.

$N^1(t)$ is first-order irregular yaw moment.

ω_e frequency of encounter.

$S_x(\omega_e)$ Pierson Moskowitz energy density spectrum.

$\varepsilon_f(\omega_e)$ phase angle for sway force.

$\varepsilon_m(\omega_e)$ phase angle for yaw moment.

$|H_y(\omega_e)|, |H_n(\omega_e)|$ the linear transfer functions at the frequency of encounter for the sway force excitation and yaw moment excitation.

$|H_y(\omega_e)|^2, |H_n(\omega_e)|^2$ are the response amplitude operators (RAO) for the sway force and moment at the frequency of encounter.

The data from Table 2.4[Ref.8] were used to determine the response amplitude operators and were nondimensionlized with respect to the series 60 model. For use with the maneuvering model of this thesis a futher nondimensionlization step is required.

For the nondimensional sway force:

$$H_y(\omega_e) = F(\omega_e) \times \frac{\frac{M_m g}{L_m}}{\frac{1}{2}\rho L_s^2 u^2} \quad (2.42)$$

For the nondimensional yaw moment:

$$H_n(\omega_e) = Y(\omega_e) \frac{M_m g \xi}{\frac{1}{2}\rho L_s^3 u^2} \quad (2.43)$$

where L_s is the mariner-type ship length.

L_m is the series 60 model length.

M_m is the displacement of series 60 model.

The frequency of encounter is function of the absolute wave frequency ω, the ship speed, the ship-to-wave angle θ, and the heading angle ψ, see Figure 2.8. The equation is

$$\omega_e = \omega - \frac{\omega^2}{g} u_1 \cos(\theta - \psi) \qquad (2.42)$$

The Pierson-Moskowitz Energy Density Spectrum $S_x(\omega)$ is used to characterize the sea state. This is calculated for a given significant wave height and for a fully developed, wind-driven sea. The characteristics of the wind speed and the corresponding significant wave height are shown in Table 2.2. A model for Pierson-Moskowitz Spectrum is

$$S_x(\omega) = \frac{\alpha g^2}{\omega^5} e^{\beta \left(\frac{g}{V\omega}\right)^4} \qquad (2.43)$$

where

α= 8.1 * 10^{-3}

β= -0.74

g= 32.174 ft/sec^2

ω= frequency of the wave in rad/sec

V= wind speed in ft/sec

The corresponding Pierson-Moskowitz Spectrum at the frequency of encounter is

$$S_x(\omega_e) = S_x(\omega) \left(1 - \frac{2\omega}{g} u \cos(\theta - \psi)\right)^{-1} \qquad (2.44)$$

Table 2.2 Characteristics of Series 60 Model

Length between perpendicular	5.0 ft(1.32 m)
Beam	0.667 ft(0.2 m)
Draft(even keel)	0.267 ft(0.08 m)
Displacement	33.27 lb(147.99 kg)
Block coefficient	0.6

Table 2.3 Characteristics of Wind-driven Sea States

Wind Speed (knots)	Sea State	Significant Wave Height	Average Period(sec)
10	2	0.6 m	2.7
20	4	2.2 m	5.3
30	6	5.0 m	8.0
40	7	8.9 m	10.7
50	8	13.9 m	13.4

Table 2.4 Nondimensional First-order Sway Force and Yaw Moment in Regular Wave

ω_e (rad/sec)	$F(\omega_e)$ = sway force /(Mgζ/L)	Sway force phase angle	$Y(\omega_e)$ =yaw moment/ (Mgζ)	Yaw moment phase angle
.293	1.3191	274	.07246	169
.361	1.9473	277	.03741	138
.433	2.5082	277	.08306	32
.509	2.9529	280	.22726	19
.588	3.2653	287	.42925	22
.679	3.3462	290	.6717	23
.756	3.0542	293	.89061	23
.845	2.364	294	.99661	26
.938	1.5397	293	1.0366	27
1.034	.6624	281	.9459	24
1.133	.21465	163	.73952	19
1.236	.73203	122	.47369	10
1.342	1.033	110	.19894	399
1.452	1.0222	101	.17588	242
1.565	.68012	87	.31972	211

M= Displaced mass

g= Acceleration of gravity

ζ= Wave amlpitude

L= Length detween perpendiculars

Table 2.5 Nondimensional Hydrodynamic Coefficients

Nondimensional Coefficients	Nondimensional Factors	Nondimensional Values (10^5)
Y_v	$\rho L^2 u$	-1243
Y_v-m	ρL^3	-1500
Y_r-m	$\rho L^3 u$	-510
$Y_{\dot{\delta}}$-mx_G	ρL^4	-27
Y_δ	$\rho L^2 u^2$	-270
N_v	$\rho L^3 u$	-351
N_r-mx_G	$\rho L^4 u$	-227
N_r-I_z	ρL^5	-68
$N_{\dot{\delta}}$	$\rho L^3 u^2$	-126
N_v	$\rho L^4 u$	-19.7

* Note :

1. The primes ' are neglected here but all coefficients are dimensionless values.
2. x_G= 0, L=length between perpendiculars.
3. u is the ship speed 15 knots, nondimensional value is 1.
4. ρ is the density of the sea water.

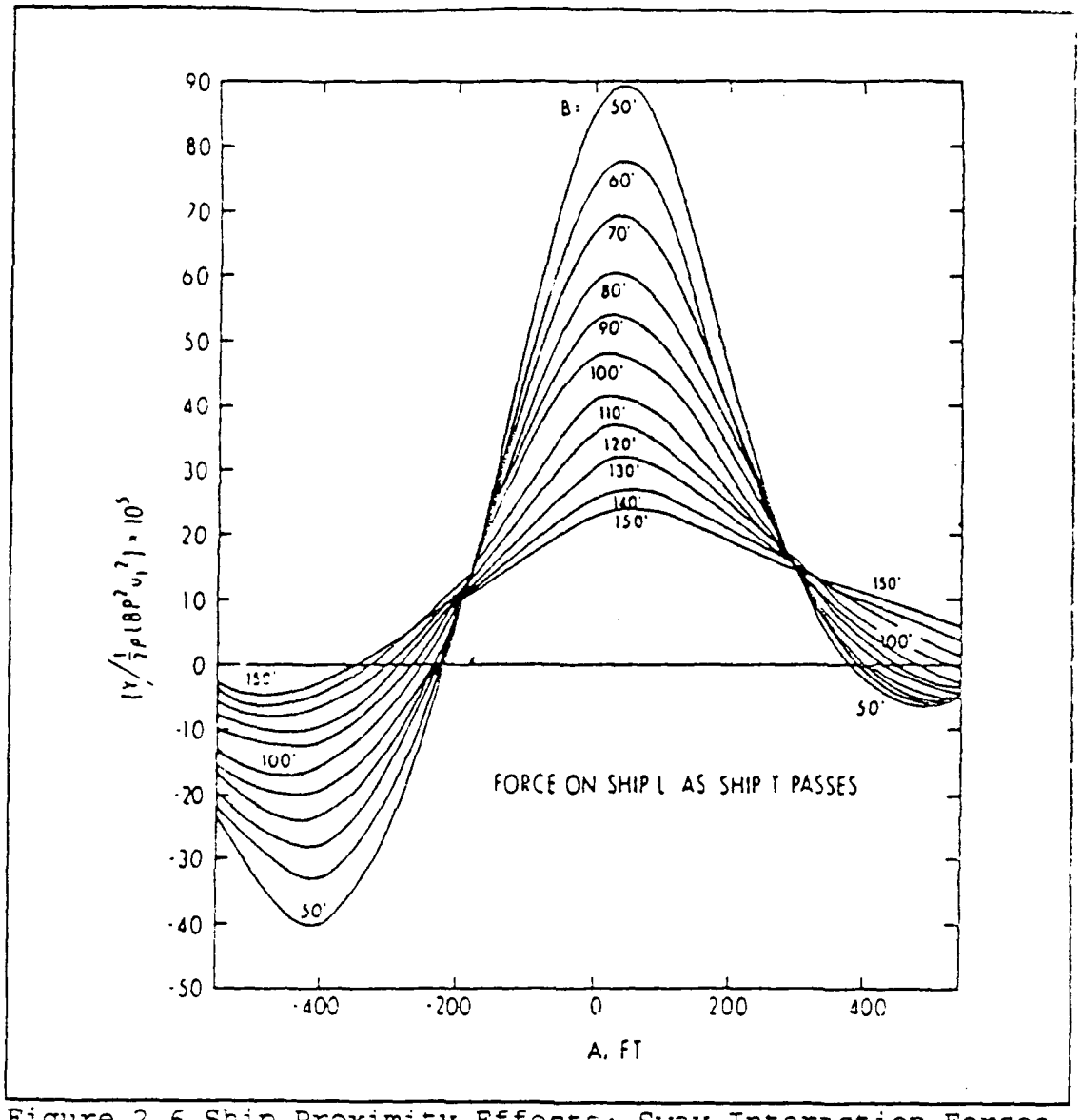

Figure 2.6 Ship Proximity Effects: Sway Interaction Forces.

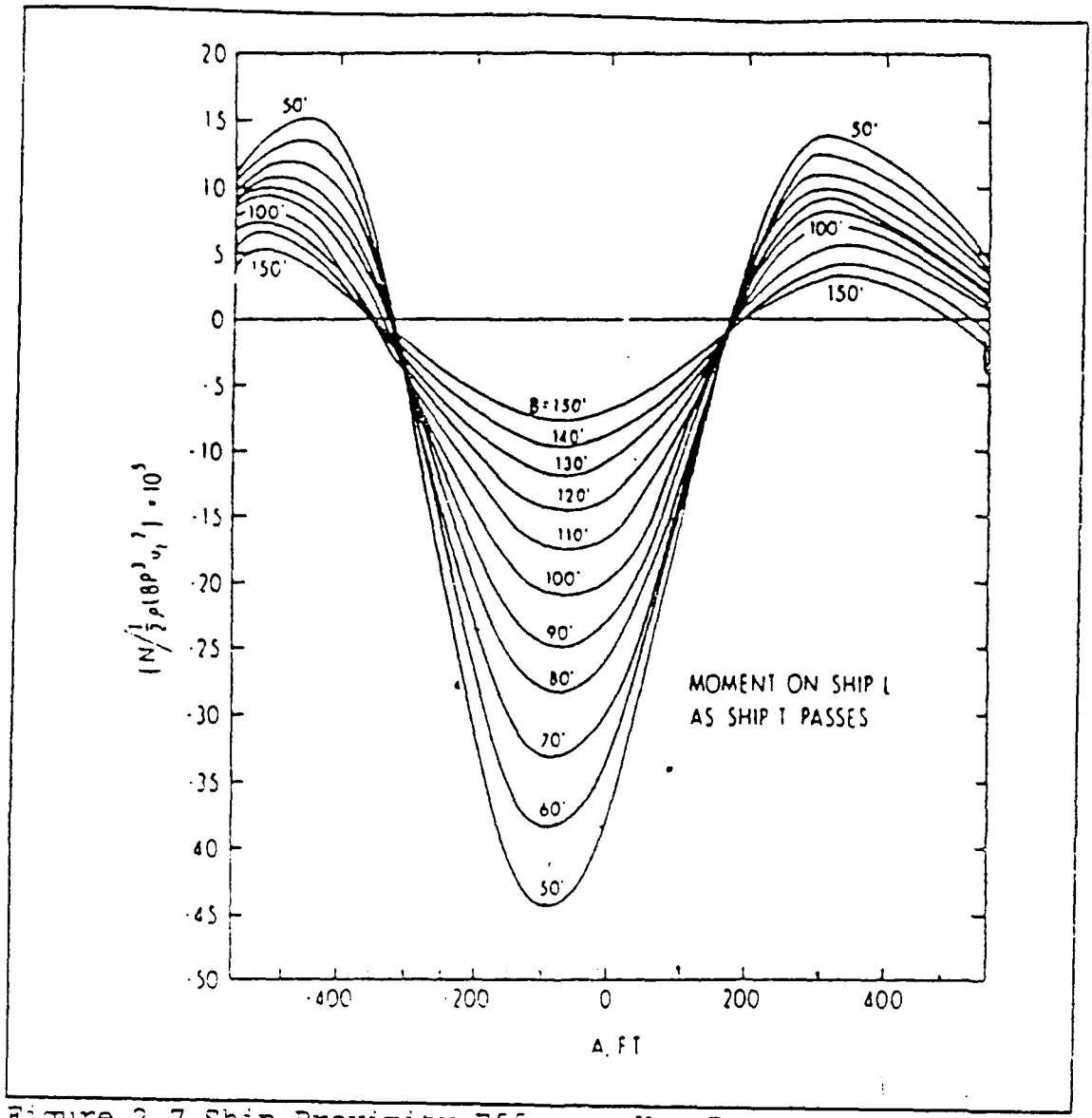

Figure 2.7 Ship Proximity Effects: Yaw Interaction Moments.

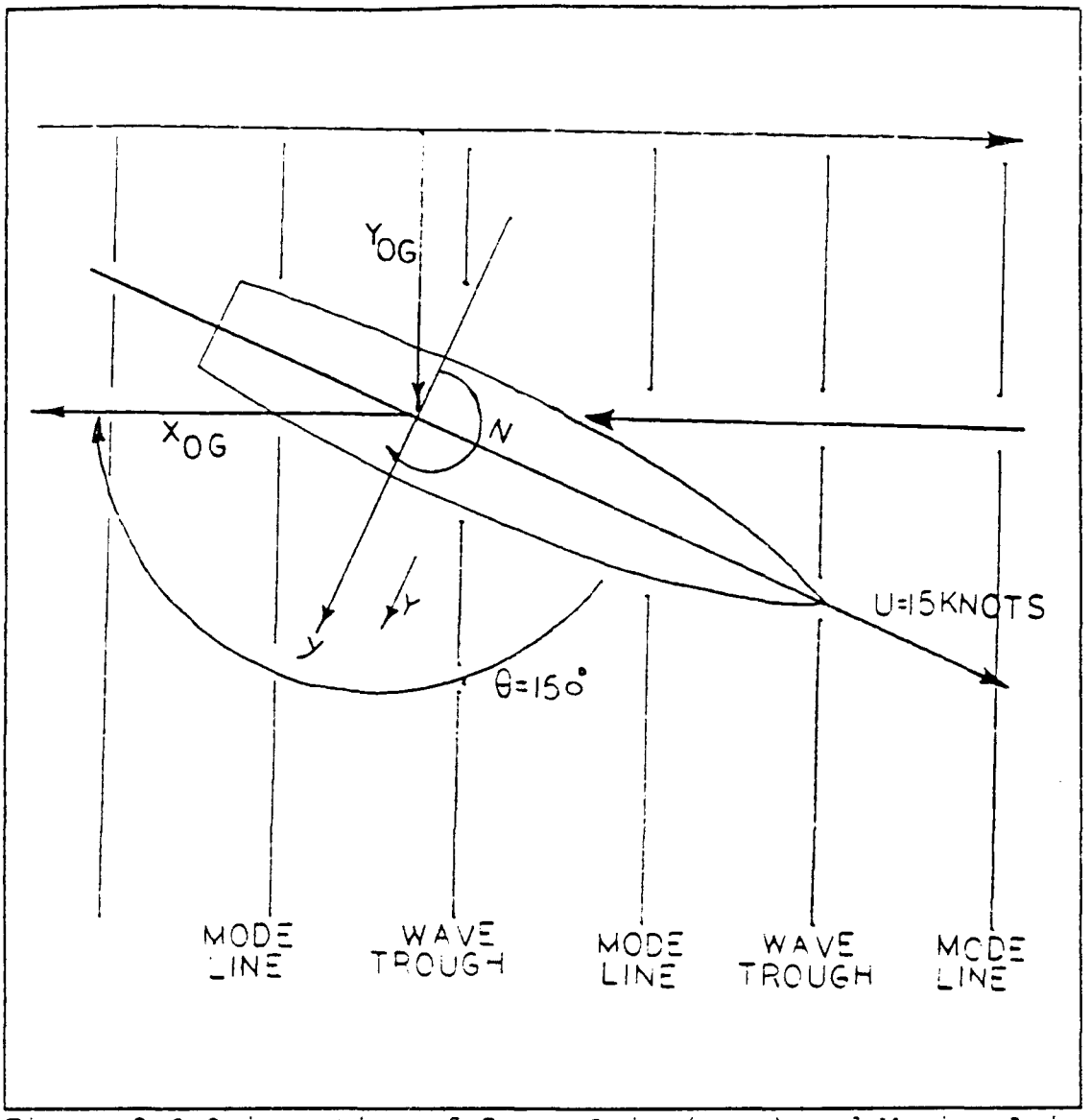

Figure 2.8 Orientation of Space Axis (x_0, y_0) and Moving Axis (x, y) for Series 60 Model in Oblique Regular Wave

III. CONTROL DESIGN

A. CONTROL METHODOLOGY

The method for conducting the Underway Replenishemnt at Sea maneuver requires the supply ship to maintain a fixed speed and heading. The conning officer of the receiving ship drives it alongside, and the measurement is the visual estimation of the relative distance from the seaman's eye. There are some basic measurement methods and sensor equipments which are utilized on the ship and can give very accurate distance measurement. The information can be fed into the computer which processes the data and automatically maneuvers the receiver ship to the desired position.

A fixed straight line and a zero point were used as the course and the center of gravity of the leading ship, and they are the references for driving the tracking ship to a position of 100 ft from this line, and from -524 ft to 524 ft with respect to this point. The controller is at the tracking ship (receiving ship). When the tracking ship approaches the leading ship (supply ship), the controller of the tracking ship will be aware of the excitation due to the interaction forces and moments from the leading ship. The dynamics of the tracking ship will converge to the sliding surface which is chosen in order to drive the ship to the desired position.

At the station keeping process, after the tracking ship and leading ship are alongside, a constant speed which is a normalized speed is considered for both ships. Also constant interaction forces and moments are exerted at this stage, which will cause a steady state error. Feedforward control is used for eliminating this error.

The feedforward control is mainly used for compensating the error of the ship lateral distance at steady state. The feedback control law is based on stability requirements, while the feedforward part is based on the desired steady state accuracy. Since the feedforward control is a function of the interaction force and moment, when the latter are zero, the former is also zero. Therefore, in general we can write

$$Control\ \ input(\delta_c) = Feedback\ \ Control(\delta_{fb}) + Feedforward\ \ Control(\delta_{ff})$$

During the control design stage the first-order wave force and moment and measurement noise are not considered, and perfect and complete state measurements are assumed. Then a kalman filter is designed for observing the unmeasurable states and the noise filter.

Figure 3.1 presents a block diagram of the optimal control design for the ship replenishment maneuver.

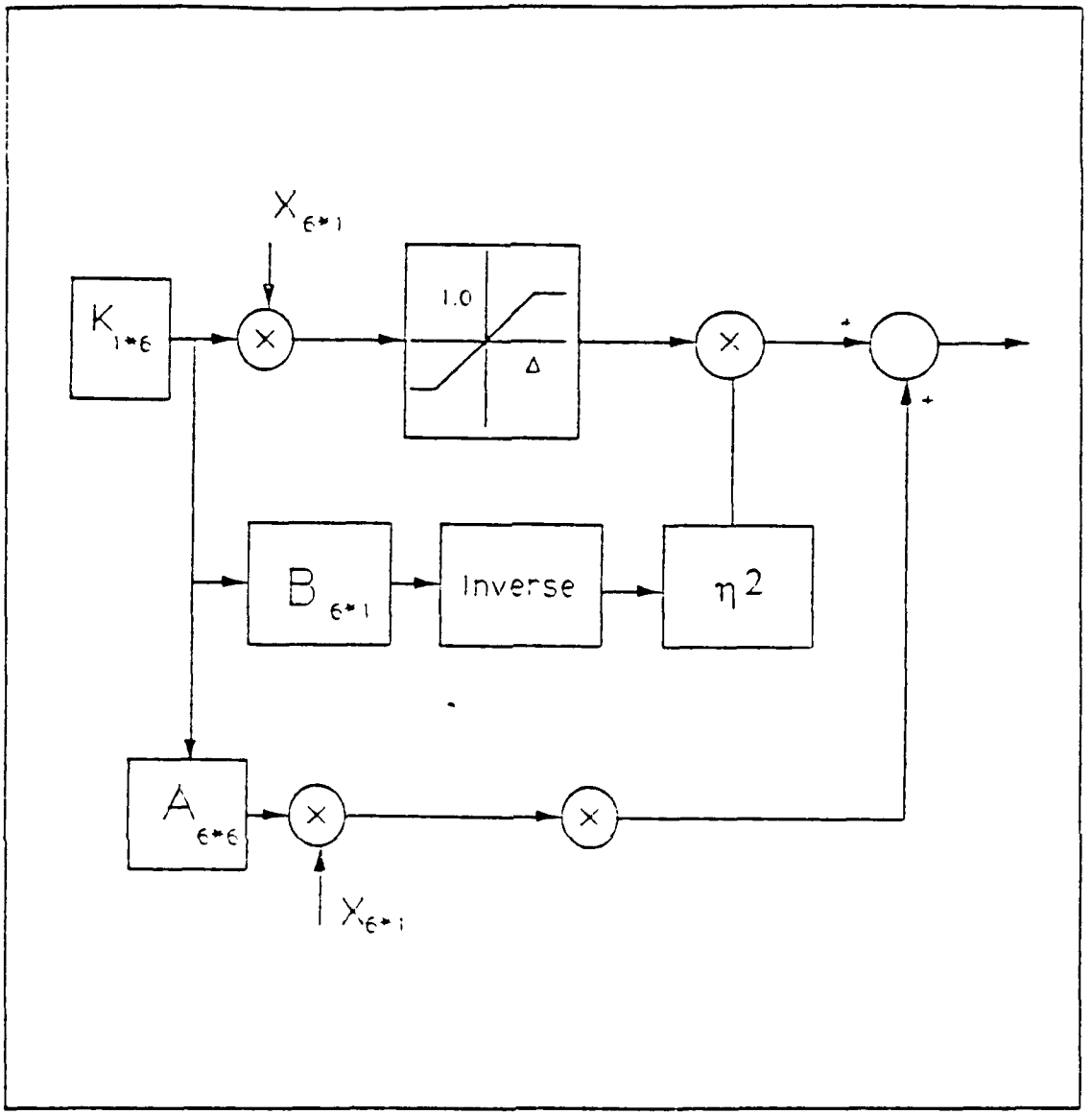

Figure 3.1 The Sliding Mode Control Design for Ship Replenishment at Sea

B. SLIDING SURFACE DESIGN FOR THE FEEDBACK CONTROL

1. Reduction of Order

In sliding mode control, the equivalent system must satisfy not only the n-dimensional state equations but also m-dimensional algebraic equations. This indicates that there exist only (n-m) indepedent equations on the sliding surface and m poles are located at the origin, where n is the number of states and m the number of control parameters(1 in our case) [Ref.10] [Ref.12].

Consider the state equation

$$\dot{x}=Ax+Bu \tag{3.1}$$

where states and matrices refer to the mathematical model described in Chapter II.

The first state equation of (3.1) describes the rudder dynamics;

$$\dot{\delta}=\frac{1}{\tau}\delta+\frac{1}{\tau}\delta_c \tag{3.2}$$

and the rest describe ψ, v, r, y, Y, and N.

The system of equations (3.1), (3.2) can be rewritten as:

$$\begin{bmatrix}\dot{x}_1\\ \dot{x}_2\end{bmatrix} = \begin{bmatrix}A_{11} & A_{12}\\ A_{21} & A_{22}\end{bmatrix}\begin{bmatrix}x_1\\ x_2\end{bmatrix}+\begin{bmatrix}B_{11}\\ B_{21}\end{bmatrix}u \qquad (3.3)$$

In this form

$\mathbf{x}_1 = [\delta]$.

$$x_2 = \begin{bmatrix}\psi\\ v\\ r\\ y\\ Y\\ N\end{bmatrix}. \qquad (3.4)$$

A_{11} = [1/τ] 1 by 1 matrix.

A_{12} = 0 1 by 6 matrix.

A_{21} = Equivalent control 6 by 1 matrix.

A_{22} = Equivalent state 6 by 6 matrix.

The linear switching surface parameters are

$K = [K_1\ K_2]$

The switching surface can be written as

$$\rho(x) = K_1x_1 + K_2x_2 \qquad (3.5)$$

where K_1 =1 and K_2 is a 1 by 6 matrix which is computed by the LQR method for the equivalent system as described later.

The equivalent control is based on the system

$$\dot{x}_2(t) = [I - A_{21}(K_2 A_{21})^{-1} K_2] A_{22} x_2(t) \tag{3.6}$$

$$x_2 = -K_2^{-1} K_1 x_1 \tag{3.7}$$

with x_2 viewed as the state and x_1 as the control input.

By substituting (3.6) into (3.7), the reduced order dynamics can be rewritten into the form:

$$\dot{x}_1 = [A_{11} - A_{12} K_2^{-1} K_1] x_1 \tag{3.8}$$

Having found $-K_2^{-1}K_1$ the switching surface and control law is completely defined.

2. LQR Method for Determination of the Sliding Surface

The control law design is based on the following: A 5 degree of rudder for path control is used when the heading deviates 5 degrees from zero or the ship reaches a lateral offset of 10.43 m (one quarter of beam). From the linear quadratic regulator theory the control should minimize the quadratic performance function:

$$J = \frac{1}{2} \int (x^T Q x + u^T R u)\, dt \tag{3.9}$$

where Q is a positive semidefinite matrix weighting on the states, and R is a positive definite control weight.

The two weights Q and R can be obtained from the criteria mentioned above and can be evaluated as follows:

Weighting on heading angle ψ:

$$q_{22}=(\frac{5}{57.3})^{-2}=131.332 \tag{3.10}$$

Weighting on side distance y:

$$q_{55}=(\frac{10.43}{290})^{-2}=772.463 \tag{3.11}$$

Weighting on rudder angle δ:

$$q_{11}=(\frac{5}{57.3})^{-2}=131.332 \tag{3.12}$$

Weighting on commanded rudder δ_c:

$$r_{11}=(\frac{5}{57.3})^{-2}=131.332 \tag{3.13}$$

The equivalent system is:

$$\dot{X}_2=A_{22}X_2+A_{21}X_1 \tag{3.14}$$

The Riccati equation is:

$$A_{22}^T K_2+K_2 A_{22}-K_2 A_{21} Q^{-1} A_{21}^T K+Q=0 \tag{3.15}$$

The equivalent control is then given by:

$$x_1 = -Q^{-1}A_{21}^T K_2 x_2 \qquad (3.16)$$

3. System Dynamics and Switches

a. Theory of Switching Control

Switching control has been successfully applied the nonlinear processes such as the "Bang-Bang" control and is widely used in optimal control. Systems with switched control law represent differential equations with discontinuous right hand side. A problem arises in that the conventional existence-uniqueness theory for ordinary differential equations is not valid. A discontinuous differential equation is defined on R^n as follows: [Ref.10] [Ref.11]

Let S be defined as $\{x:\rho(x)=0\}$, where ρ is a function from R^n to R, and S is (n-1) dimensional which represents the switching boundary. The switching dynamics are then defined:

$$\begin{cases} \dot{x}=f^+(x) : x=\rho(x) \geq 0 \\ \dot{x}=f^-(x) : x=\rho(x) \leq 0 \end{cases} \qquad (3.17)$$

where f^+ and f^- are smooth functions from R^n to R and are not matched on S so that the dynamics are discontinuous at S. The mechanism of the switches are operated as $\rho(x)$ changes sign which implies that the state trajectory passes through the surface and across it.

From the ideal switching law, existence of a sliding mode requires infinitely fast switching. But in actual systems imperfections exist in the facilities responsible to the switching control such as delay, hysteresis, saturation, etc., which force the switches with a finite frequency. The ideal switching can still be considered as long as the frequency of the switching is much higher than the dynamic response of the system. This regularization of the switching dynamics is schematically depicted Figure 3.2 and Figure 3.3.

The value ρ represents the switching variable: when $\rho \geq +1$, the dynamics are described by +r, and when $\rho \leq -1$, they are described by -r, where r is chosen as 1. A linear relation of x and $\rho(x)$ within this saturation region is described by the switching function.

Existence of the sliding mode requires stability of the state trajectory to the sliding surface $\rho(x)=0$ and asymptotic stablility within the region of attraction which is the region between $+\Delta$ and $-\Delta$.

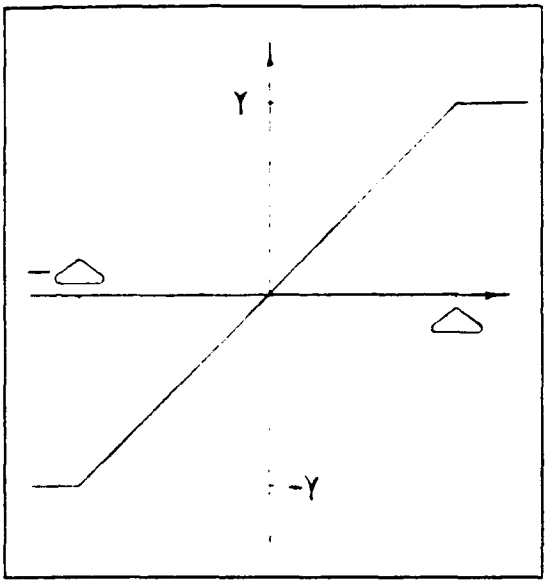

Figure 3.2 Saturation Switch

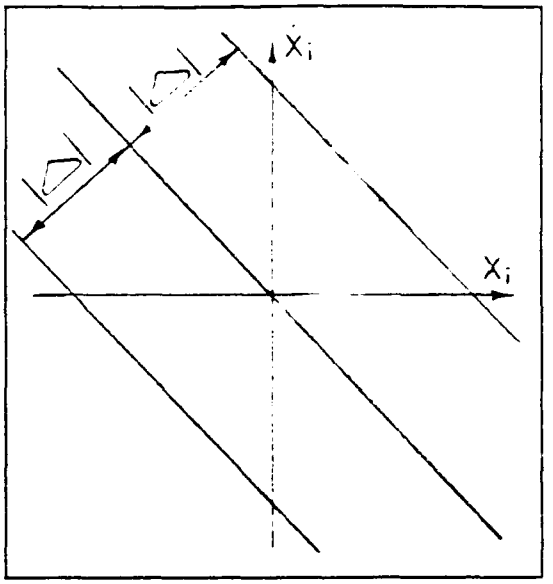

Figure 3.3 Effects of the boundary Layer Regulation

b. The Lyapunov Function

The second method of Lyapunov provides a characteristic function for analyzing the existence of the sliding mode. The Lyapunov function $v(t,x,\rho)$ is continuously differentiable with respect to all of its variabless and satisfies the following conditions: [Ref.12]

- $v(t,x,\rho)$ is positive definite with respect to ρ.
- The total time derivative of $v(t,x,\rho)$ for the system has a negative supremum for all $x\epsilon\Omega$ except for x on the switching surface where the control inputs are undefined.

The structure of the function $v(t,x,\rho)$ is determined by the ease which one can compute the switching parameters, such as pole placement, Root locus, LQR, or other

state space control theory, for application of variable structure control design. For all single input system a suitable Lyapunov function is $v(t,x) = 0.5\rho^2(x)$, which is a function of ρ depending on the control and has a negative derivative function with respect to time

$$\frac{1}{2}\frac{d\rho^2}{dt} = \rho\frac{d\rho}{dt} < 0 \qquad (3.18)$$

In the domain of attraction the state trajectory converges to the surface and is restricted to the surface for all subsequent times. The feedback gains associated with the optimal design are computed from Linear Quadratic Regulator theory. The weighting matrices for control and state associated with the cost function are obtained from (3.10) to (3.13).

4. Feedback Control Law

The method of determination of the switching surface $\rho(x)=0$ is by Lyapunov function. The stability function guarantees that a sliding mode exist at every $t \geq t_0$, where t_0 is the time when the state trajectory intercepts the surface.

The existence of the sliding mode implies that:

- $d\rho(x)/dt < 0$.
- $\rho(x)=Kx =0$, where the K is the surface parameters (feedback gains), and x is the state vector.

From the chain rule

$$\dot{\rho}(x) = \frac{d\rho}{dx}\dot{x} = K\dot{x} < 0 \tag{3.19}$$

we substitute the constraint equation

$$\dot{x} = Ax + Bu \tag{3.20}$$

and the definition

$$\dot{\rho} = -\eta^2 sign(\rho(x)) \tag{3.21}$$

where η is the weighting for the switching structure. This form guarantees the existence of a sliding mode and will operate as the sign of the state trajectory changes.

Combining (3.19), (3.20) and (3.21)

$$\frac{d\rho(x)}{dx}\dot{x} = -\eta^2 sign(\rho(x)) \tag{3.22}$$

where $d\rho(x)/dx = K$ and substituting (3.22), then the control law is written as

$$u = -\left(\frac{d\rho(x)}{dx}B\right)^{-1}\frac{d\rho(x)}{dx}Ax - \left(\frac{d\rho(x)}{dx}B\right)^{-1}\eta^2 sign(\rho(x)) \tag{3.23}$$

There are two parts in this feedback control. They are a feedback structure term for the first part, and the second part is for the switching structure.

In general the steps for the control design are:

- Determining the reduced order dynamical equations governing the system motion on the switching surface.
- Choosing the switching surface parameters K for a linear switching surface $\rho(x)=0$, so that the system is stable in the sliding surface that has been chosen.
- Augmenting the control law.

5. Switching Surface Design

Generally, the stability of the closed loop system depends on the design of the switching surface. The design of the switching surface depends on the choice of the surface parameters and the dynamics of the system equation.

The switching surfaces are designed such that the state trajectory is restricted to $\rho(x)=0$, and that stability is guaranteed.

Again from the reduced order dynamics the state equation can be written as:

$$\begin{aligned} \dot{x}_1 &= A_{11}x_1 + A_{12}x_2 + B_{11}u \\ \dot{x}_2 &= A_{21}x_1 + A_{22}x_2 + B_{21}u \end{aligned} \qquad (3.24)$$

The rudder dynamics, first equation of (3.3), will be responsible for the control phase of the second equation of (3.3), which has an order n-1. The equivalent control gives the equivalent system in the form

$$\dot{x}_2 = A_{22}x_2 + A_{21}x_1 \tag{3.25}$$

where

x_2 is the (n-1)th-order equivalent state vector.

x_1 is the 1st-order equivalent control input.

A_{22} is the equivalent state matrix (n-1) by (n-1) matrix.

A_{21} is the equivalent control matrix (n-m) by m matrix.

The gain K_2 results by minimizing the cost function

$$J_2 = \int_{-\infty}^{\infty} [x_2^T Q_2 x_2 + x_1^T R_2 x_1]\, dt \tag{3.26}$$

where

$$R_2 = [q_{11}^2] \tag{3.27}$$

$$Q_2 = diag(|q_{22}^2 \;\; 0 \;\; 0 \;\; q_{55}^2 \;\; 0 \;\; 0|) \tag{3.28}$$

The weighting factors are as indicated by (3.10), (3.11), and (3.12), (3.13).

Since (A_{21},A_{22}) is controllable, it is possible to effectively use classical feedback control techniques to compute a K_2 and K_1 such that $(A_{22}+A_{21}K_1^{-1}K_2)$ has the desired characteristics. Having found $[K_1\ K_2]$, the linear switching surface is:

$$[K_1 \quad K_2]x=0. \tag{3.29}$$

C. SLIDING SURFACE DESIGN FOR FEEDFORWARD CONTROL

1. Introduction

There are two types of disturbances that were considered in this thesis. These are time varying low frequency disturbances at passing process, and constant disturbances at station keeping process.

A steady state error in the station keeping process indicates that feedback control is not enough. The compensation is achieved by feedforward control.

The design objective is to eliminate the steady state error. Prediction of disturbance and cancellation process is done by the feedforward control generated at time t. The disturbances were assumed to be the same at one time step before $(t-\Delta t)$ and one time after $(t+\Delta t)$

$$\begin{aligned} \Delta Y &= Y(t+\Delta t) - Y(t) \\ \Delta N &= N(t+\Delta t) - N(t) \end{aligned} \tag{3.30}$$

And

$$\begin{aligned} \Delta Y &= Y(t) - Y(t-\Delta t) \\ \Delta N &= N(t) - N(t-\Delta t) \end{aligned} \tag{3.31}$$

By the assumption that Δt is small and we have slowly varying interaction forces and moments as the tracking ship passes the leading ship. The differences will approach to zero

$$\begin{cases} \lim_{\Delta t \to 0} \Delta Y = 0 \\ \lim_{\Delta t \to 0} \Delta N = 0 \end{cases} \tag{3.32}$$

2. The Feedforward Control Law

The steady state Conditions are:

$$\begin{aligned} &\dot{r} = 0 \\ &\psi = 0 \Rightarrow r = 0 \\ &\dot{y} = 0 \Rightarrow \psi = -r \\ &\delta = 0 \Rightarrow \delta = \delta_c \\ &\dot{v} = 0 \end{aligned} \tag{3.33}$$

The separation distance is assumed to be y=0, which is the desired position in which the tracking ship will be located.

We substitute (3.33) into the state equations and we get

$$a_1\delta + b_1 v = c_1 \tag{3.34}$$

$$a_2\delta + b_2 v = c_2 \tag{3.35}$$

where

$$a_1 = Y_\delta (N_{\dot{v}} - mX_G) - N_\delta (Y_{\dot{v}} - m) \tag{3.36}$$

$$b_1 = Y_v (N_{\dot{v}} - mX_G) - N_v (Y_{\dot{v}} - m) \tag{3.37}$$

$$c_1 = -(Y + f_1)(N_{\dot{v}} - mX_G) + (Y_{\dot{v}} - m)(N + n_1) \tag{3.38}$$

$$a_2 = Y_\delta (N_t - I_z) - N_\delta (Y_t - mX_G) \tag{3.39}$$

$$b_2 = Y_v (N_t - I_z) - N_v (Y_{\dot{v}} - mX_G) \tag{3.40}$$

$$c_2 = -(N_t - I_z)(Y + f_1) + (Y_t - mX_G)(N + n_1) \tag{3.41}$$

Simultaneous solutions of (3.34) and (3.35), provide the state variables at steady state. The results are:

$$\delta_s = \frac{(c_1 \times b_2) - (c_2 \times b_1)}{(a_1 \times b_2) - (a_2 \times b_1)} \tag{3.42}$$

$$v_s = \frac{(c_1 \times a_2) - (c_2 \times a_1)}{(b_1 \times a_2) - (b_2 \times a_1)} \tag{3.43}$$

$$\psi_s = -v_s \tag{3.44}$$

The results of these algebraic equations provide the amount of the control needed.

3. Switching Surface Design For Feedforward Control

As mentioned above rudder angle, heading angle, and lateral separation rate are depend on the interaction forces and moments at steady state. If constant disturbances act on the ship then these three states will not go to zero and a steady state error will be presented. An appropriate compensation input will be found to eliminate this error. The steady state switching surface is:

$$\rho_s(x) = K_1 \delta_s + K_{11} \psi_s + K_{12} v_s + K_{15} N + K_{16} Y \tag{3.45}$$

4. Augment of Automatic Control Law

A subsliding surface was designed for this feedforward control input. (An subscript s indicates that the states are for feedforward calculation)

Substitute the feedforward control switching surface (3.45) into the control law and augment the reference input as

$$\delta_r = -(KB)^{-1}KAx_s - (KB)^{-1}\eta^2 sign(\rho_s) \qquad (3.46)$$

where

δ_r is the feedforward control rudder input.

ρ_s is the switching surface for feedforward control at steady state condition.

η is the weighting factor for switching control.

$$x_s = \begin{bmatrix} \delta_s \\ \psi_s \\ V_s \\ 0 \\ 0 \\ N \\ Y \end{bmatrix} \qquad (3.47)$$

x_s is the state vector at steady state.

The augmented control law for tracking design is completed and the schematic block diagram is shown in Figure 3.4.

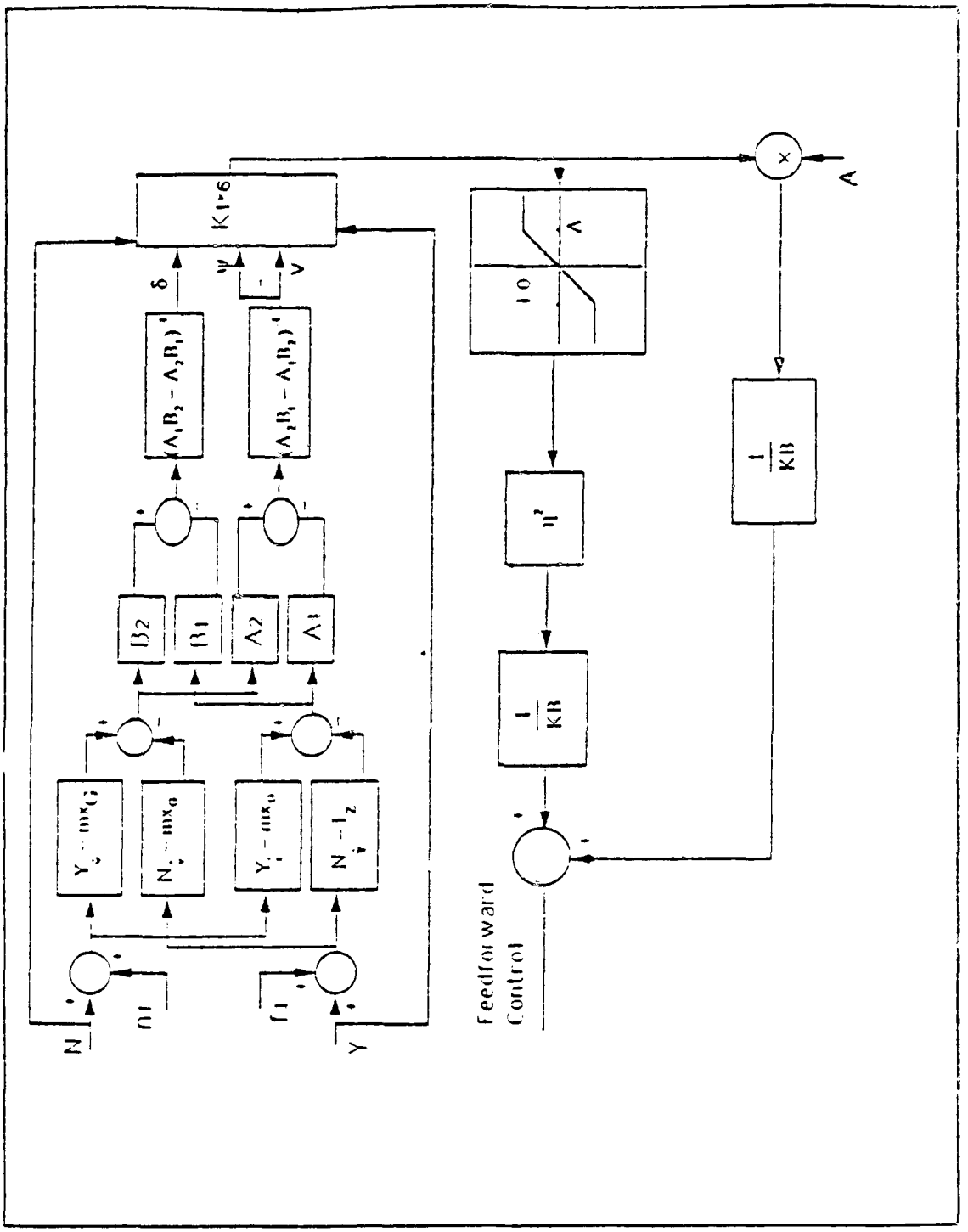

Figure 3.4 The Configuration of the Feedforward Control

* Note for Fig 3.4:

$$B_1 = (N_{\dot{v}} - mx_G)\, Y_v - (Y_{\dot{v}} - m)\, N_v \qquad (3.48)$$

$$B_2 = (N_{\dot{r}} - I_z)\, Y_v - (Y_{\dot{v}} - mx_G)\, N_v \qquad (3.49)$$

$$A_1 = (N_{\dot{v}} - mx_G)\, Y_\delta - (Y_{\dot{v}} - m)\, N_\delta \qquad (3.50)$$

$$A_2 = (N_{\dot{r}} - I_z)\, Y_\delta - (Y_{\dot{r}} - mx_G)\, N_\delta \qquad (3.51)$$

f_1, n_1 : 1st-order wave force and moment.

N, Y : Interaction forces and moments.

5. Simulation at Calm Sea

a. Introduction

Fortran Program SHIP4QQ.FOR(see Appendix B) was used to simulate the UNREP in the horizontal plane using controller designed by LQR. Simulation is performed with a perfect and full state feedback at this stage. Interaction forces and moments are calculated by the bilinear rule. The surge velocity is simulated as 15 knots. The time step is .005 dimensionless seconds which corresponds to 10 Hz sampling rate. Two data files TABLE1.DAT and TABLE2.DAT contained the data points from Figure 2.6 and Figure 2.7.

b. Simulation Condition Specification

Two types of ship maneuvering processes are considered in this control test. These are the passing maneuver and the station keeping process. The passing maneuver is a process in which the tracking ship is passing the leading ship at constant speed while keeping a desired course. The station keeping process is a process in which interaction forces and moments are constant after both ships are driven alongside, where the same course and speed for the leading and tracking ship are maintained at this stage.

In this chapter, the sea state is considered as a calm sea. Perfect measurements from the sensors are assumed. The initial conditions for the tracking ship are specified as:

- One normalized separation distance, $y(0)=1$.

- Initial heading angle 5 degrees, $\psi(0)=.087$ rad.
- Simulation starts at -4000 ft longitudinal distance, and ends at 8000 ft.
- The leading ship travels twice as fast as the tracking ship during the passing process.

The weighting factor η in the switching structure of the feedback control dominates the sensitivity of the control law, the stability of the state trajectory in the zone of the attraction, and the capability of the design to remain stable under external disturbances. Too small a value indicates that the system may be slow or even unstable, too high a value may cause a chattering problem. The chattering problem will not be discussed here[Ref.14][Ref.12].

D. SIMULATION RESULTS AT CALM SEA

1. Passing Process, η=1, Δ=0.12

Results for this case are presented in Figure 3.4. The four graphs in this and all similar figures show clockwise from the upper left corner the interaction force and moment, the actual rudder angle, the tracking ship lateral deviation from the desired position(100 ft), and the ship heading in radians. All variables are presented versus the ship-to-ship longitudinal separation with 0 corresponding to the two ships alongside. It can be seen from the figure that the control objectives are met. The effect of the interaction forces is evident by the rudder activity at about 0 ft longitudinal distance.

2. Passing Process, η=1, Δ=0.06

The effects of reducing the boundary layer thickness are shown in Figure 3.5. The results are virtually identical to those of Figure 3.4 which means that for the above range of variation, Δ has no significant effect. It should be mentioned, though, that this is true under the current assumptions of calm sea and perfect feedback, and it may no longer be the case under the general conditions studied in the next chapter.

3. Passing Process, η=8, Δ=0.12

The effects of increasing the switching gain η are shown in Figure 3.6. In order to demonstrate this effect, the commanded rudder angle is presented instead of the interaction forces. It can be clearly seen that increasing η results in more control chattering and increased overshoot of the commanded path. Both of these are operationally dangerous and should be avoided in practice.

4. Passing Process, η=0.5, Δ=0.12

The effects of reducing the value of the switching gain are shown in Figure 3.7. The control response is now very sluggish and the objectives of the underway replenishment maneuver are not met.

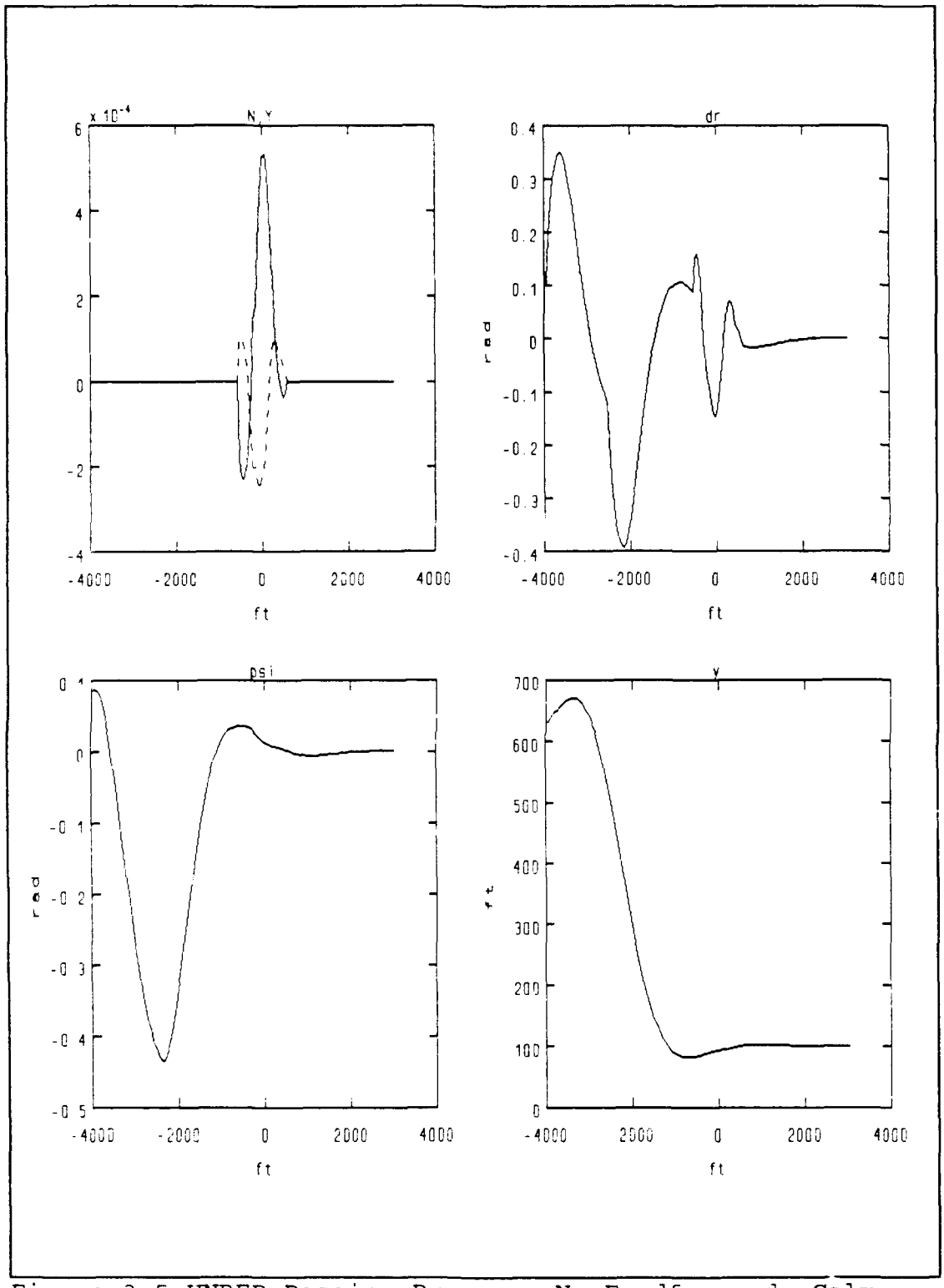

Figure 3.5 UNREP Passing Process, No Feedforward, Calm Sea(Prefect Feedback, η=1, Δ=0.12)

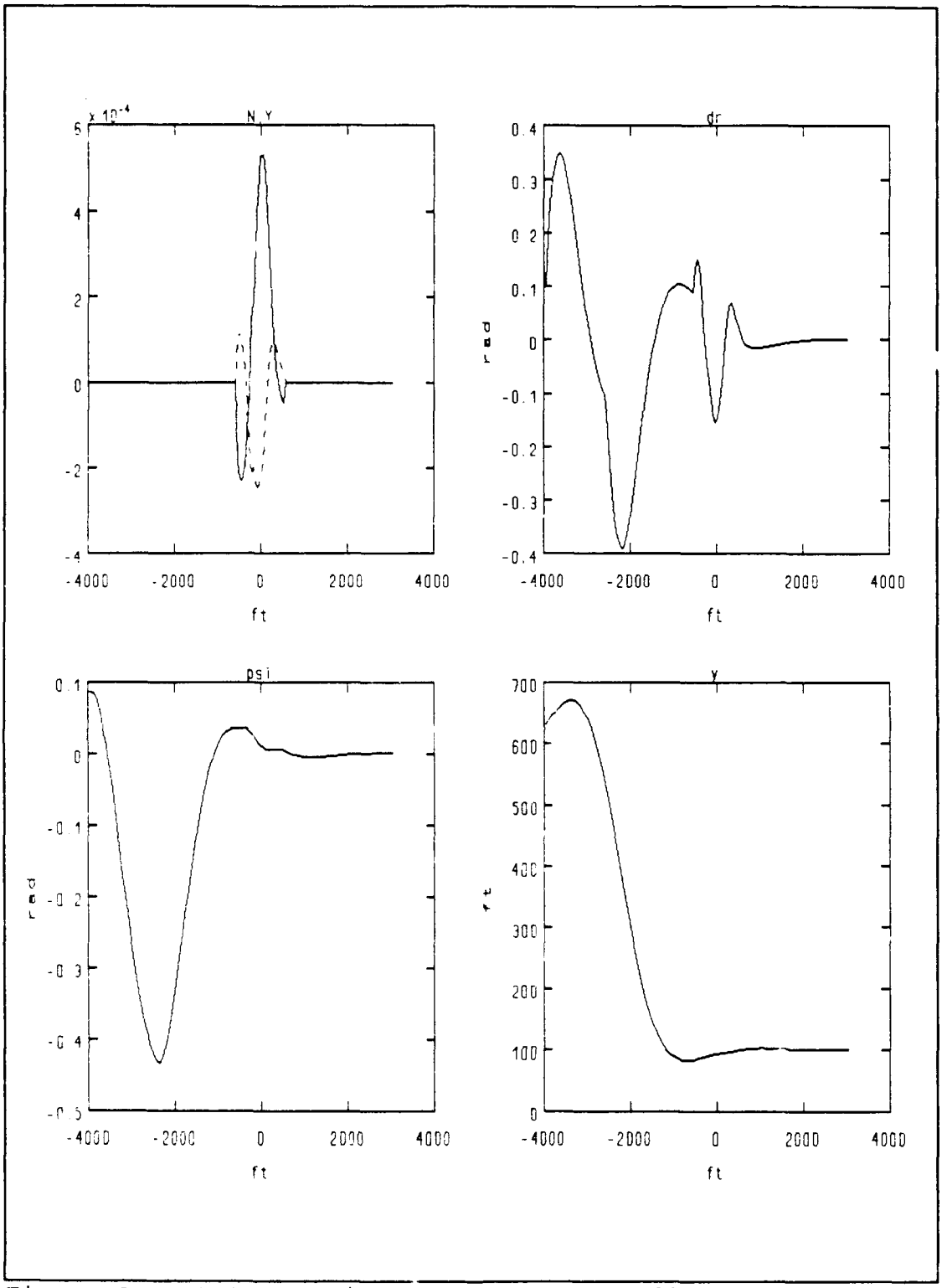

Figure 3.5 UNREP Passing Process, No Feedforward, Calm Sea(Perfect Feedback, η=1, Δ=0.06)

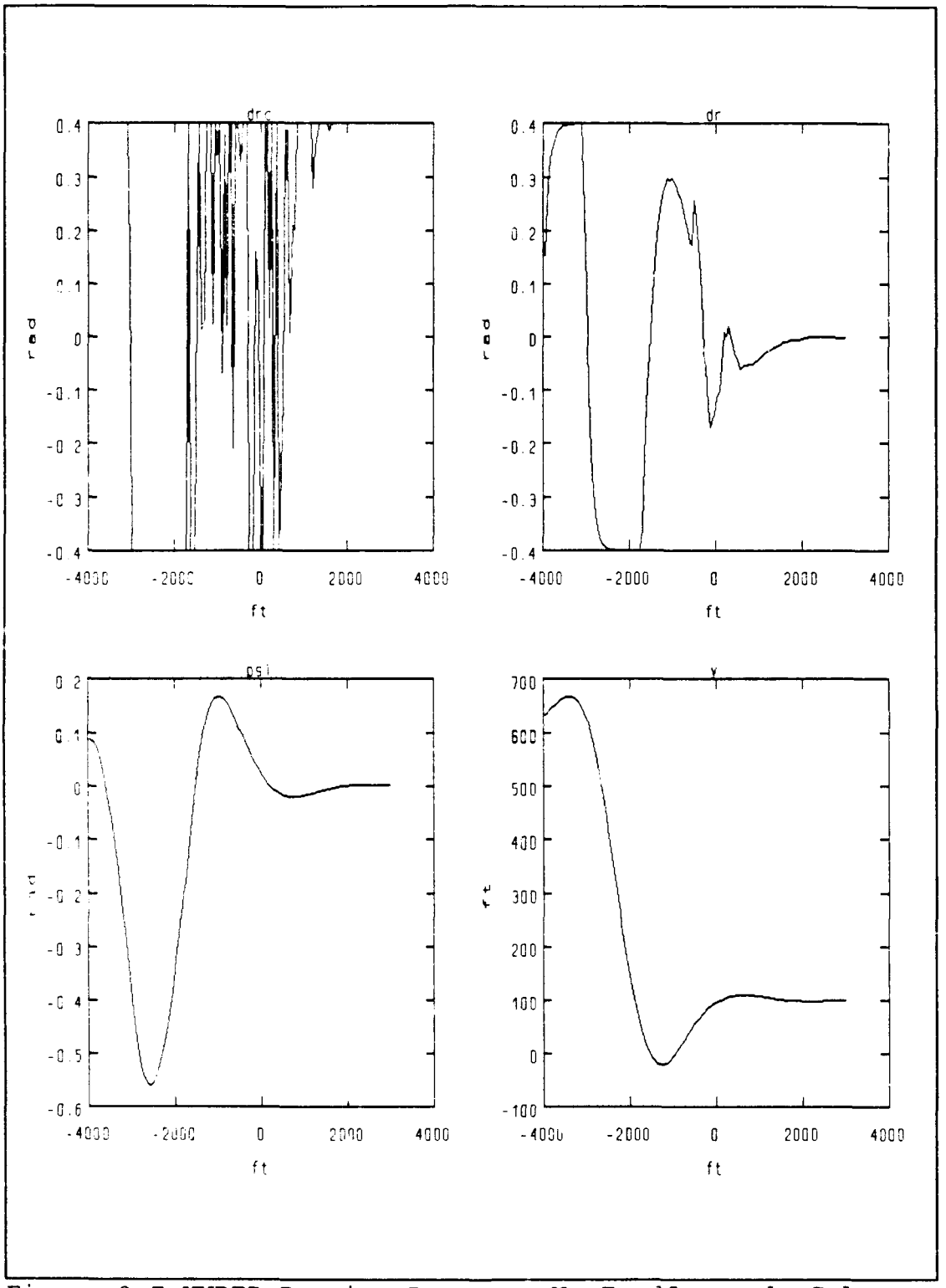

Figure 3.7 UNREP Passing Process, No Feedforward, Calm Sea(Perfect Feedback, η=8, Δ=0.12)

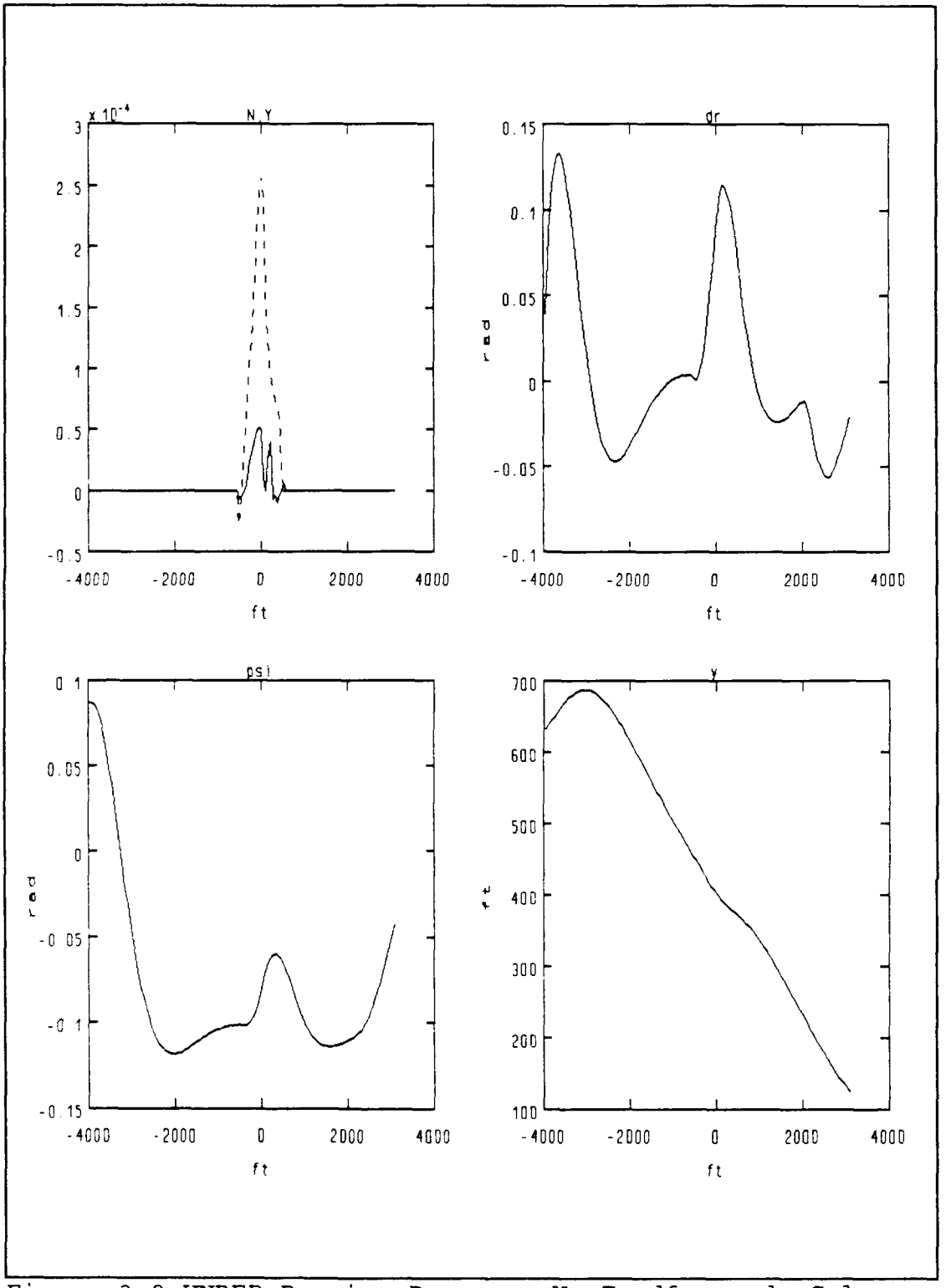

Figure 3.8 UNREP Passing Process, No Feedforward, Calm Sea(Perfect Feedback, η=0.5, Δ=0.12)

5. Station Keeping Process, η=1, Δ=0.12, No Feedforward

During the station keeping process where the two ships travel alongside for some time, constant interaction force and moment will develop, see Figure 3.8. As a result in the absence of the feedforward term, a nonzero steady state error will be present. Although the feedback control stabilizes the system, it cannot ensure the required steady state accuracy.

6. Passing Process, η=1, Δ=0.12

The simulations that follow include the feedforward term in the control lawas developed previously. The results are shown in Figure 3.9. Comparing these to Figure 3.4. where feedforward was not included we can see that for the passing process the effects of the feedforward term are very small except for the increased rudder action at 0 ft longitudinal position, as expected.

7. Passing Process, η=4, Δ=0.06

As seem from Figure 3.10 increasing $\eta$and decreasing Δ results in more path accuracy and increased control activity. The tighter control law in this case helps however during the station keeping process in the following two figures.

8. Station Keeping Process, η=1, Δ=0.12

The effect that the feedforward term has on path accuracy is evident by comparing the results of this simulation Figure 3.11, with those at the no feedforward case, Figure 3.8. Although the transient response during the

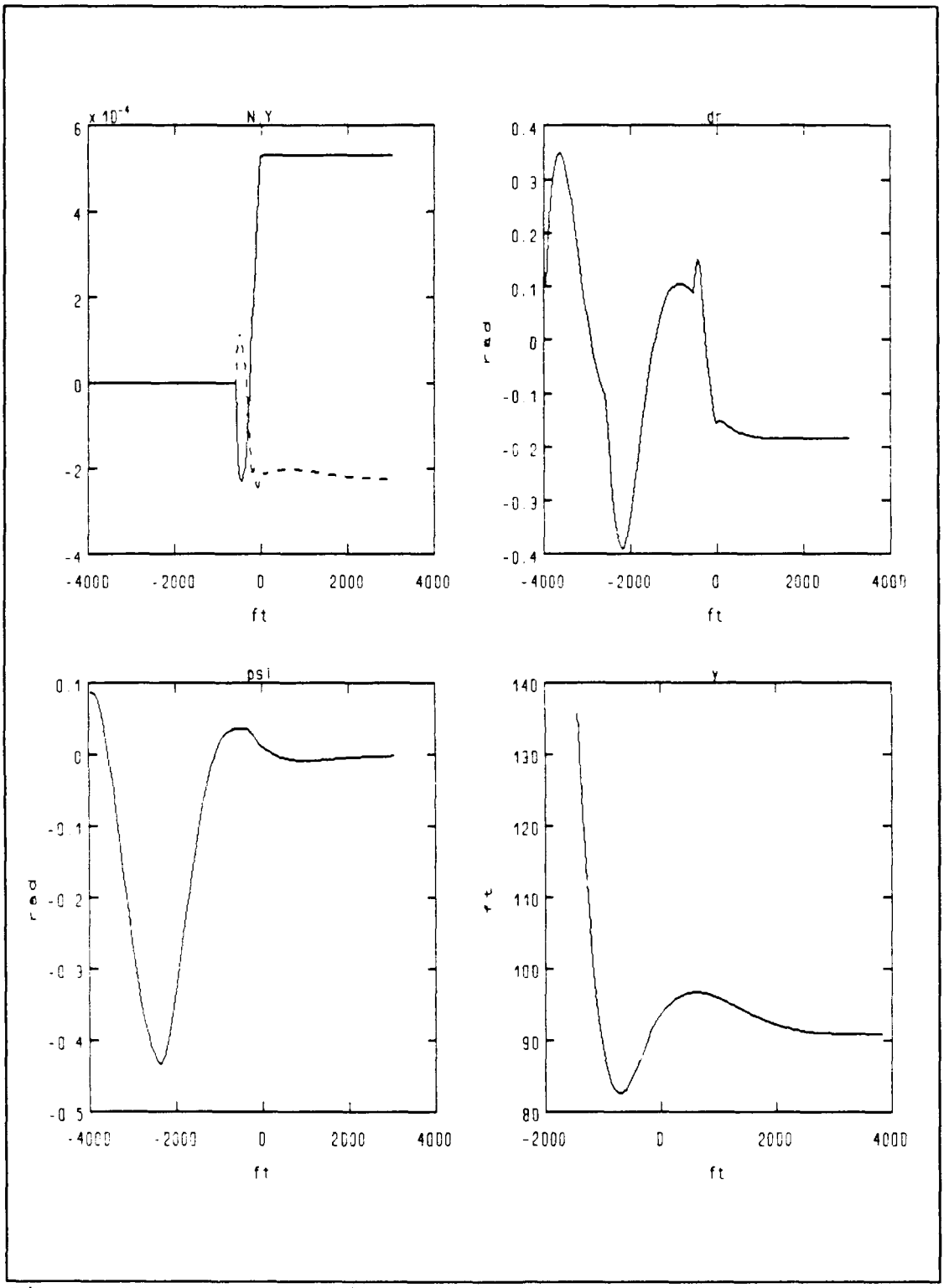

Figure 3.9 UNREP Station Keeping Process, No Feedforward, Calm Sea(Perfect Feedback, η=1, Δ=0.12)

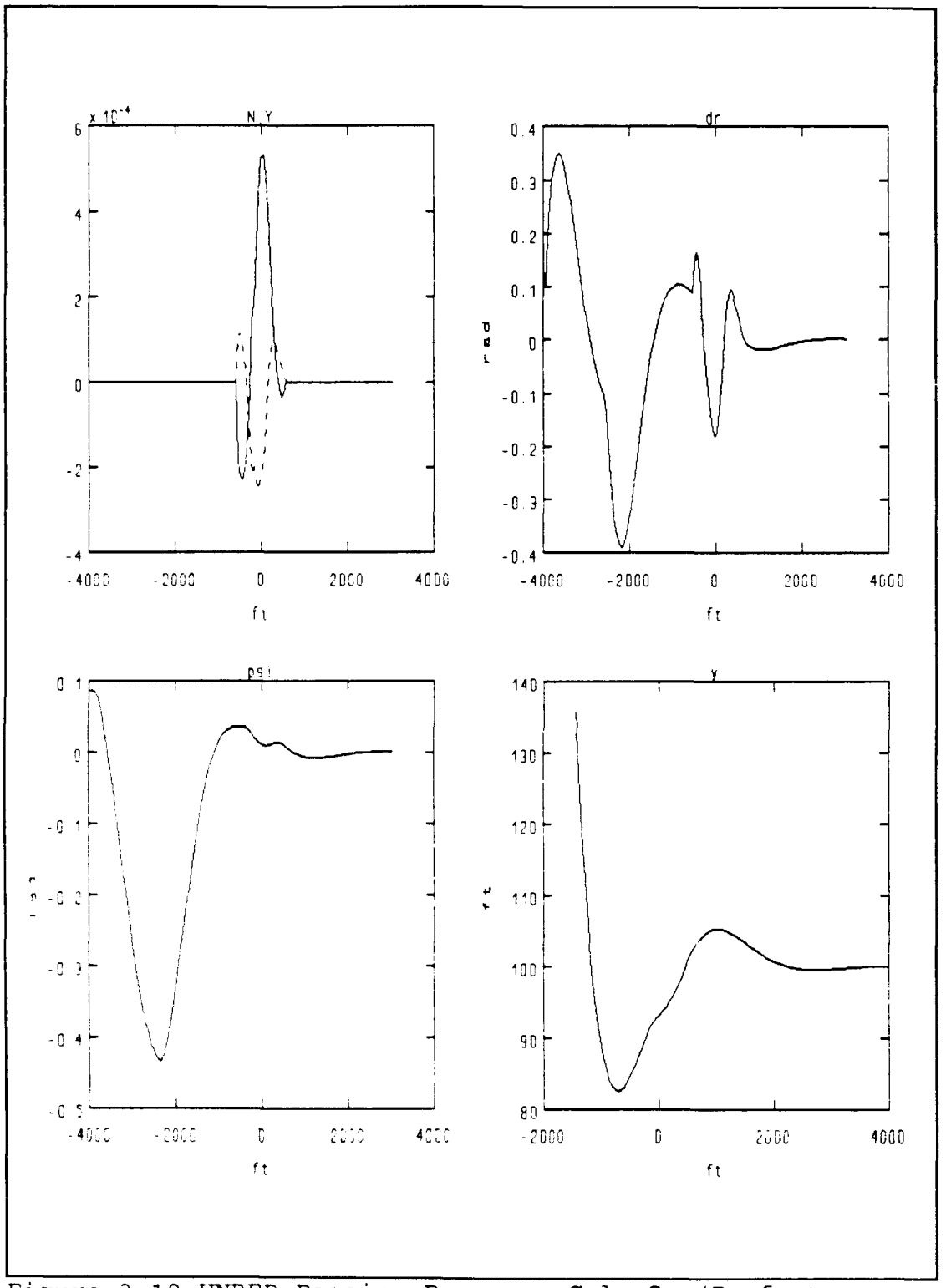

Figure 3.10 UNREP Passing Process, Calm Sea(Perfect Feedback, Disturbance Compensation, η=1, Δ=0.12)

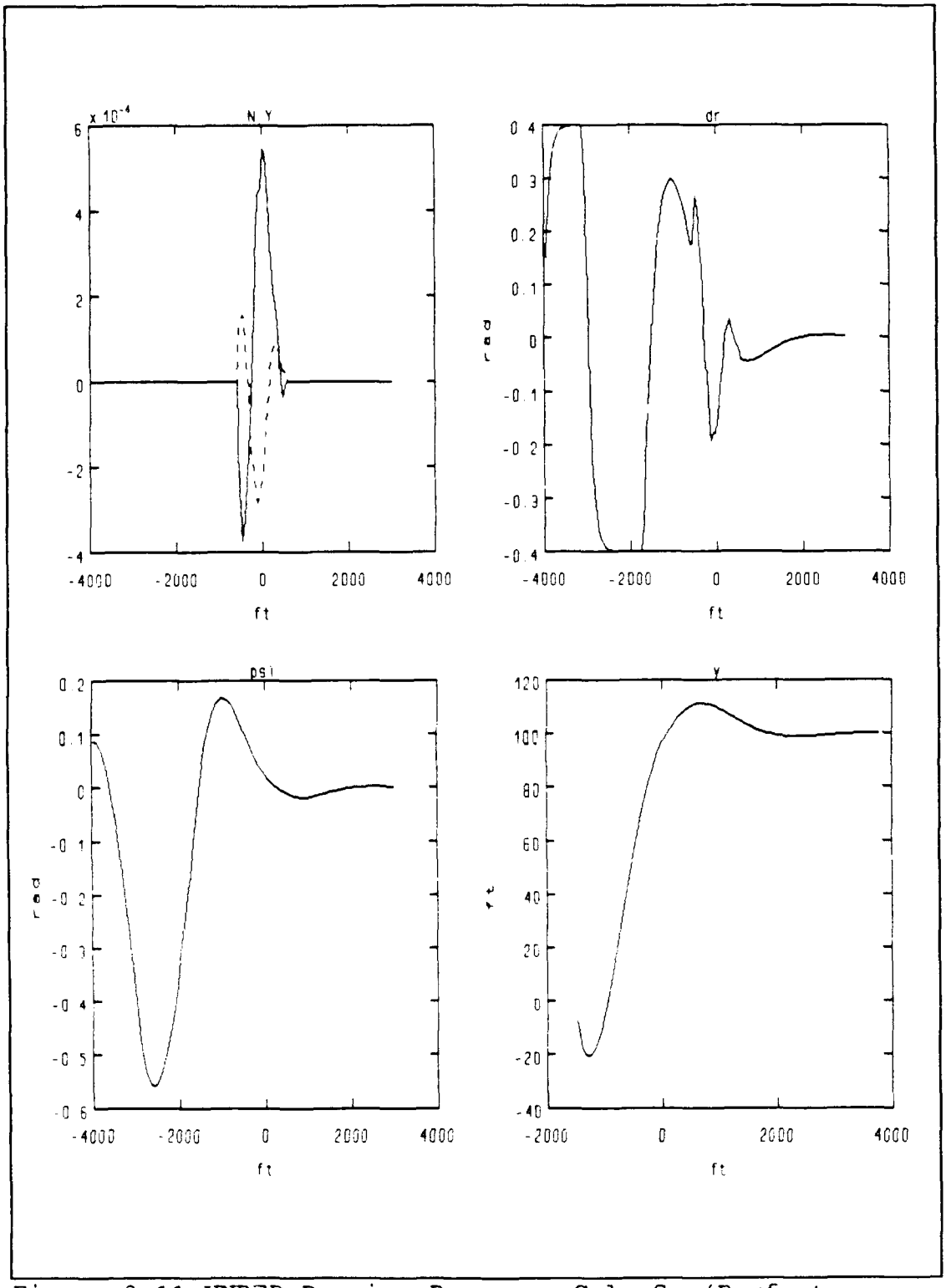

Figure 3.11 UNREP Passing Process, Calm Sea(Perfect Feedback, Disturbance Compensation, η=4, Δ=0.06)

approach phase is identical, the steady state path deviation becomes much smaller and asymptotically reaches zero.

9. Station Keeping Process, η=4, Δ=0.06

The results of this simulation are shown in Figure 3.12 where we can clearly see the increased rudder action and path overshoot. These result from increasing η and decreasing Δ as in the passing process.

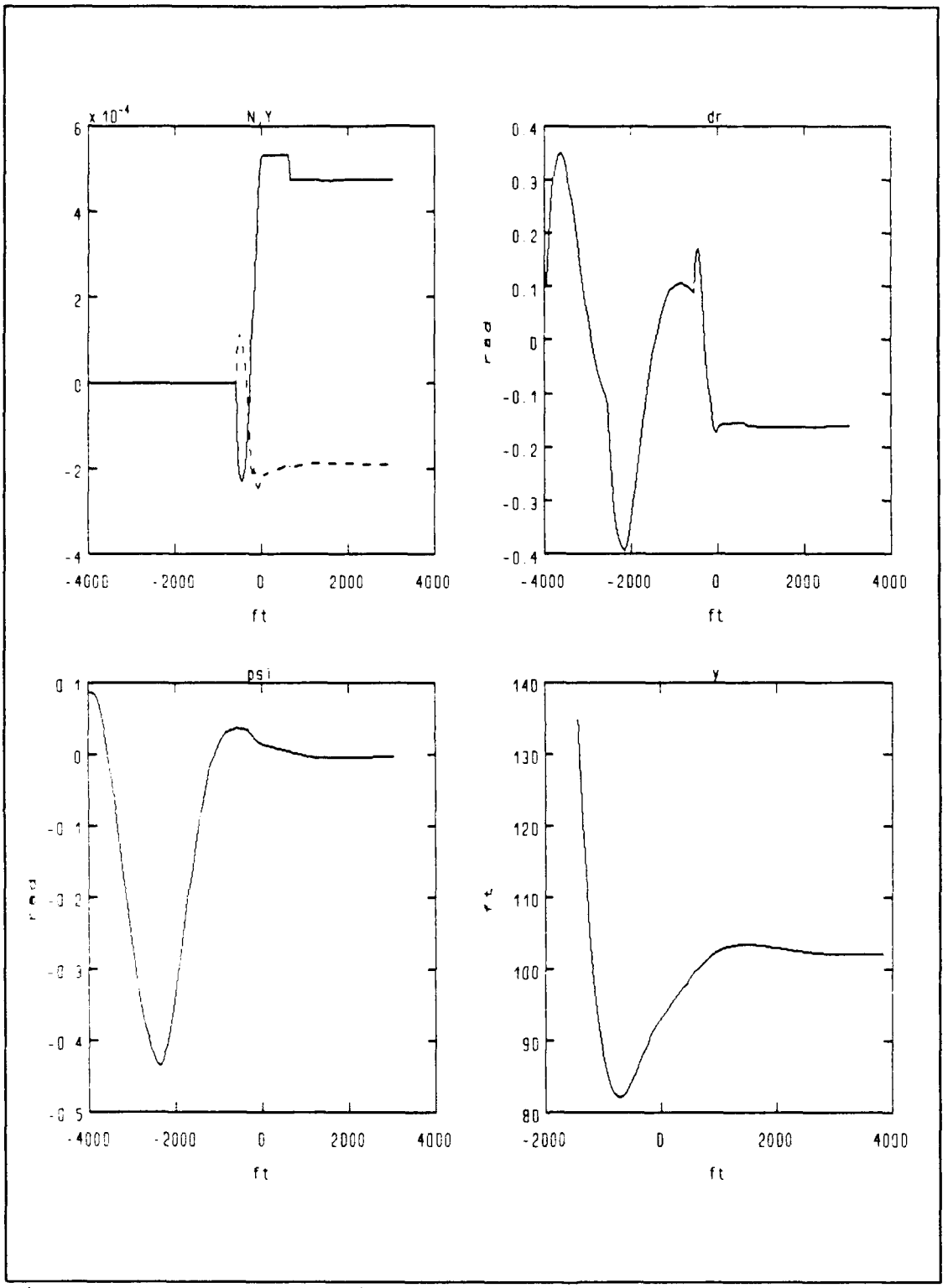

Figure 3.12 UNREP Station Keeping Process, Calm Sea(Perfect Feedback, Disturbance Compensation, η=1, Δ=0.12)

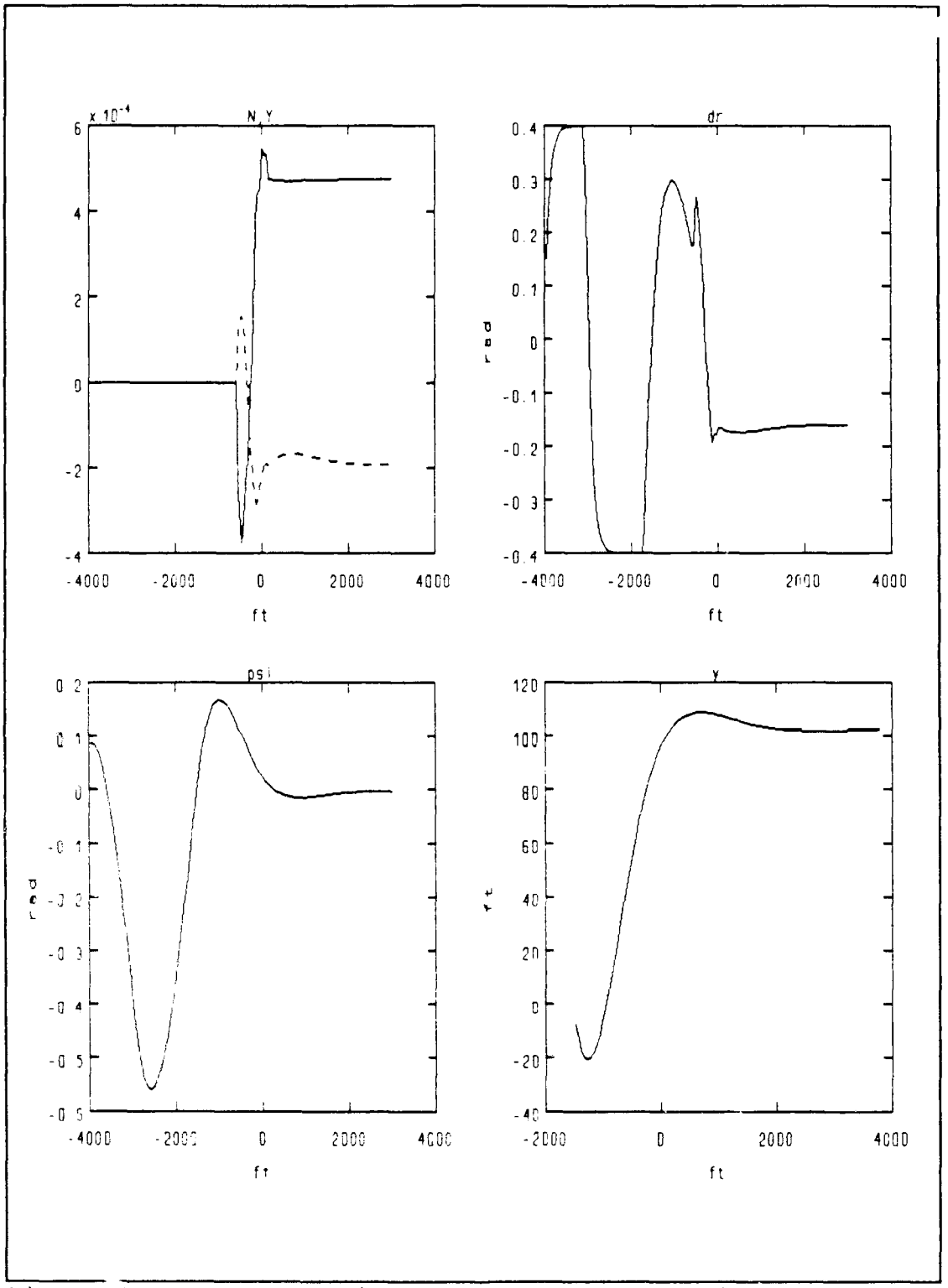

Figure 3.13 UNREP Station Keeping Process, Calm Sea(Perfect Feedback, Disturbance Compensation, η=4, Δ=0.06)

E. REMARKS

A sliding mode controller has been designed for the UNREP which utilized a LQR method. The controller have been proved to be very effective for a time varying disturbance(passing). Disturbance compensation was achieved by means of a feedforward term in the automatic controller.

The results demonstrate excellent tracking and path keeping characteristics in the presence of strong interaction forces and moments without any compromise in the stability and robustness properties at calm seas.

In this control test results all states are measurable, but in reality for a ship operating at sea not all states can be measured. So a Kalman filter design is needed as done in Chapter IV.

IV. KALMAN FILTER

A. INTRODUCTION

1. Disturbances

As was demonstrated in the previous chapter the optimal sliding mode control law was able to guarantee stability and steady state accuracy. For that it required knowledge of all states including the interaction forces and moments. An observer is therefore necessary in order to provide an estimate as accurate as possible of all system states. The first order wave forces can be effectively modeled as white noise components since they vary very rapidly compared to the dynamics of the maneuvering ship. A shaping filter is introduced in order to model the interaction force Y and moment N as exponentially correlated noise driven by white noise. In other words

$$\begin{aligned} \dot{N} &= -\frac{1}{T_N} N + \frac{1}{T_N} W_N \\ \dot{Y} &= -\frac{1}{T_N} Y + \frac{1}{T_N} W_Y \end{aligned} \tag{4.1}$$

where w_N, w_Y are white noise components and T_N and T_Y are time constants of the filter which are approximately equal to one (the time that it takes to travel ine ship length).

The power spectral density of Y and N is

$$Q_v=\begin{bmatrix} Q_N & 0 \\ 0 & Q_Y \end{bmatrix} \tag{4.2}$$

where Q_N and Q_Y are estimated using

$$Q_N=2\sigma_N^2 T_N \tag{4.3}$$

$$Q_Y=2\sigma_Y^2 T_Y \tag{4.4}$$

The root mean aquare values of N and Y denoted by σ_N and σ_Y can be estimated using the typical curves for the interaction forces shown in Figure 4.1. This calculation gives

$$Q_v=\begin{bmatrix} 1.548\times10^{-8} & 0 \\ 0 & 8.97\times10^{-8} \end{bmatrix} \tag{4.5}$$

2. Measurement Noise

The measurable states in this study are heading angle(ψ), yaw rate(r), and lateral separation distance(y).

The output equation is

$$y_m=\begin{bmatrix}\psi\\ r\\ y\end{bmatrix}=\begin{bmatrix}0&1&0&0&0&0&0\\0&0&0&1&0&0&0\\0&0&0&0&1&0&0\end{bmatrix}\begin{bmatrix}\delta\\ \psi\\ v\\ r\\ y\\ N\\ Y\end{bmatrix}+V_n \qquad (4.6)$$

where y_m is the output vector, the output matrix

$$C=\begin{bmatrix}0&1&0&0&0&0&0\\0&0&0&1&0&0&0\\0&0&0&0&1&0&0\end{bmatrix}$$

and V_n is the measurement noise. The power spectral density R_v of V_n can be evaluated using the numerical values in Table 4.1. The weighting matrix R_v is written in the form

$$R_v=\begin{bmatrix}rv_{11}&0&0\\0&rv_{22}&0\\0&0&rv_{33}\end{bmatrix} \qquad (4.7)$$

Table 4.1 The Power Spectral Density of Measurement Noises

Measurement	Source	R_v	σ	τ
ψ	gyro compass	rv_{11} = $4.612*10^{-8}$	0.2	0.1 sec
r	rate gyro	rv_{22} = $3.218*10^{-7}$	0.1 /s	0.1 sec
v	radar	rv_{33} = $4.502*10^{-6}$	3.3 ft	0.1 sec

* Note:

σ: Random standard deviation from the true value(units are degrees for heading angle and yaw rate, ft for y).

τ: The correlation time .

All values of R_v are in nondimensional values.

B. DESIGN OF KALMAN FILTER

In order to avoid enlarging the plant noises and measuremant noises, an optimal stochastic observer is required. The state vector and the covariance error are described as follows

$$\begin{aligned} E[x(t_0)] &= \overline{x}_0 \\ E[[x(t_0)-\overline{x}_0][x(t_0)-\overline{x}_0]^T] &= p_0 \end{aligned} \tag{4.8}$$

The estimate of the state at t_0 is assumed to be

$$\hat{x}(t_0) = \overline{x}_0 \tag{4.9}$$

The disturbance in the state equations has

$$\begin{aligned} E[w(t)] &= 0 \\ E[w(t)w^T(t)] &= Q(t)\delta(t-\tau) \end{aligned} \tag{4.10}$$

The measurement noise has

$$\begin{aligned} E[v(t)] &= 0 \\ E[v(t)v^T(t)] &= R(t)\delta(t-\tau) \end{aligned} \tag{4.11}$$

Design of the Kalman Filter is based on the cost function

$$J=\frac{1}{2}\left[(x_0-\bar{x}_0)^T P_0^{-1}(x_0-\bar{x}_0)\right] + \frac{1}{2}\int_{t_0}^{t}\left[w^T Q^{-1} w+(y_m-Cx)^T R^{-1}(y_m-Cx)\right]dt \tag{4.12}$$

where the first term minimizes the error in the initial estimate, the second term minimizes the effect of w, and the third term minimizes the error in the estimate of x.

The Kalman Filter has the familiar form

$$\frac{d\hat{x}}{dt}=A\hat{x}+B_1 u+L(y_m-C\hat{x}) \tag{4.13}$$

L is the time-varing Kalman gain matrix,

$$L=PC^T R^{-1} \tag{4.14}$$

P is the solution of the Riccati differential equation,

$$\dot{P}=AP+PA^T+B_2 Q B_2^T-PC^T R^{-1} CP \tag{4.15}$$

B_2 is the disturbance matrix; and

$P(t_0)=P_0$.

At steady state P is the solution to the algebraic Riccati equation

$$AP+Pa^T+B_2 Q B_2+PC^T R^{-1} CP=0 \tag{4.16}$$

In such a case the Kalman filter gain matrix is time-invariant and the Kalman filter is a full order observer with its gains tuned in an optimal way to the system at hand.

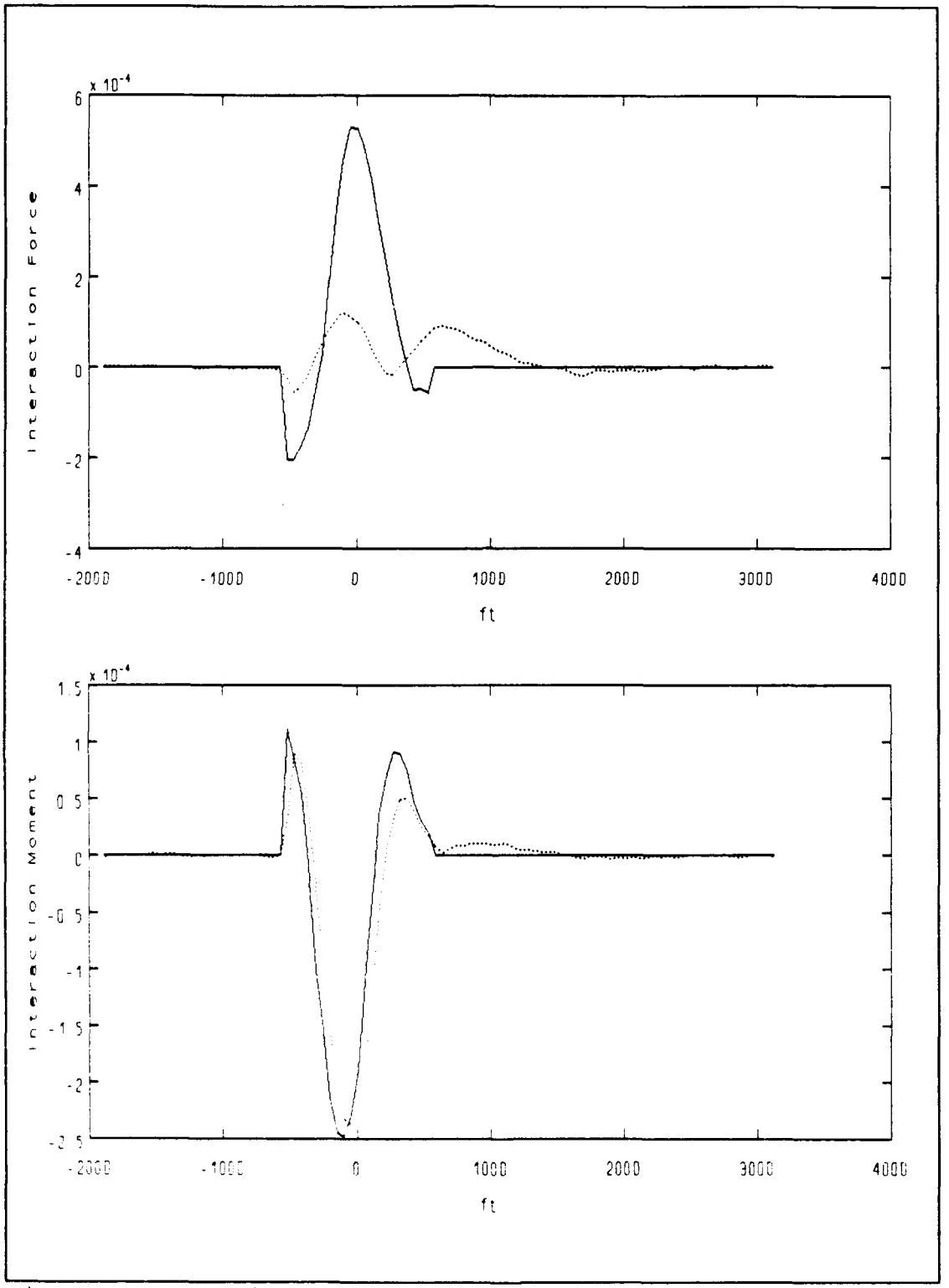

Figure 4.1 Turning Phase UNREP Passing Process, Open Sea, Disturbance Compensation η=1, Δ=0.12

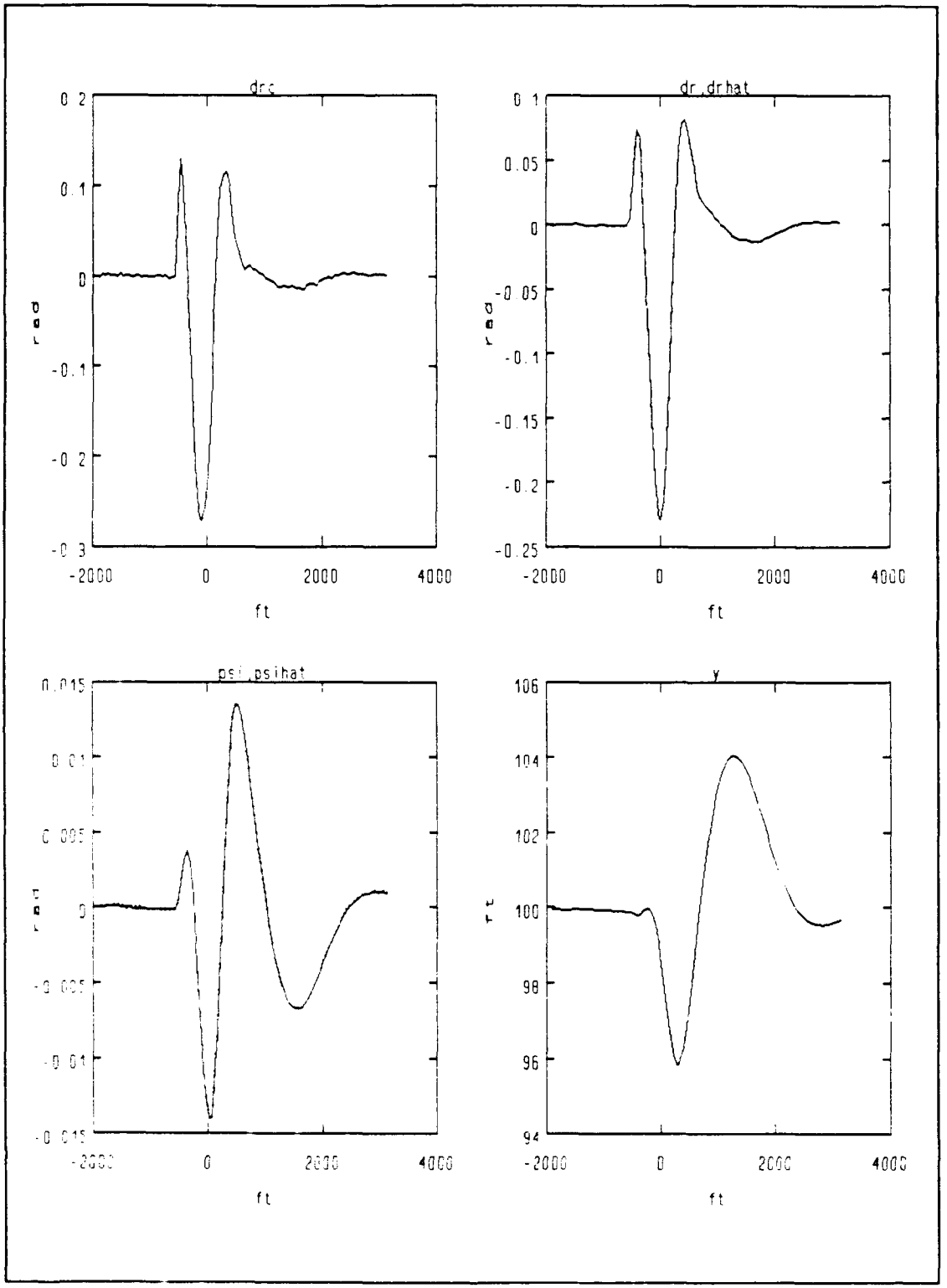

Figure 4.1 Turning Phase-(continued)

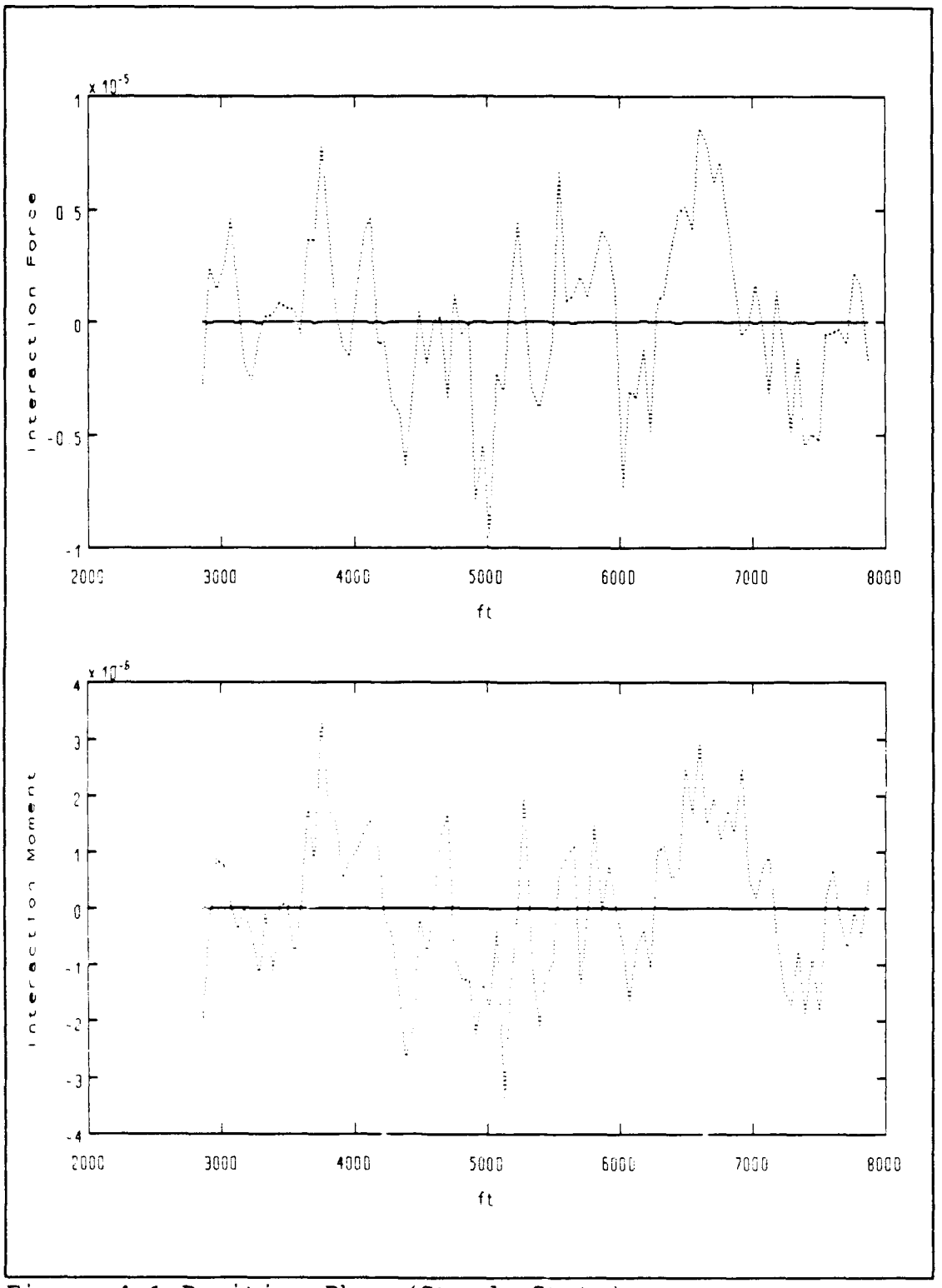

Figure 4.1 Position Phase(Steady State)

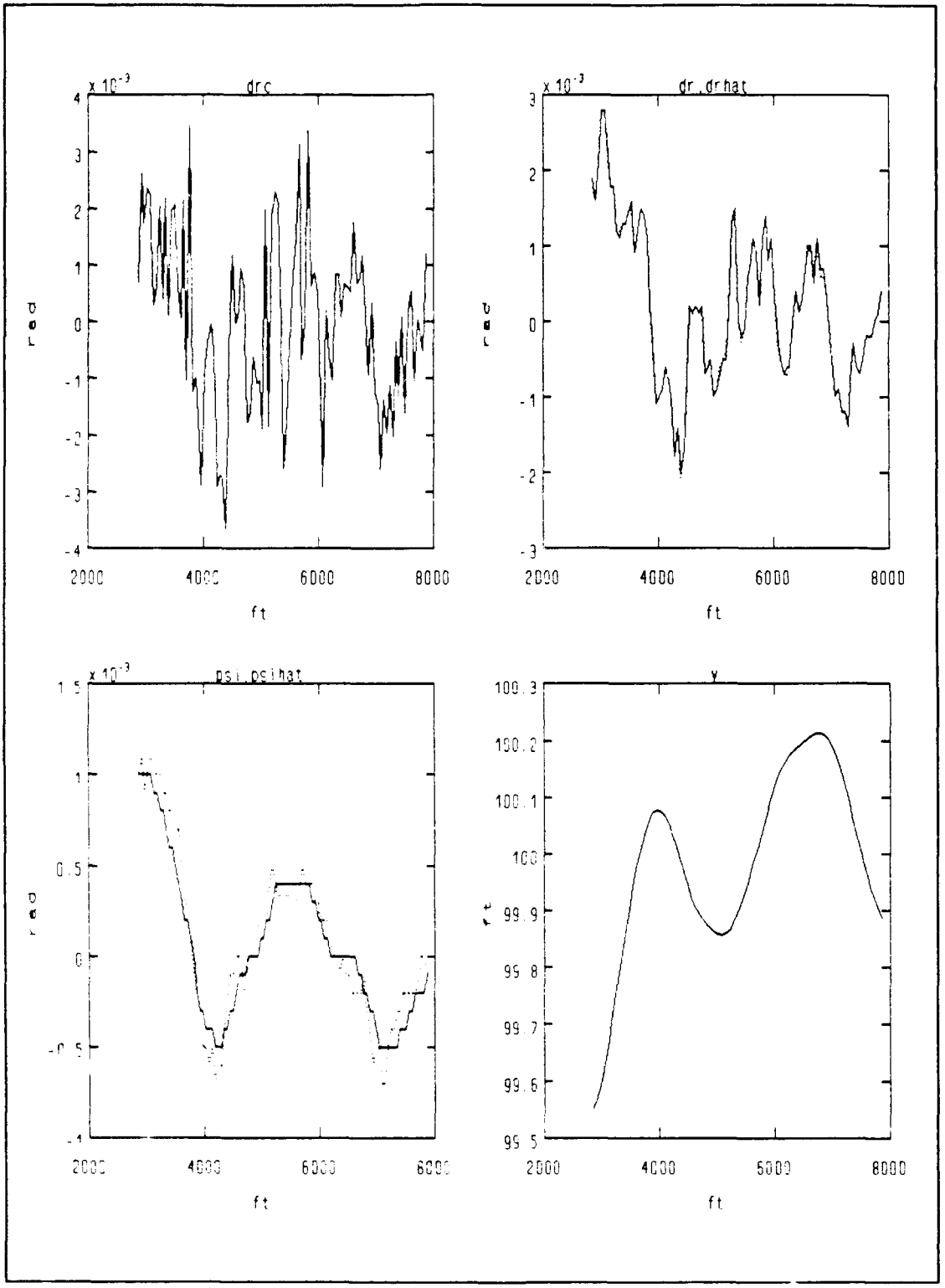

Figure 4.1 Position Phase-(continued)

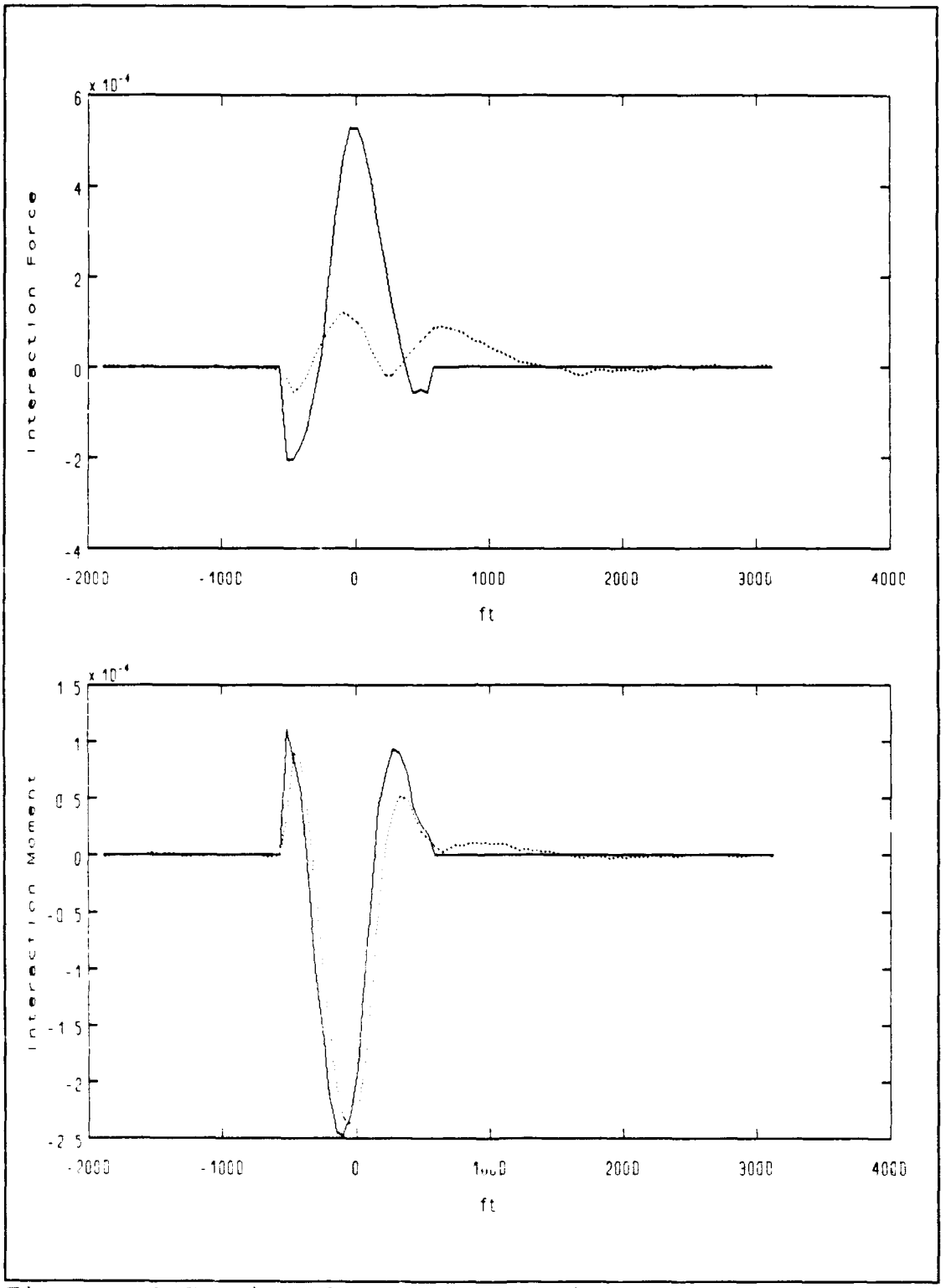

Figure 4.2 Turning Phase UNREP Passing Process, Open Sea, Disturbance Compensation η=4, Δ=0.06

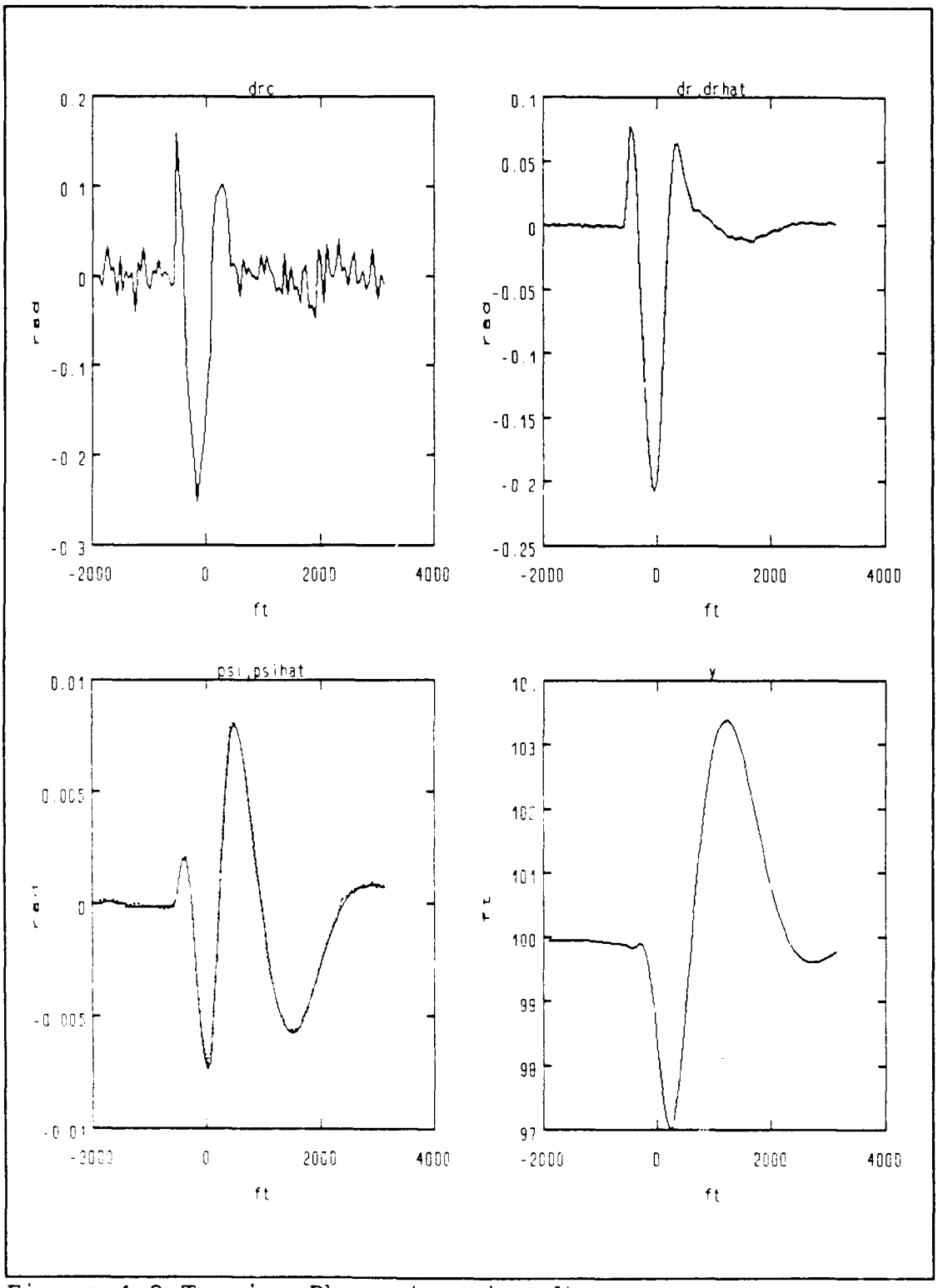

Figure 4.2 Turning Phase-(continued)

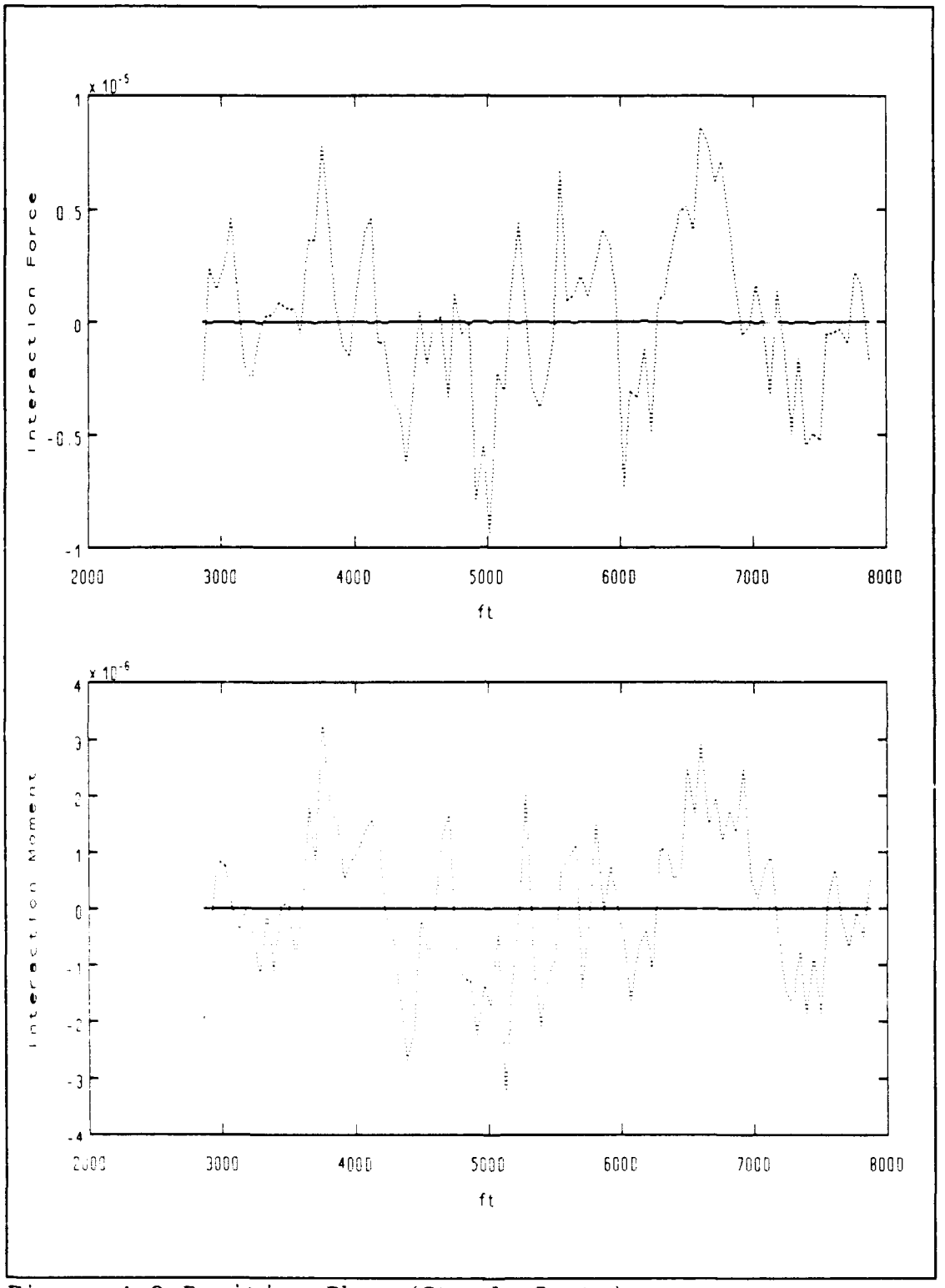

Figure 4.2 Position Phase(Steady State)

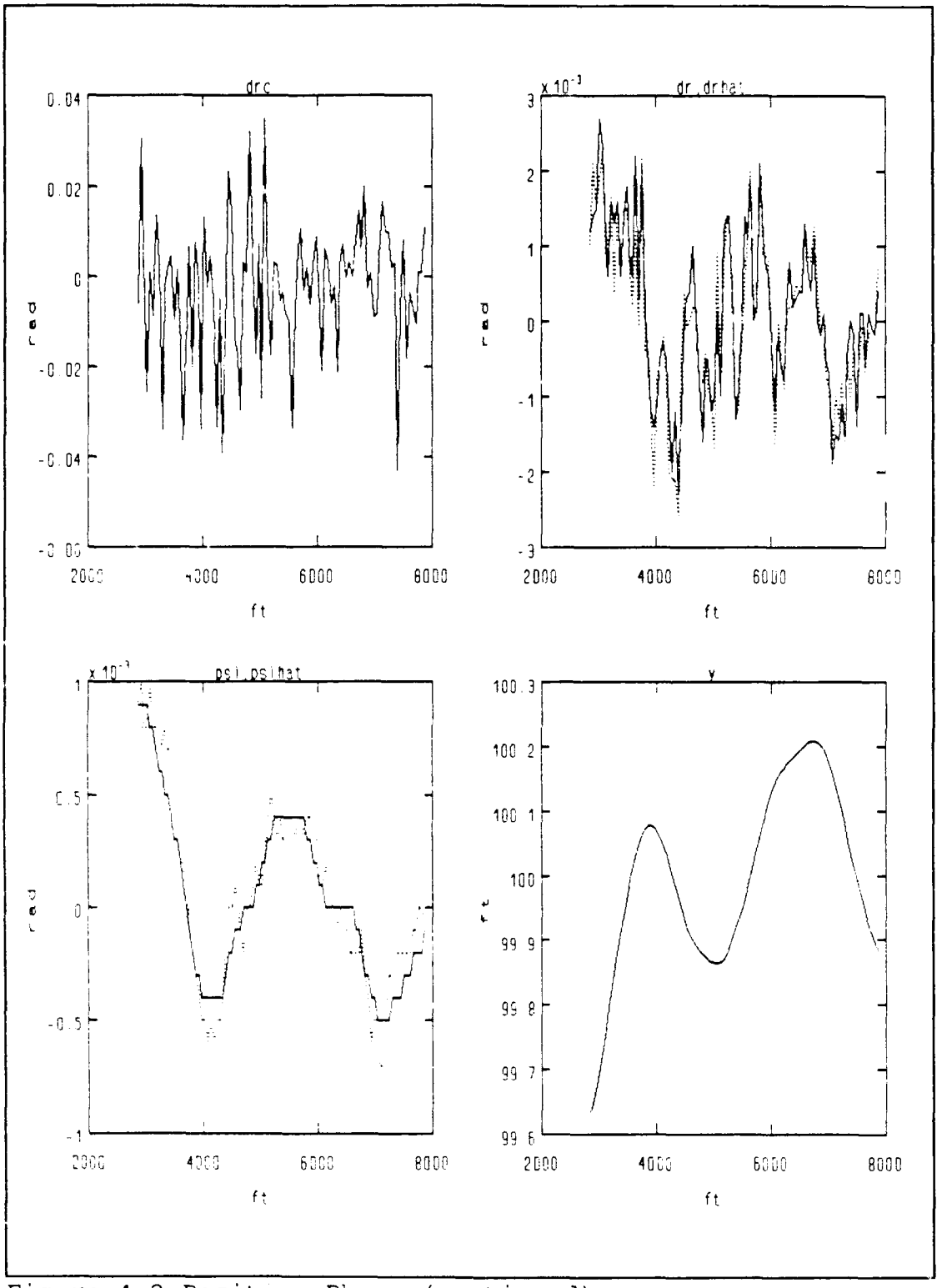

Figure 4.2 Position Phase-(continued)

C. SIMULATION AT OPEN SEA

1. Introduction

In the following we present results for both the passing and the station keeping process. The sliding mode linear quadratic Gaussian compensator is used along with the feedforward term developed in chapter III. All results are based on UNREP in a random sea of significant wave height of 16 ft. Solid curves in the graphs denote the actual values of the variables while dotted curves correspond to the estimated values from the Kalman filter.

2. Passing Process, Δ=0.12, η=1

The results of the simulation are shown in Figure 4.1. Convergence to the desired track is achieved. The steady state deviation of the tracking ship from the commanded path is minimal. The steady state use of the rudder angle is also very satisfactory.

3. Passing Process, η=4, Δ=0.06

The results of the simulation are shown in Figure 4.2. Initial conditions were selected on the desired path so this simulation demonstrates the effects of the passing ship disturbance. The two ships are located beam-to-beam at 0 ft longitudinal distance. The maximum deviation of the tracking ship is $\pm$ 3 ft.

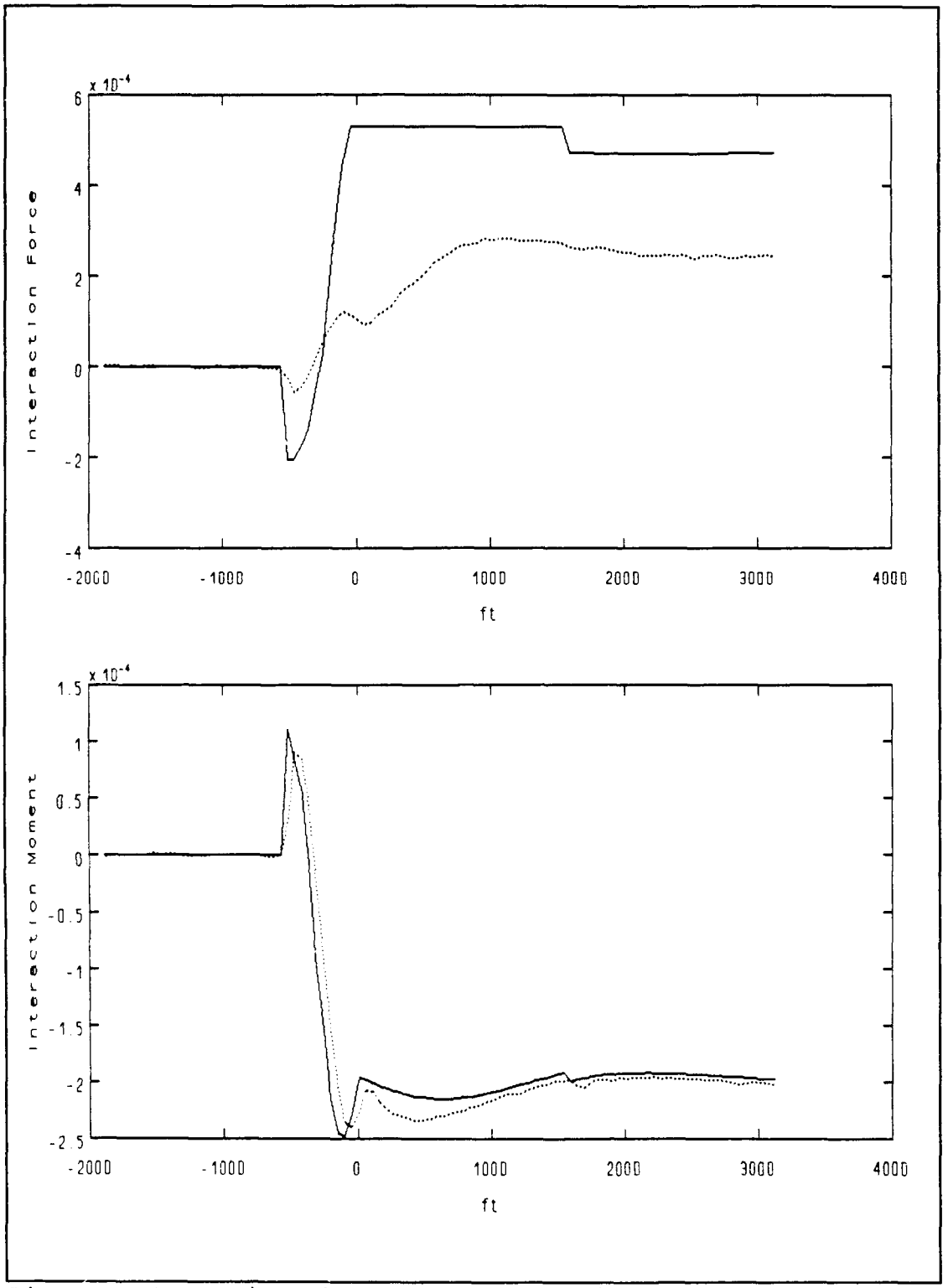

Figure 4.3 Turning Phase Station Keeping Process, Open Sea, Disturbance Compensation η=1, Δ=0.12

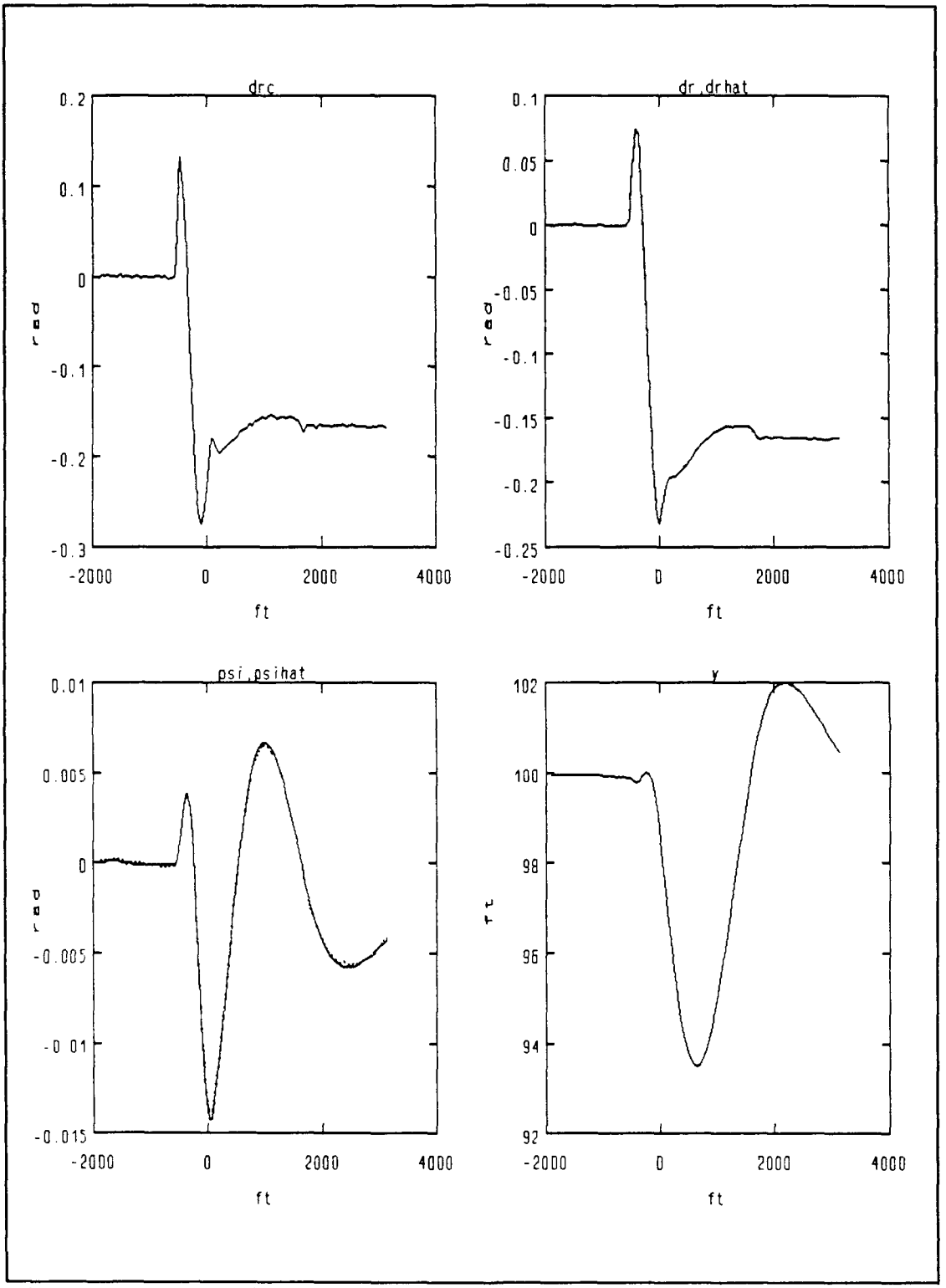

Figure 4.3 Turning Phase-(continued)

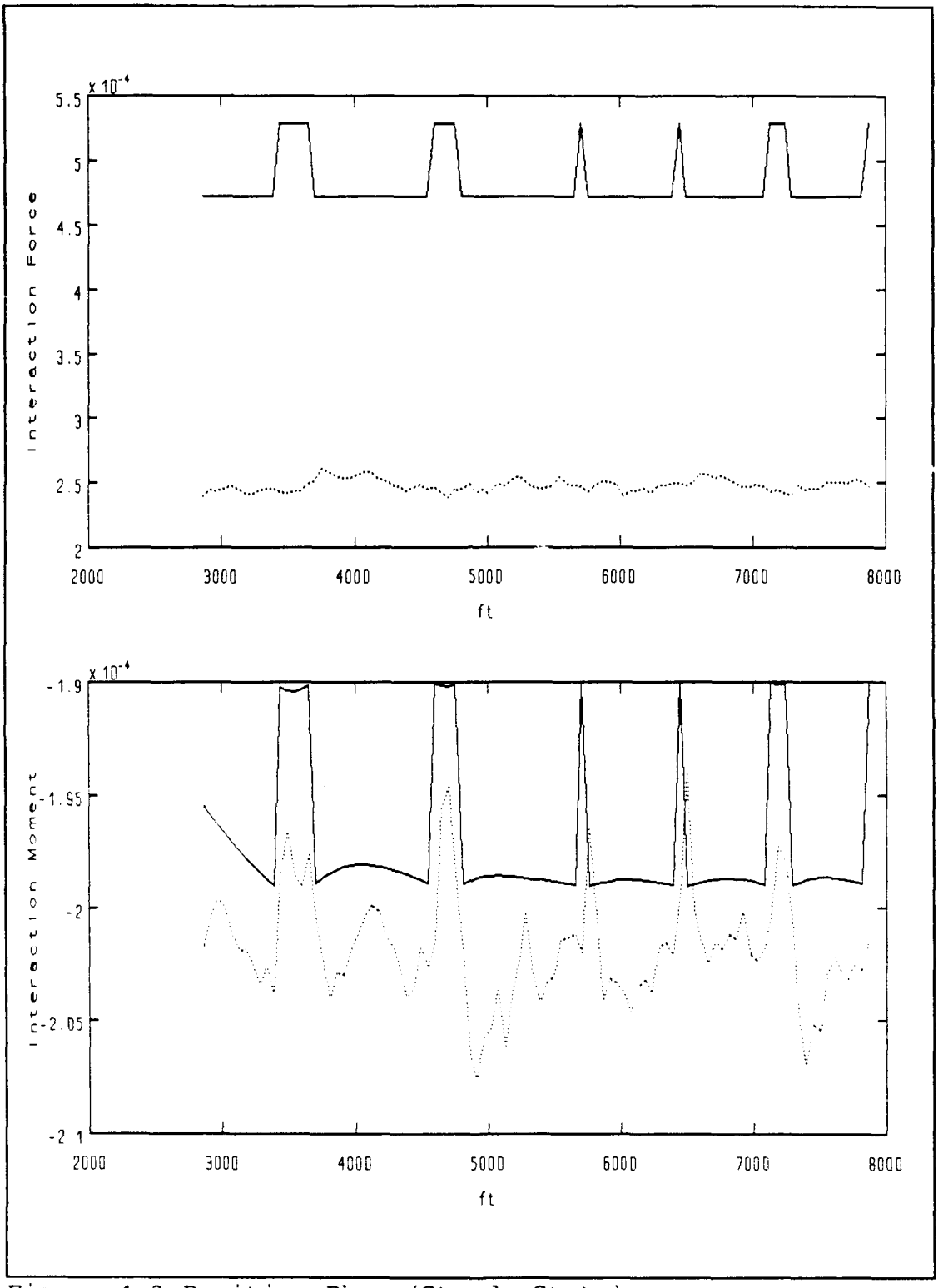

Figure 4.3 Position Phase(Steady State)

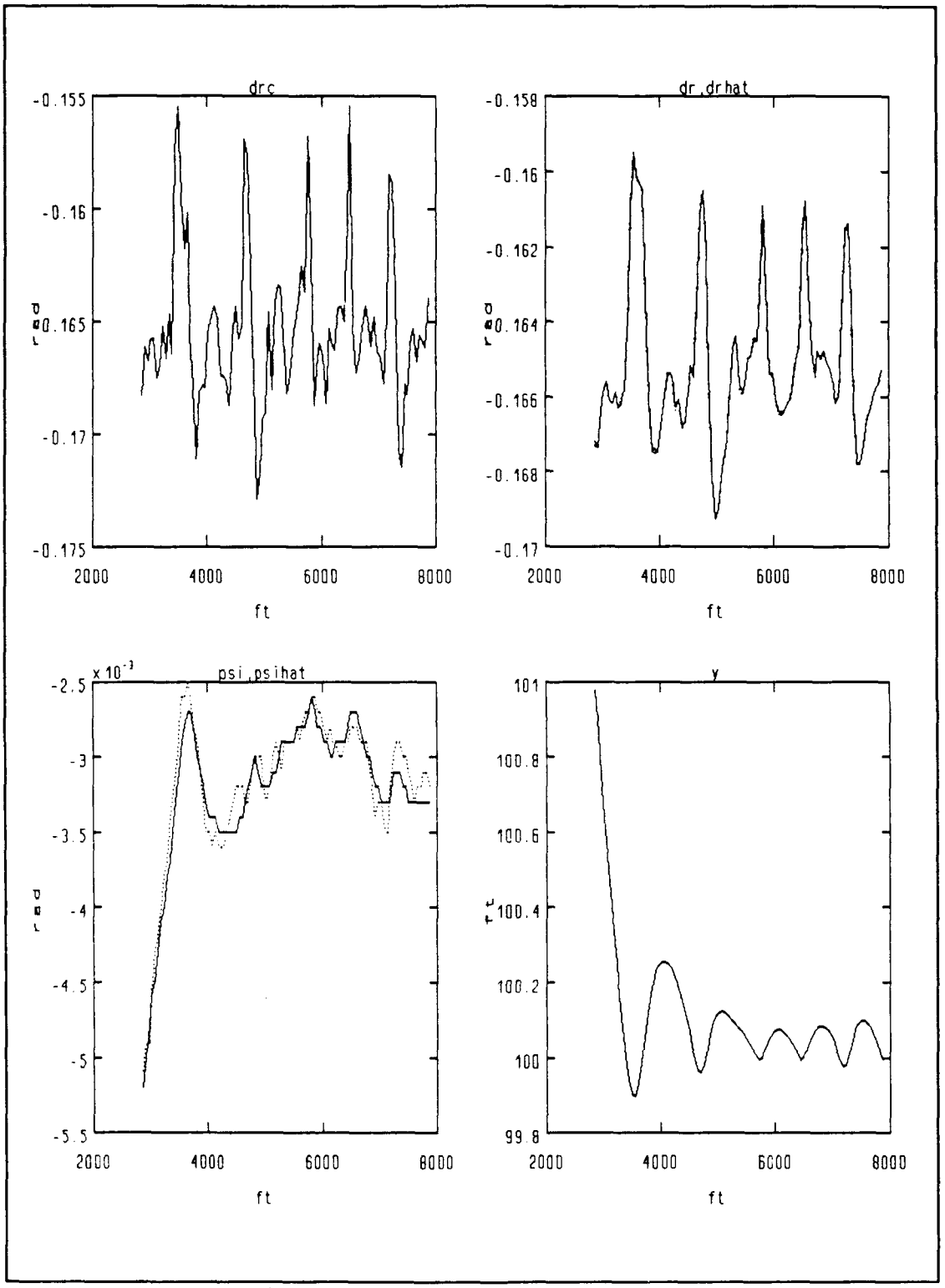

Figure 4.3 Position Phase-(continued)

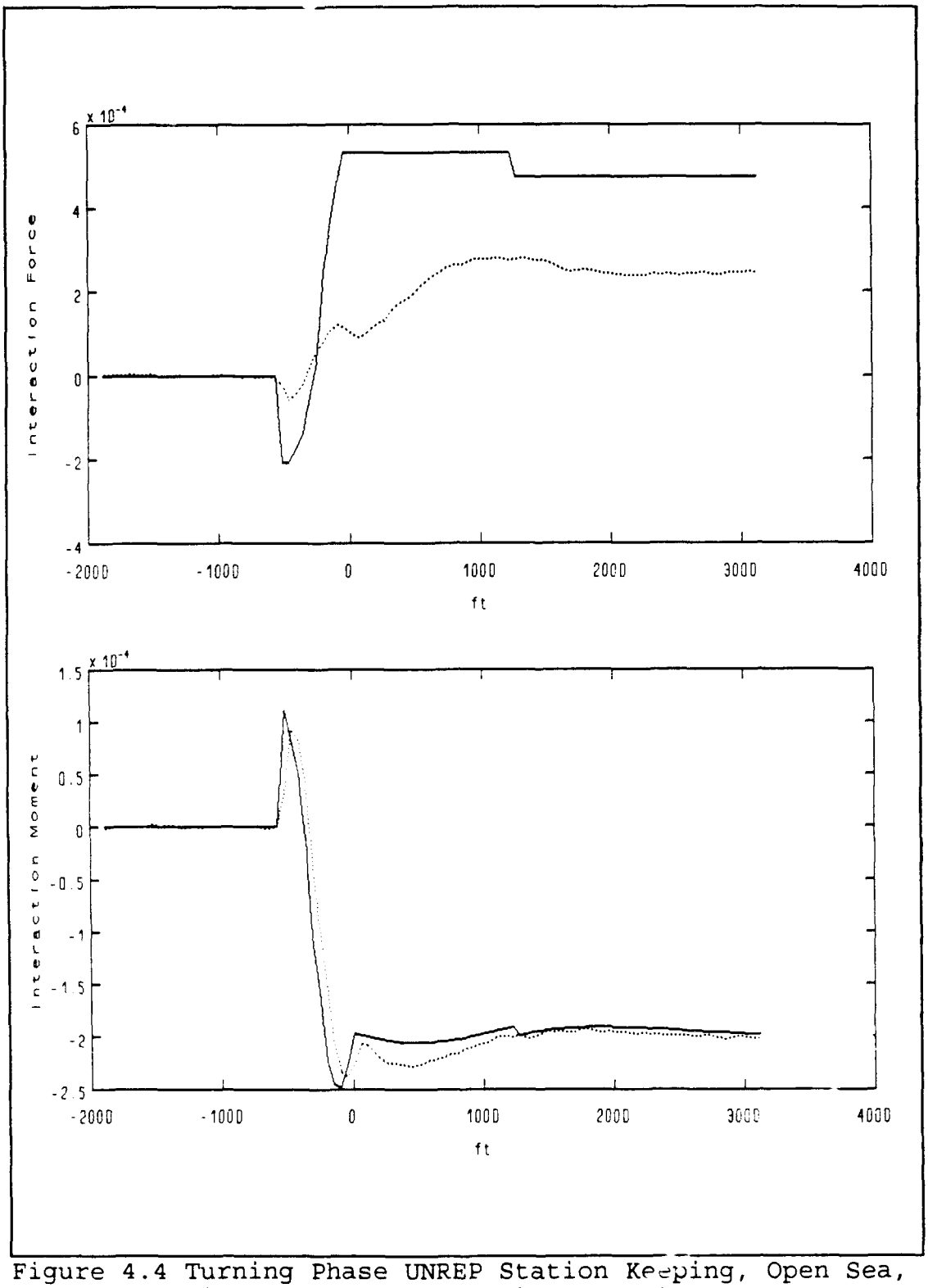

Figure 4.4 Turning Phase UNREP Station Keeping, Open Sea, Disturbance Compenastion η=4, Δ=0.06

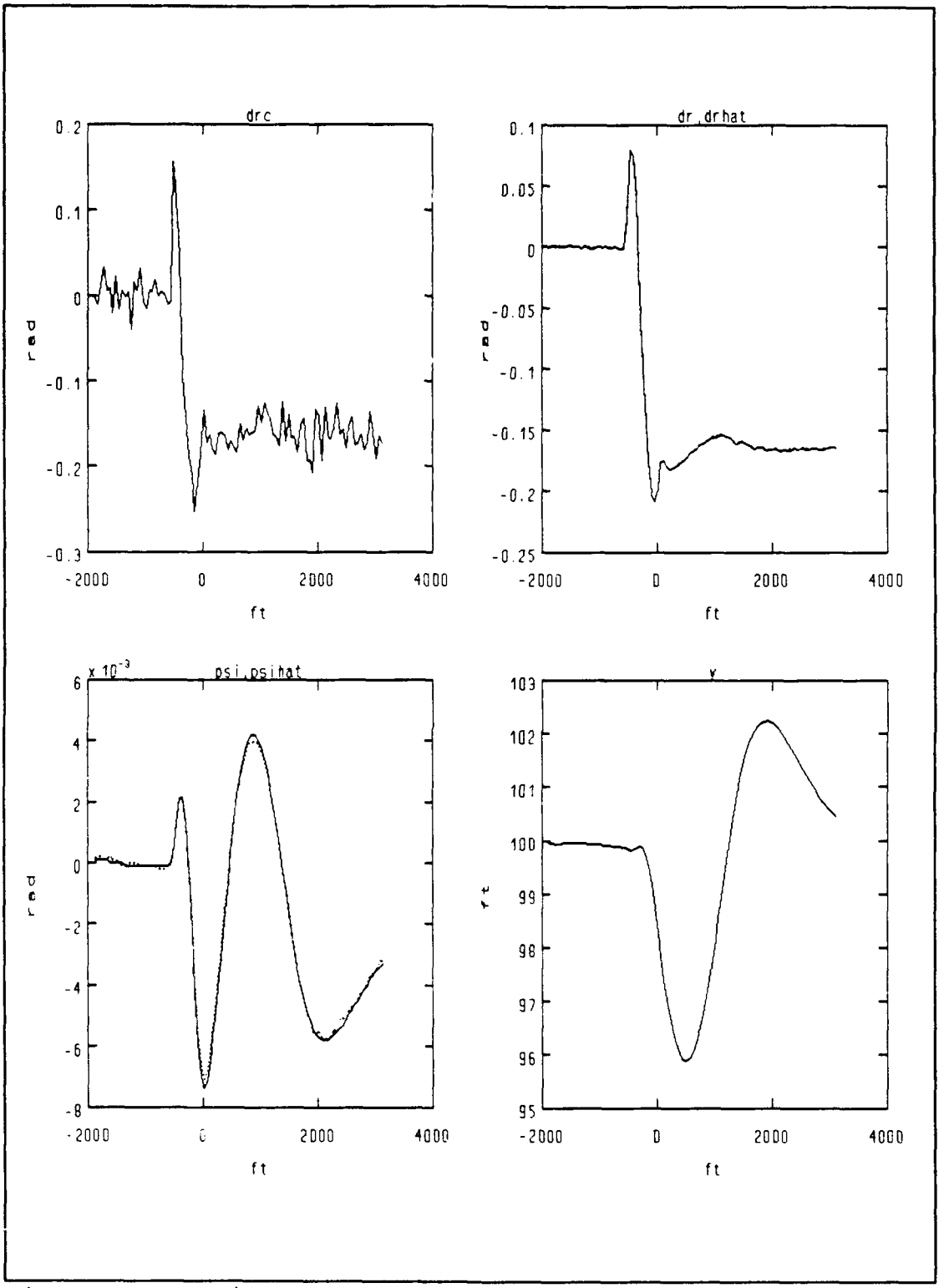

Figure 4.4 Tuning Phase-(continued)

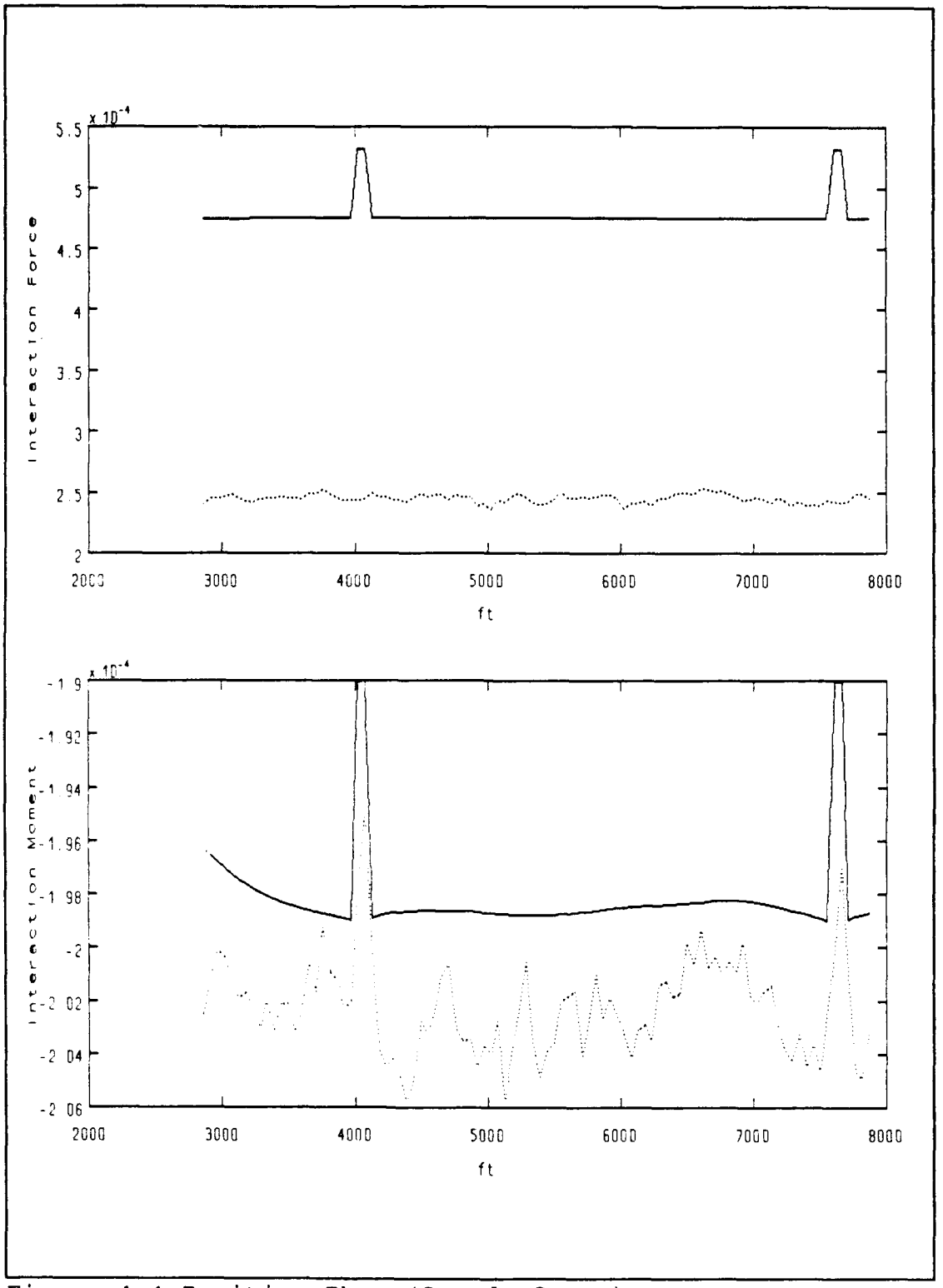

Figure 4.4 Position Phase(Steady State)

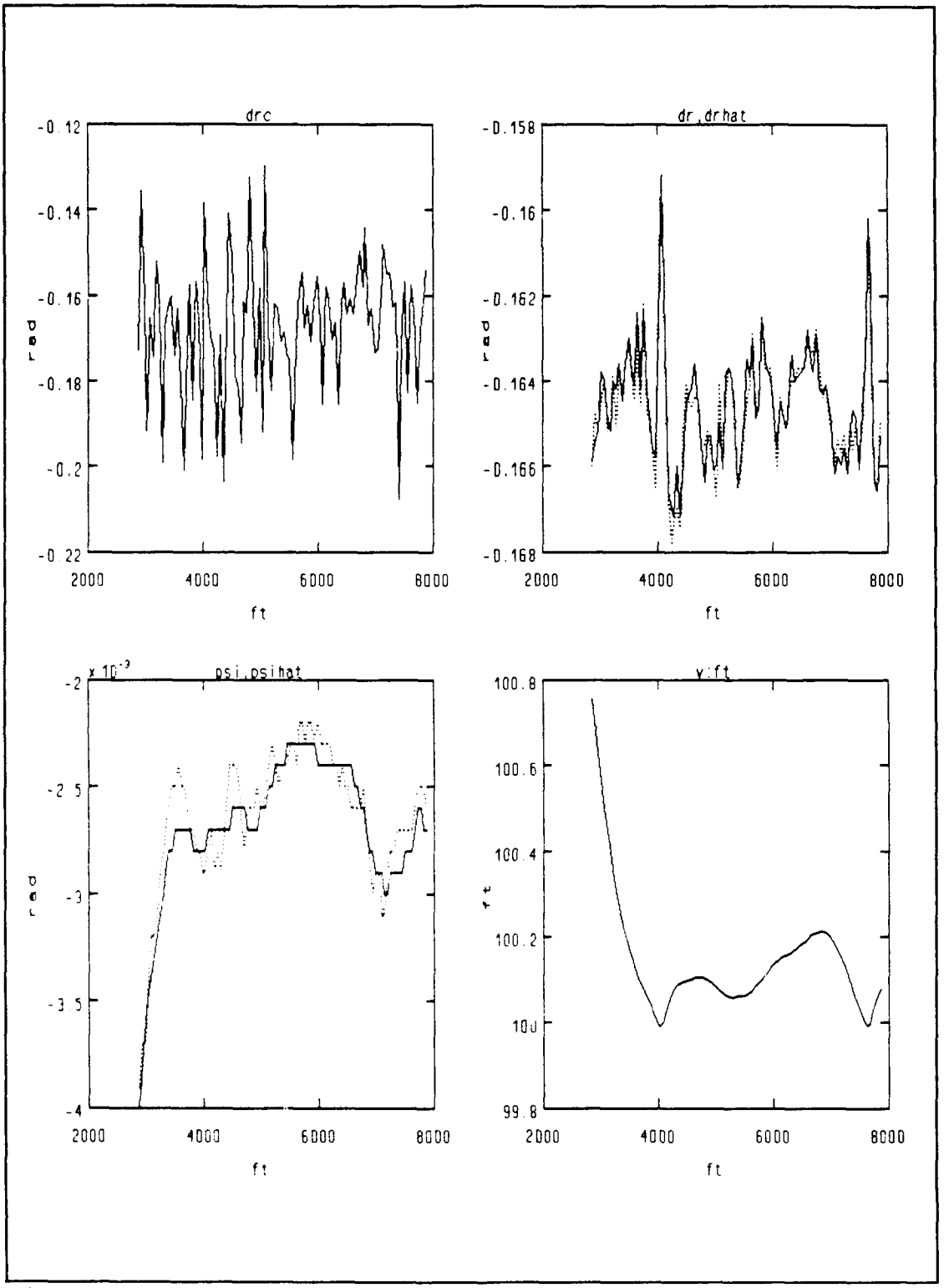

Figure 4.4 Position Phase-(continued)

4. Station Keeping Process, η=1, Δ=0.12

The results of this simulation are shown in Figure 4.3. Steady state accuracy is maintained. There appears to exist an error in the estimates of Y and N despite the zero steady state error in the path deviation. This is attributed to the existence of the first order wave force and moment. Since there is no explicit estimation scheme for these, their effect is effectively combined by the observer into an equivalent interaction force and moment which of course differ from the actual.

5. Station Keeping process, η=4, Δ=0.06

The results of this simulation are shown in Figure 4.4. Compared to the simulation shown in Figure 4.3 we can see the effects of the tighter control law in this case. Both the transient and steady state path deviation are reduced while the rudder activity is slightly increased.

D. CONCLUSIONS AND REMARKS

The sliding mode Linear Quadratic Gaussian compensator was able to adequately control the lateral motion of a surface ship during underway replenishment in an open sea. The feedforward term ensured state path accuracy in the presence of interaction forces and moments as well as first order wave effects. The Kalman filter was able to minimize the effects of the measurement noises and external random disturbances while at the same time it provided the controller with an accurate

estimate of the states needed for control. Different control options were considered with regards to their transient and steady state characteristics. These comparisons provided insight towards appropriate selection of the boundary layer thickness and switching gain of the sliding mode control.

Suggestions for further research include the application of integral control instead of disturbance estimation and compensation for eliminating the steady state path error. Furthermore, the effects of constant disturbances, such as currents, and slowly varying second order wave draft forces should be investigated.

APPENDIX A. SUMMARY FOR COMPUTER PROGRAMS

The complete listing of the computer programs written and used in this thesis are in APPENDIX B and APPENDIX C.

The MATLAB program in APPENDIX B is used for calculating feedback gains and observer gains using the LQR method, which are utilized for sliding surface design and Kalman filter design.

The FORTRAN program in APPENDIX C is a complete listing for PASSING PROCESS simulation. The modified program for the STATION KEEPING PROCESS is not listed here, the only change is the following FORTRAN code logic expression:

```
if (b.ge.0) b=0.
```

APPENDIX B. MATLAB LQR DESIGN PROGRAM FOR UNREP SLIDING MODE CONTROLLER AND KALMAN GAINS

```
mass=0.0;
xg=0.0;
iz=0.0;
tr=.2;
nvdot=-19.7e-5;
xudot=-850e-5;
xu=-120e-5;
yv=-1243e-5;
yvdot=-1500e-5;
yr=-510e-5;
yrdot=-27e-5;
ydr=270e-5;
nv=-351e-5;
nr=-227e-5;
nrdot=-68e-5;
ndr=-126e-5;
xn=4.62e-5;
yn=-.52e-5;
nn=.26e-5;
ap1=yvdot*nrdot-vrdot*nvdot
a32=(yrdot*nv-yv*nrdot)/ap1;
a33=(yrdot*nr-yr*nrdot)/ap1;
a35=yrdot/ap1;
a36=-nrdot/ap1;
ap2=nvdot*yrdot-nrdot*yvdot
a42=(nv*yvdot-nvdot*yv)/ap2
a43=(nr*yvdot-yr*nvdot)/ap2
a45=yvdot/ap2
a46=-nvdot/ap2
b21=(ndr*yrdot-ydr*nrdot)/ap1;
b31=(ndr*yvdot-ydr*nvdot)/ap2
a=[0 0 1 0 0 0;0 a32 a33 0 a35 a36;0 a42 a43 0 a45 a46; ...
   1 1 0  0 0 0;0 0 0 0 -1 0;0 0 0 0 0 -1];
b=[0 b21 b31 0 0 0]';
aab=b31*a32-b21*a42;
```

```
aa1=(a42*a35-a45*a32)/aab;
aa2=a35*a42/aab;
bb1=(a35*b31-a45*b21)/aab;
bb2=a36*a42/aab;
tau=.2;
ad=1;
a11=[-1/tau];
a12=[0 0 0 0 0 0];
bb=[1/tau 0 0 0 0 0 0]';
aa=[a11 a12;b a];
q=diag([131.3 0 0 771.69 0 0]);
qq=diag([131.3 131.3 0 0 771.69]);
r=[131.3];
c=[1 0 0 0 0 0;0 0 1 0 0 0;0 0 0 1 0 0];
[k,s]=lqr(a,b,q,r);
ss=[1 k]
gg=inv(ss*bb)*ss*aa
kn=inv(ss*bb);
ca=aa-bb*(gg-kn1);
cc=[0 1 0 0 0 0 0;0 0 0 1 0 0 0;0 0 0 0 1 0 0];
g1=[0 0 0 0 0 1 0;0 0 0 0 0 0 1]';
q1=[1.548e-8 0;0 8.97e-8];
rr=diag([4.612e-8 3.213e-7 4.502e-6]);
l=lqe(aa,g1,cc,q1,rr)
f=aa-l*cc*aa
bf=bb-l*cc*bb
```

APPENDIX C. UNREP SIMULATION PROGRAM: SLIDING MODE CONTROLLER DESIGNED BY LQR METHOD

```
      program shipdynamics
c*************************************************************
c   Simulation program for UNREP
c
c   Written by LT FU, HSU-SHENG SIMON
c
c  The program controls one rudder input with a sliding mode
c   design for path keeping and tracking.
c
c   Speed is constant 1 normalized value.
c
c   The initial conditions for ship are follows: 1
c   nondimensional leteral seperation distance, -4000 ft
c   longitudinal distance, 0.087 rad heading angle.
c
c    The disturbances include interaction forces and moments,
c    and first-order wave sway force and yaw moment.
c
c    The observed states: yaw rate, lateral separation rate,
c    interaction forces and moments.
c
c    The measurements: heading angle, lateral separation
c    distance, and rudder angle.
c
c    The outputs of the program are written to files, these
c    files are then accessed by the MATLAB to generat output
c    graphics.
c
c   This program utilized subroutines for different functions
c    that are required:
c      subroutine locate: find the interaction forces and
c                         moments at the real time and use
c                        subroutine trlint as interpolation.
c      subroutine trlint: incooprate with subroutine locate.
```

```
c      subroutine randm : generate random signal.
c      subroutine trap  : Trapzoid integration.
c      subroutine first : first order wave calculation.
c
c    Two data files for interaction forces and moments:
c      Table1.dat: interaction forces.
c      Table2.dat: interaction moments.
c*************************************************************
      real mass,nrdot,nvdot,nr,nv,ndr,nn
      real k1,k2,k3,k4,k5,k6,k7,kn,iz,mo,a,b,l
      real w,coef,f1,n1,wn,wy,we2(5),ws
      real ol(7,3),ae(7,7),ba(7,1),bc(7,2),bd(7,2),sf2(5),
     1     ym2(5)
      real time
c
      dimension aa(23),bb(11),table1(23,11),table2(23,11)
      data aa/-550,-500,-450,-400,-350,-300,-250,-200,-150,
     1        -100,-50,0,50,100,150,200,250,300,350,400,
     1         450,500,550/
      data bb/50,60,70,80,90,100,110,120,130,140,150/
      data ol/0,2.6383,-1.4846,6.6537,.165,.0167,-.0133,
     1        0,.9536,-3.8899,21.5836,-.911,.1926,-.1238,
     1        0,.0017,3.3203,-.0651,2.566,.0107,.0507/
c
      m     =23
      n     =11
      l     =527.8
      iseed =17
c
      mass =    0.0
      xg   =    0.0
      iz   =    0.0
      nvdot=-  19.7*1.e-5
      tr   =     .2
      xudot=- 850.0*1.e-5
      xu   =- 120.0*1.e-5
      yv   =-1243.0*1.e-5
      yvdot=-1500.0*1.e-5
      yr   =- 510.0*1.e-5
      yrdot=-  27.0*1.e-5
      ydr  =  270.0*1.e-5
```

```
      nv    =- 351.0*1.e-5
      nr    =- 227.0*1.e-5
      nrdot=-  68.0*1.e-5
      ndr   =- 126.0*1.e-5
      xn    =    4.62*1.e-5
      yn    =-    .52*1.e-5
      nn    =     .26*1.e-5
c
c     define system matrix
c
      do 60 i  =1,7
       do 70 j =1,7
        ae(i,j)=0.0
        ba(i,1)=0.0
        bc(i,1)=0.0
        bd(i,1)=0.0
        bc(i,2)=0.0
        bd(i,2)=0.0
70     continue
60    continue
      ae1     = nrdot*yvdot-yrdot*nvdot
      ae2     = nvdot*yrdot-nrdot*yvdot
      ae(1,1)=-1/tr
      ae(2,4)= 1.
      ae(3,1)= (ndr*yrdot-ydr*nrdot)/ae1
      ae(3,3)= (yrdot*nv-yv*nrdot)/ae1
      ae(3,4)= (yrdot*nr-yr*nrdot)/ae1
      ae(3,6)= yrdot/ae1
      ae(3,7)=-nrdot/ae1
      ae(4,1)= (ndr*yvdot-ydr*nvdot)/ae2
      ae(4,3)= (yvdot*nv-yv*nvdot)/ae2
      ae(4,4)= (nr*yvdot-nvdot*yr)/ae2
      ae(4,6)= yvdot/ae2
      ae(4,7)=-nvdot/ae2
      ae(5,2)= 1.
      ae(5,3)= 1.
      ae(6,6)=-1.
      ae(7,7)=-1.
      ba(1,1)= 1/tr
      bc(6,1)= 1.
      bc(7,2)= 1.
```

```
      bd(3,1)= yrdot/ae1
      bd(3,2)=-nrdot/ae1
      bd(4,1)= yvdot/ae2
      bd(4,2)=-nvdot/ae2
c
      open(10,file='sim.dat',status='old')
      open(11,file='sim1.res',status='new')
      open(12,file='sim2.res',status='new')
      open(13,file='sim3.res',status='new')
      open(14,file='table1.dat',status='old')
      open(15,file='table2.dat',status='old')
      open(16,file='sim4.res',status='new')
      open(18,file='sim5.res',status='new')
      open(19,file='sim6.res',status='new')
      open(20,file='simo1.res',status='new')
      open(21,file='simo2.res',status='new')
c
c100
      do 40 i=1,m
       read(14,30)(table1(i,j),j=1,n)
       read(15,30)(table2(i,j),j=1,n)
30     format(11f7.2)
40    continue
c
c
      read(10,*)stime,delta
      read(10,*)s1,s2,s3,s4,s5,s6,s7
      read(10,*)k1,k2,k3,k4,k5,k6,k7,kn
      read(10,*)sigsat,eta,eta1,psi,y,xref,yref,ws
c
      ws=ws*.51444/.3048
c
c     define state v,r,dr,drc,psi,y
c
      isim=stime/delta
      v   =0.0
      u   =1.0
      r   =0.0
      dr  =0.0
      drc =0.0
      x   =0.0
```

```
      y    =0.0
      yf   =0.0
      mo   =0.0
c
c     estimated states
c
      odr  =0.0
      opsi =0.0
      ov   =0.0
      or   =0.0
      oy   =0.0
      oyf  =0.0
      omo  =0.0
c
c     simulation start
c
      do 1 i=1,isim
      if (b.ge.(3.5*xref)) stop
c
c     First order wave
c
       call first(psi,ws,time,f1,n1)
c
c     White noise
c
       call randm(iseed,wn)
       call randm(iseed,wy)
       wn=(wn*1.e-5)
       wy=(wy*1.e-5)
c
c      Interaction Force and Moment
c
       a =yref+y*l
       b =x*l-xref
       call locate(bb,n,a,nx)
       call loctae(aa,m,b,my)
       call trlint(m,n,my,nx,table1,bb,aa,a,b,yf)
       call trlint(m,m,my,nx,table2,bb,aa,a,b,mo)
       yf=yf*1.e-5
       mo=mo*1.e-5
       if (b.lt.(-550).or.b.gt.550) then
```

```
            yf=0.0
            mo=0.0
           endif
      c
           a1=mass-yvdot
           b1=mass*xg-yrdot
           c1=yv*v+(yr-mass)*r+ydr*dr+yf+f1
           a2=mass*xg-nvdot
           b2=iz-nrdot
           c2=nv*v+(nr-mass*xg)*r+ndr*dr+mo+n1
           a3=mass-xudot
      c
           drdot =-dr/tr+drc/tr
           psidot= r
           vdot  = (c1*b2-c2*b1)/(a1*b2-a2*b1)
           rdot  = (c1*a2-c2*a1)/(a2*b1-a1*b2)
           ydot  = sin(psi)+v*cos(psi)
           xdot  = cos(psi)-v*sin(psi)
           yfdot =-yf+wy
           modot =-mo+wn
      c
      c    Euler Integration for Actual States
      c
           dr =dr +drdot *delta
           psi=psi+psidot*delta
           v  =v  +vdot  *delta
           r  =r  +rdot  *delta
           y  =y  +ydot  *delta
           x  =x  +xdot  *delta
           yf =yf +yfdot *delta
           mo =mo +modot *delta
      c
      c    Measurement Noises
      c
           call randm(iseed,rnpsi)
           call randm(iseed,rnr)
           call randm(iseed,rny)
           rnpsi=rnpsi*0.0035
           rnr  =rnr  *0.0002
           rny  =rny  *0.0063
           psime=psi  +rnpsi
```

```
      rme  =r    +rnr
      yme  =y    +rny
c
c     Feedforward Control Rudder Angle Design
c
      aa1   = ydr*nvdot-ndr*yvdot
      bb1   = nvdot*yv-yvdot*nv
      cc1   =-(oyf+f1)*nvdot+(omo+n1)*yvdot
      aa2   = ydr*nrdot-ndr*yrdot
      bb2   = yv*nrdot-nv*yvdot
      cc2   = (omo+n1)*yrdot-(oyf+f1)*nrdot
      drc0  = (cc1*bb2-cc2*bb1)/(aa1*bb2-aa2*bb1)
      v0    = (cc1*aa2-cc2*aa1)/(bb1*aa2-bb2*aa1)
      psi0  =-v0
      sigma1=s1*drc0+s2*psi0+s3*v0+s6*omo+s7*oyf
      if (abs(sigma1).lt.sigsat) satsgn1=sigma1/sigsat
      if (sigma1.le.-sigsat)     satsgn1=-1.0
      if (sigma1.gt. sigsat)     satsgn1= 1.0
      a0    =-eta1**2*kn*satsgn1
      dr0   = drc0+(k1*drc0+k2*psi0+k3*v0+k6*omo+k7*oyf)-a0
c
c     rudder input calculation
c
      sigma=s1*odr+(s2*opsi+s3*ov+s4*or+s5*oy+s6*omo+s7*oyf)
      if (abs(sigma).lt.sigsat) satsgn=sigma/sigsat
      if (sigma.le.-sigsat)     satsgn=-1.0
      if (sigma.ge. sigsat)     satsgn= 1.0
c
      drchat=-(k1*odr+k2*opsi+k3*ov+k4*or+k5*oy+k6*omo+
     1          k7*oyf)
      drcbar= eta**2*kn*satsgn
      drc   = drchat-drcbar+dr0
      drf   = drchat-drcbar
c
      if (drc.ge. 0.4) drc= 0.4
      if (drc.le.-0.4) drc=-0.4
c
c     Observed States
c
      ob1=ae(1,1)*odr+ae(1,2)*opsi+ae(1,3)*ov+ae(1,4)*or+
     1    ae(1,5)*oy+ae(1,6)*omo+ae(1,7)*oyf
```

```
      ob2=ae(2,1)*odr+ae(2,2)*opsi+ae(2,3)*ov+ae(2,4)*or+
     1     ae(2,5)*oy+ae(2,6)*omo+ae(2,7)*oyf
      ob3=ae(3,1)*odr+ae(3,2)*opsi+ae(3,3)*ov+ae(3,4)*or+
     1     ae(3,5)*oy+ae(3,6)*omo+ae(3,7)*oyf
      ob4=ae(4,1)*odr+ae(4,2)*opsi+ae(4,3)*ov+ae(4,4)*or+
     1     ae(4,5)*oy+ae(4,6)*omo+ae(4,7)*oyf
      ob5=ae(5,1)*odr+ae(5,2)*opsi+ae(5,3)*ov+ae(5,4)*or+
     1     ae(5,5)*oy+ae(5,6)*omo+ae(5,7)*oyf
      ob6=ae(6,1)*odr+ae(6,2)*opsi+ae(6,3)*ov+ae(6,4)*or+
     1     ae(6,5)*oy+ae(6,6)*omo+ae(6,7)*oyf
      ob7=ae(7,1)*odr+ae(7,2)*opsi+ae(7,3)*ov+ae(7,4)*or+
     1     ae(7,5)*oy+ae(7,6)*omo+ae(7,7)*oyf
      ob23   =bd(3,1)*(n1)+bd(3,2)*f1
      ob24   =bd(4,1)*(n1)+bd(4,2)*f1
      odrdot =ob1+ol(1,1)*(psime-opsi)+ol(1,2)*(rme-or)+
     1        ol(1,3)*(yme-oy)+ba(1,1)*drc
      opsidot=ob2+ol(2,1)*(psime-opsi)+ol(2,2)*(rme-or)+
     1        ol(2,3)*(yme-oy)
      ovdot  =ob3+ol(3,1)*(psime-opsi)+ol(3,2)*(rme-or)+
     1        ol(3,3)*(yme-oy)+ob23
      ordot  =ob4+ol(4,1)*(psime-opsi)+ol(4,2)*(rme-or)+
     1        ol(4,3)*(yme-oy)+ob24
      oydot  =ob5+ol(5,1)*(psime-opsi)+ol(5,2)*(rme-or)+
     1        ol(5,3)*(yme-oy)
      omodot =ob6+ol(6,1)*(psime-opsi)+ol(6,2)*(rme-or)+
     1        ol(6,3)*(yme-oy)
      oyfdot =ob7+ol(7,1)*(psime-opsi)+ol(7,2)*(rme-or)+
     1        ol(7,3)*(yme-oy)
c
c     Eular Integration for Estimate States
c
      odr =odr +odrdot *delta
      opsi=opsi+opsidot*delta
      ov  =ov  +ovdot  *delta
      or  =or  +ordot  *delta
      oy  =oy  +oydot  *delta
      oyf =oyf +oyfdot *delta
      omo =omo +omodot *delta
cc
      time=i*delta
      if (mod(i,20).eq.0) then
```

```
        write(11,20)time,psi,v,y,r,dr
20      format(f10.4,1x,f10.4,1x,f10.4,1x,f10.4,1x,f10.4,
     1         1x,f10.4)
        write(12,*)x,y,a,b
        write(13,*)drchat,drcbar,drc,drf
        write(16,*)yf,mo,dr0
        write(19,*)wy,wn
        write(20,50)odr,opsi,ov,or,oy
50      format(f10.4,1x,f10.4,1x,f10.4,1x,f10.4,1x,f10.4)
        write(21,*)omo,oyf
        write(18,*)f1,n1
       endif
1      continue
       stop
       end
c303
ccccccccccccccccccccccccccccccccccccccccccccccccccccccccccccccccc
c
       subroutine locate(xx,n,x,j)
c
c     This is a subroutine for finding the interaction forces
c      and moments. For location the interaction forces and
c      moments in the input file TABLE1.DAT and TABLE2.DAT
c      correspond the lateral distance and longitudinal

c      distance.
c
       dimension xx(n)
c
       do 20 i=1,n
        if (x.eq.xx(i)) j=i
20     continue
       do 10 i=1,n-1
        if (x.gt.xx(i).and.x.lt.xx(i+1)) then
         j=i
        endif
10     continue
       return
       end
c
ccccccccccccccccccccccccccccccccccccccccccccccccccccccccccccccccc
```

```
c
      subroutine trlint(m,n,i,j,ya,x1a,x2a,x1,x2,y)
c
c     This subroutine is used for calculating the interaction
c     forces and moments, the data get from SUB LOCATE and the
c     values calculated by interpolation.
c
      dimension ya(m,n),x1a(n),x2a(m)
      real t,u,t1,u1
c
c
      y1=ya(i  ,j  )
      y2=ya(i  ,j+1)
      y3=ya(i+1,j  )
      y4=ya(i+1,j+1)
c
      t=(x1-x1a(j))/(x1a(j+1)-x1a(j))
      u=(x2-x2a(i))/(x2a(i+1)-x2a(i))
c
      t1=y1+u*(y3-y1)
      u1=y3+u*(y4-y2)
      y =t1+t*(u1-t1)
c
      return
      end
ccccccccccccccccccccccccccccccccccccccccccccccccccccccccccccccccc
      subroutine randm(iseed,rndm)
c
c     generate a gaussian random number
c     iseed - input a integer variable seed
c             output seed is changed during execution for next

c               call
c     rndm  - gaussian random variable with zero mean and unit

c               variance
c
      real rndm,rnd1,rnd2
      integer iseed,jr,kr,mr
      parameter (jr=5243,kr=55397,mr=262139)
       iseed=mod(iseed*jr+kr,mr)
```

```
        rnd1 =(iseed+.5)/mr
        iseed=mod(iseed*jr+kr,mr)
        rnd2 =(iseed+.5)/mr
        rndm =sqrt(-2.*log(rnd1))*cos(6.2831853*rnd2)/2.5
       return
       end
ccccccccccccccccccccccccccccccccccccccccccccccccccccccccccccccccc
       subroutine trap(nt,vx,vy,out)
c
c     numerical integration routine using the trapezoidal rule
c
       dimension vx(1),vy(1)
       real out
c
       n1=nt-1
       out=0.0
       do 1 i=1,n1
        out1=.5*(vx(i)+vx(i+1))*(vy(i+1)-vy(i))
        out =out+out1
1      continue
       return
       end
ccccccccccccccccccccccccccccccccccccccccccccccccccccccccccccccccc
       subroutine first(psi,ws,time,f1,n1)
c
c      This subroutine is used for calculating the sway force
c      and yaw moment component from first-order wave
c      excitation.
c
c      The inputs of the subroutine are:
c      (1) The encounter frequency(we):
c
c        we=w-(w^2)/g*u*cos(theta-psi)
c           w         is the actual wave frequency.
c           theta(θ)  is the wave-to-ship angle.
c           psi(ψ)    is the ship heading.
c           g         is the acceleration of gravity.
c           u         is the ship forward speed(15 knots).
c
c      (2) The wind speed(ws).
```

```
c
c     (3) The RAO of sway force and RAO of yaw moment are the
c         function of encounter frequency .
c     (4) The Pierson-Moskowitz spectrum is the function of we
c         and wind speed .
c        The associated force and moment are calculated from
c     Trapizoid Intergration and be the outputs of the
c     subroutine.
c         The phase angles correspond to the sway force and
c     moment are generated by random process (irregular wave)
c     (epsf,epsm) from 0 to 2π
c397
      real sf(19),ym(19),wee(19),wf(19),wm(19),vecx(19),
     1     vecm(19)
      real we,alpha,beta,ws,g,epsf,epsm,sx(19),psi,w1(19),
     1     w2(19)
      real raom(19),raof(19),time,model,l,lm,rho,u1,omega,
     1     w(19),s(19)
      real f1,n1
      data sf/1.3191,1.9473,2.5082,2.9529,3.2653,3.3462,
     1       3.0542,2.3640,1.5397,.6624,.21465,.73203,1.033,
     1        1.0222,.68012,.27829,.37778,.55739,.46259/
      data ym/.07246,.03741,.08306,.22726,.42925,.6717,
     1      .89061,.99661,1.0366,.9459,.73952,.47369,.19894,
     1        .17588,.31972,.34974,.25216,.07516,.15072/
      data wee/.293,.361,.433,.509,.588,.679,.756,.845,
     1       .938,1.304,1.133,1.236,1.342,1.452,1.565,1.682,
     1         1.801,1.925,2.052/
      data wf/274,277,277,280,287,290,293,294,292,281,163,
     1        122,110,101,87,40,313,290,280/
      data wm/169,138,32,19,22,23,23,26,27,24,19,10,339,
     1        242,211,197,185,146,24/
c
      model= 33.27
      lm   = 5.
      l    = 527.8
      rho  = 1.9905
      g    = 32.2
      u1   = 26.0
      alpha=  8.1*.001
      beta =-  .74
```

```
      ised = 17
      omega=  2.0
      time = time*l/u1
c
c     Pierson-Moskowitz Spectrum
c
      do 1 i  =1,19
       raof(i)=sf(i)*model*g/lm
       raom(i)=ym(i)*model*g
       w1(i)=(1+sqrt(1-4*u1*cos(2.618-psi)/g))/
     1       (2*u1*cos(2.618-psi)/g)
       w2(i)=(1-sqrt(1-4*u1*cos(2.618-psi)/g))/
     1       (2*u1*cos(2.618-psi)/g)
       if (w1(i)*w2(i).lt.0) then
        if (w1(i).gt.0) w(i)=w1(i)
        if (w2(i).gt.0) w(i)=w2(i)
       endif
       if (w1(i)*w2(i).gt.0) then
        if (abs(w1(i)).gt.abs(w2(i))) w(i)=abs(w1(i))
        if (abs(w2(i)).gt.abs(w1(i))) w(i)=abs(w2(i))
       endif
       s(i)    =(alpha*(g**2)/(w(i)**5))*
     1          exp(beta*(g/(ws*w(i)))**4)
       sx(i)   =s(i)/(1-(2*w(i)/g)*u1*cos(2.618-psi))
       vecx(i)=sqrt(2*sx(i)*raof(i))*
     1          cos(wee(i)*time-wf(i)*3.14/180)
       vecm(i)=sqrt(2*sx(i)*raom(i))*
     1          cos(wee(i)*time-wm(i)*3.14/180)
1     continue
c
c     Force and Moment calculation
c
      call trap(19,vecx,wee,f1)
      call trap(19,vecm,wee,n1)
      f1=f1/(.5*rho*l**2*u1**2)
      n1=n1/(.5*rho*l**3*u1**2)
      return
      end
```

LIST OF REFERENCES

1. Uhrin J.J. III, *Sampled Data Adaptive Digital Computer Control of Surface Ship Maneuvers*, M.S. Thesis US Naval Postgraduate School, June 1976.

2. George J. Thaler and Uhrin J.J. III, "Replenishment at Sea, an Automatic System" Naval Engineering Journal, Dec 1979, Vol. 91, No6.

3. Samuel H. Brown and Joseph G. Dimmick, "Simulation Analysis of Steering Control During Underway Replenishment" Journal of Ship Research, Vol. 27, No. 4, Dec 1983, pp 236-251.

4. Reidav Alvested, "Automatic Control of Underway Replenishment Maneuvers in a Random Sea" Journal of Ship Research, Vol. 22, No. 1, March 1978, pp 20-28.

5. Manley ST. Denis and Willard J. Pierson, "On the Motions of Ship in Confused Sea" Annual Meeting of Society of Naval Architects and Marine Engineers in New York, Nov 1953.

6. S. H. Brown and R. Alvestad, "Hybrid Computer Simulation of Maneuvering During Underway Replenishment" David W. Taylor Naval Ship Research and Development Center, 27-529, July 1973.

7. S. H. Brown and R. Alvestad, "Sensitivity Study of Control Parameters During Underway Replenishment Simulations including Approximate Nonlinear Sea Effects" David W. Taylor Naval Ship Research and Development Center, 77-0003, Jan. 1977.

8. S. H. Brown and Joseph G. Dimmick, "Simulation Analysis of Automatic and Quickened Manual Control During Underway Replenishment" DTNSRDC-801007, June 1981.

9. S. H. Brown and R. Alvestad, " Hybrid Computer Simulation of Maneuvering During Underway Replenishment" A004603, Feb. 1975.

10. J.J. E. Slotine, *Tracking Control of Nonlinear System Using Sliding Surface*, MIT M.S. Thesis, May 1983.

11. V. I. Utkin, *Sliding Modes and Their Application in Variable Structure System*, Moscow 1974.

12. R. A. Decorlo, S. H. Zak, and G. P. Matthews, "Variable Structure Control of Nonlinear Multivariable System: A tutorial" Proceeding of the IEEE, Vol. 76, No. 3, Mar. 1988.

13. Philip Mandel, *Principle of the Naval Architecture, Ship Maneuvering and Control*, 1967.

14. Sur, Joo-No, *Design and Investigation of a Dive Plane Sliding Mode Compensator for an Autonomous Underwater Vehicle*, NPGS M. S. Thesis, Sep 1989.

INITIAL DISTRIBUTION LIST

1. Defense Technical Information Center — 2
   Cameron Station
   Alexandria, Virginia 22304-6145

2. Library, Code 52 — 2
   Naval Postgraduate School
   Monterey, California 93943-5002

3. Department Chairman, Code ME — 1
   Department of Mechanical Engineering
   Naval Postgraduate School
   Monterey, California 93943-5000

4. Professor Fortis A. Papoulias — 2
   Code ME/Pa
   Department of Mechanical Engineering
   Naval Postgraduate School
   Monterey, California 93943-5000

5. Professor George J. Thaler, Code 62Tr — 1
   Department of Electrical and
   Computer Engineering,
   Naval Postgraduate School
   Monterey, California 93943-5100

6. Library — 2
   Chinese Naval Academy
   Kaohsiung, Taiwan, R.O.C

7. LT Fu, Hsu-Sheng — 2
   99, Lu-Kuan 2nd Village, Kuei-San,
   Taoyuan, Taiwan, R.O.C

8. LT Chu, Hui-Shen — 1
   32424, No. 9, 72 Lane, Moutung Rd,
   Chung-Li, Taoyuan, Taiwan, R.O.C

9. Naval Engineering Curricular Officer, Code 34 — 2
   Department of Mechanical Engineering
   Naval Postgraduate School
   Monterey, California 93943-5004

10. Professor H. A. Titus, Code 62Ts 1
Department of Electrical and Computer
Engineering, Naval Postgraduate School,
Monterey, California 93943-500